

**GAIT ANALYSIS METHODS FOR ASSESSING FALL RISK IN OLDER ADULTS
WITH UNILATERAL TRANSFEMORAL AMPUTATION**

by

Allison Joy Luther

B.S. in Biomedical Engineering, Rose-Hulman Institute of Technology, 2011

Submitted to the Graduate Faculty of
Swanson School of Engineering in partial fulfillment
of the requirements for the degree of
Master of Science

University of Pittsburgh

2013

UNIVERSITY OF PITTSBURGH
SWANSON SCHOOL OF ENGINEERING

This thesis was presented

by

Allison Luther

It was defended on

February 28, 2013

and approved by

Ray Burdett, PhD, PT, CO, CPed, Associate Professor,
Department of Rehabilitation Science and Technology, University of Pittsburgh

April Chambers, PhD, Director, Human Movement & Balance Laboratory,
Research Assistant Professor, Department of Bioengineering, University of Pittsburgh

Mark Redfern, PhD, Vice Provost for Research, University of Pittsburgh,
Professor, Departments of Bioengineering, Otolaryngology, Physical Therapy and
Rehabilitation, University of Pittsburgh

Thesis Advisor: Rakié Cham, PhD, Associate Professor, Department of Bioengineering,
University of Pittsburgh

Copyright © by Allison Luther

2013

**GAIT ANALYSIS METHODS FOR ASSESSING FALL RISK IN OLDER ADULTS
WITH UNILATERAL TRANSFEMORAL AMPUTATION**

Allison Luther, M.S.

University of Pittsburgh, 2013

The risk of falling in older adults has been widely investigated among the able-bodied population but there is little evidence identifying fall risk among older adults who have a unilateral transfemoral amputation. Older adult amputees have a loss of muscular control at the ankle and knee joints in the prosthetic limb and decreased muscle strength in the sound limb from aging. Previous research has investigated minimum foot clearance (MFC) to understand the risk of tripping while walking, and results show MFC decreases with age in able-bodied individuals. Changes in MFC have not been examined for older adults with unilateral transfemoral amputation, and in general, the methods for determining MFC must be modified for deviations in amputee gait. The first objective of this thesis was to develop a methodology for identifying MFC in older adult unilateral transfemoral amputees while walking over a level surface and during stair ambulation. Comparisons were made between the prosthetic limb and sound limb. Six older adult unilateral transfemoral amputees completed multiple walking and stair ambulation trials. Results showed 4 of 6 subjects had smaller MFC with the prosthetic limb compared to the sound limb while walking over a level surface. During stair ascent and descent, horizontal clearance of the prosthetic foot with respect to the step edge was typically greater than the sound limb. The methodology developed in this thesis allowed for identification of MFC regardless of unilateral transfemoral amputee gait style. The second objective was to investigate stumble recovery following obstruction of the prosthetic limb during swing. Results showed an

elevating recovery strategy yielded a shorter recovery duration and smaller trunk deviation in the sagittal and frontal planes in comparison to a lowering strategy. The final objective was to develop a geometric model of the prosthetic limb for determining the mass, center of mass, and mass moment of inertia of its segments. Published anthropometric methods for determining inertial properties in able-bodied individuals cannot be applied due to the amputation. The developed geometric model of the prosthetic limb successfully produced the inertial properties, and the model results were comparable to direct measurements taken for each segment.

TABLE OF CONTENTS

NOMENCLATURE.....	XIX
PREFACE.....	XX
1.0 INTRODUCTION.....	1
1.1 THE SIGNIFICANCE OF FALLS	1
1.1.1 Impact of Falls in the Older Adult Population	1
1.1.2 Causes for Falling in Older Able-Bodied Adults	2
1.1.3 Lower Limb Loss and Falls in Older Adult Amputees	5
1.1.4 Causes for Falling in Unilateral Transfemoral Amputees.....	6
1.2 PROSTHETIC KNEE JOINTS	7
1.2.1 Prosthetic Knee Joint Technology.....	7
1.2.2 Research Comparing Prosthetic Knee Joints	9
1.2.3 Classifying Older Adult Amputees Based on Functional Status.....	13
1.3 THE BIOMECHANICS OF GAIT AND STAIR AMBULATION.....	17
1.3.1 Normal Gait.....	17
1.3.2 Unilateral Transfemoral Amputee Gait	19
1.3.3 Stair Ascent and Descent in Able-Bodied Individuals	22
1.3.4 Stair Ascent and Descent in Unilateral Transfemoral Amputees	25
1.3.5 Responses to Stumbling in Older Adults.....	26
1.3.6 Responses to Stumbling in Unilateral Transfemoral Amputees	27

1.4	INERTIAL PROPERTIES OF THE PROSTHETIC LIMB	28
1.5	IMPORTANCE OF UNILATERAL TRANSFEMORAL AMPUTEE GAIT RESEARCH IN OLDER ADULTS	33
2.0	SPECIFIC AIMS.....	35
3.0	METHODS FOR ASSESSING MINIMUM FOOT CLEARANCE AND STUMBLE RECOVERY IN OLDER ADULTS WITH UNILATERAL TRANSFEMORAL AMPUTATION.....	37
3.1	STUDY PARTICIPANTS.....	37
3.1.1	Subject Recruitment.....	37
3.1.2	Subject Overviews	38
3.2	METHODS.....	45
3.2.1	Experimental Protocol	45
3.2.1.1	Laboratory Visit 1.....	45
3.2.1.2	Laboratory Visit 2.....	47
3.2.1.3	Laboratory Visit 3.....	59
3.2.1.4	Laboratory Visit 4.....	60
3.2.2	Method for Minimum Foot Clearance during Level Surface Walking....	60
3.2.3	Method for Foot Clearance during Stair Ascent	70
3.2.4	Method for Foot Clearance during Stair Descent	73
3.2.5	Method for Stumbling Perturbation Outcome Measures.....	75
3.3	RESULTS.....	77
3.3.1	Minimum Foot Clearance during Level Surface Walking	77
3.3.2	Stair Ascent	101
3.3.3	Stair Descent	106
3.3.4	Responses to Stumbling.....	106

3.4	DISCUSSION.....	119
3.4.1	Minimum Foot Clearance during Level Surface Walking	119
3.4.2	Stair Ambulation Minimum Foot Clearance	123
3.4.3	Responses to Stumbling.....	125
4.0	GEOMETRIC MODELING OF THE PROSTHETIC LIMB.....	127
4.1	METHODS.....	127
4.1.1	Experimental Measurements.....	127
4.1.2	Geometric Modeling of the Prosthetic Limb.....	129
4.2	RESULTS	132
4.3	DISCUSSION.....	134
5.0	CONCLUSIONS	137
APPENDIX A. AMPUTEE MOBILITY PREDICTOR ASSESSMENT.....		142
APPENDIX B. SUPPORTING OUTCOME MEASURES FOR LEVEL SURFACE WALKING		146
APPENDIX C. FOOT CLEARANCE RESULTS FOR STAIR AMBULATION		159
APPENDIX D. RESPONSES TO STUMBLING		162
APPENDIX E. EQUATIONS FOR THE GEOMETRIC MODEL OF THE PROSTHETIC LIMB USED TO DETERMINE SEGMENT INERTIAL PROPERTIES		171
BIBLIOGRAPHY		178

LIST OF TABLES

Table 1. Coding system modifiers and Medicare Functional Classification Level descriptions used by the U.S. Health Care Financing Administration [30].	14
Table 2. Comparison of mean spatial-temporal gait parameters for normal gait and unilateral transfemoral amputee gait in adults (age range 20-56 years) [45].	21
Table 3. Comparison of the mean (standard deviation) values between the sound and prosthetic limb for the phases of gait in unilateral transfemoral amputees (age range 20-56 years) [45].	21
Table 4. Comparison of mean (standard deviation) maximal knee flexion values between middle-aged able-bodied and unilateral transfemoral amputee adults [49].	22
Table 5. Comparison of mean (standard deviation) spatial-temporal gait parameters during stair descent for young and old adults [54].	24
Table 6. Inclusion and exclusion criteria for participation in the research study.	38
Table 7. Overview of the subjects presented in the results of this thesis. Subjects 1 and 4 are the same individual but a different prosthetic knee joint was used at each visit. Full study participation refers to those who were involved in the on-going research study.	39
Table 8. Criteria for determining K-level after performing the AMP evaluation [42].	46
Table 9. Experimental conditions for biomechanical analysis during laboratory visits 2 and 4. Pilot study experimental conditions are noted with an asterisk.	49
Table 10. Prosthetic knee joint models used in the study.	59
Table 11. Subject 1 MFC values during the swing phase. Highlighted values are the MFC events identified by a clear local minimum point during the swing phase.	81
Table 12. Subject 2 MFC values during the swing phase. Highlighted values are the MFC events identified by a clear local minimum point during the swing phase.	83
Table 13. Subject 3 MFC values during the swing phase. Highlighted values are the MFC events identified by a clear local minimum point during the swing phase.	85

Table 14. Subject 4 MFC values during the swing phase. Highlighted values are the MFC events identified by a clear local minimum point during the swing phase. 87

Table 15. All forefoot clearance values for the sound limb of subject 5 during swing. Highlighted values correspond to the overall smallest clearance value for each location in the swing phase (32.5%, 67.5%, and the identified MFC point). 90

Table 16. All resulting clearance values for the prosthetic limb of subject 5 during swing. Highlighted values correspond to the overall smallest clearance value for each location in the swing phase (32.5% and 67.5%). MFC could not be determined for the prosthetic limb during swing due to no local minimum point in the trajectory data. 92

Table 17. Subject 5 clearance values during the swing phase. For each swing phase the smallest value among all forefoot markers is reported at MFC, 32.5% and 67.5% of the swing phase, along with the associated marker position. Highlighted values are the MFC events identified by a clear local minimum point during the swing phase. 93

Table 18. All forefoot clearance values for the sound limb of subject 6 during swing. Highlighted values correspond to the overall smallest clearance value for each location in the swing phase (32.5% and 67.5%). MFC results are not available for the toe tip position because no identifiable local minimum point for this trajectory was present during swing. 96

Table 19. All resulting clearance values for the prosthetic limb of subject 6 during swing. Highlighted values correspond to the overall smallest clearance value for each location in the swing phase (32.5% and 67.5%). MFC results that were not able to be identified are indicated with N/A. 99

Table 20. Subject 6 MFC values during the swing phase. For each swing phase the smallest value among all forefoot markers is reported at 32.5% and 67.5% of the swing phase, along with the associated marker position. A MFC event could not be identified by a clear local minimum point during the swing phase for all forefoot markers, thus MFC is reported as N/A. 100

Table 21. Average minimum resultant, horizontal, and vertical clearances (standard deviation) for the forefoot positions of the sound and prosthetic feet during stair ascent. The forefoot position with the smallest average clearance is presented. Horizontal clearance values are negative because the foot has not passed over the step edge. 101

Table 22. Average inferior heel clearance (standard deviation) for the sound and prosthetic feet during stair descent. 106

Table 23. Outcome for all stumble perturbation trials and the associated recovery strategy and recovery duration. 107

Table 24. Average maximum and minimum trunk angles and average angular velocity while walking unperturbed over a level surface. Negative frontal plane trunk angles signify trunk tilt to the left of vertical. 108

Table 25. Trunk angles in the sagittal and frontal planes at foot-obstacle contact, and the maximum and minimum trunk angles occurring during the stumble recovery duration. Negative frontal plane trunk angles signify trunk tilt to the left of vertical.....	108
Table 26. Trunk angular velocity at foot-obstacle contact and the maximum and minimum trunk angular velocity occurring during the stumble recovery duration.....	109
Table 27. Measurements of the foot, shank, and thigh segments needed for the geometric model of the prosthetic limb.	128
Table 28. The prosthetic limb segment inertial properties found using the geometric modeling approach along with the direct measurements taken during laboratory visit 3.....	133
Table 29. Socket inertial properties for the geometric modeling approach and the direct measurements taken during laboratory visit 3.	133
Table 30. Amputee Mobility Predictor evaluation form used during visits 1 and 4 [42].	142
Table 31. Average gait speed (standard deviation) across three level surface walking trials....	148
Table 32. Average cadence (standard deviation) across three level surface walking trials.	148
Table 33. Average stride duration (standard deviation) for 9 strides taken with each limb while walking on a level surface, and the resulting symmetry indices (positive index denotes prosthetic limb value is larger than sound limb).	149
Table 34. Average single-limb stance duration (standard deviation) for 12 stance phases with each limb while walking on a level surface, and the symmetry index results (negative index value denotes sound limb duration is greater than prosthetic limb duration).....	150
Table 35. Average double-limb support duration (standard deviation) for 12 steps taken with each limb while walking on a level surface. Sound limb double-limb support periods occur when the sound limb is the leading foot, and prosthetic limb double-limb support occurs when the prosthetic limb is the leading foot. A negative symmetry index represents the sound limb value is greater than the prosthetic limb.	151
Table 36. Average step length (standard deviation) for 12 steps taken with each limb while walking on a level surface, and the resulting symmetry indices (positive index denotes prosthetic limb value is larger than sound limb).	151
Table 37. Average step length (standard deviation) for 12 steps taken with each limb while walking on a level surface, and the resulting symmetry index (positive index denotes prosthetic limb value is larger than sound limb).	152
Table 38. Mean (standard deviation) minimum foot clearance distances during stair ascent for all subjects. The gray highlighted values signify the overall minimum clearance for the forefoot. The resultant clearance was not analyzed for the inferior heel marker; a dash indicates N/A. ..	160

Table 39. Mean (standard deviation) minimum foot clearance distances during stair descent for all subjects. The gray highlighted values signify the overall minimum clearance for the forefoot. The resultant clearance was not analyzed for the forefoot markers; a dash indicates N/A. 161

Table 40. Average trunk angles and angular velocity while walking unperturbed over a level surface for subjects 3 and 6..... 162

Table 41. Trunk angles in the sagittal and frontal planes during the stumble recovery durations for subjects 3 and 6. 163

Table 42. Trunk angular velocity during the stumble recovery durations. 163

LIST OF FIGURES

Figure 1. Trajectory of shoe toe tip for an able-bodied adult during the swing phase. Minimum foot clearance occurs at a visible local minimum point around midswing.....	4
Figure 2. Example gait cycle for the right limb, with phases and temporal variables labeled [47].	18
Figure 3. Stadium solid geometry used by Kingma and Yeadon [67].	30
Figure 4. Geometric model of the residual limb used by Fowler and Goldberg. Design consists of a proximal cylinder followed by a series of frustum and a distal paraboloid [75].	31
Figure 5. Diagrams of marker placement for the full research study marker set. The pilot study marker set did not include markers on the forefoot of the shoe (the static trial only markers), medial and lateral break markers, medial and lateral heel markers, or inferior heel markers.	48
Figure 6. Schematic of the laboratory area, instrumented with 14-Vicon motion capture cameras, 2-Bertec force plates embedded in a level surface walkway, and a Solo-Step ceiling mounted harness system.	50
Figure 7. View of the level surface walkway and the two embedded force plates. The black line spans the length of the walkway; the two force plates are outlined.....	51
Figure 8. Ramp with a 5-degree incline and embedded Bertec force plate.	52
Figure 9. Ramp with a 5-degree incline and an uneven surface.	53
Figure 10. Walkway with an uneven surface.	54
Figure 11. Staircase used for stair ascent and descent trials.	55
Figure 12. (A) The stumbling condition obstacles in the lowered position. (B) One obstacle in the raised position with the remaining two obstacle slots outlined.	57

Figure 13. (A) One of three stumbling device mechanisms housed underneath the laboratory flooring structure. When the springs are decompressed, the electromagnet holds the steel platform down so the top of the obstacle is flush with the walkway floor. Bolts in the four corners of the mechanism allow for fine-tuning the height of the obstacle within its slot in the walkway. (B) Set up of the stumbling device underneath the flooring structure. 57

Figure 14. (A) Forefoot markers along the shoe sole, from left to right: toe tip, front forefoot, middle forefoot, and break forefoot; the break and toe markers are labeled. (B) Anterior view of the shoe; forefoot markers on the lateral side of the shoe sole are shadowed on the medial side. 61

Figure 15. Typical toe marker vertical trajectory for the prosthetic limb. Initial forefoot motion points are circled. 63

Figure 16. Typical prosthetic limb force plate contact. Initial forefoot motion and heel-strike events found using vertical trajectories of the toe and superior heel markers, respectively, are identified. Heel-strike events were accurately identified using trajectory data and an approximate 167 ms difference was seen between initial forefoot motion and physical toe-off of the shoe leaving the floor. 64

Figure 17. Typical superior heel marker vertical trajectory for the prosthetic limb. Heel-strike points are circled. 65

Figure 18. Example of different sound limb and prosthetic limb toe tip patterns during gait. The sound limb toe tip trajectory has a local minimum point as the foot moves through the swing phase while the prosthetic limb does not have a minimum foot clearance point. 66

Figure 19. Example of the forefoot marker trajectories of the sound limb during swing phase (shoe figures included for visual identification of foot position during swing; not drawn to scale). The toe tip MFC occurs at approximately 50% of the swing phase while the break forefoot MFC occurs at approximately 60%. 68

Figure 20. Typical swing phase displaying a plateau instead of a clear local minimum point. When this occurred, MFC was evaluated based on the clearance values found at 32.5% and 67.5% of swing. 69

Figure 21. Typical sound limb toe motion during stair ascent. Red circles highlight initial forefoot motion points for each step. 71

Figure 22. Resultant (A), horizontal (B & E), and vertical (C & D) clearance distances for the foot during ascent (toe tip marker shown as an example for the forefoot). Prior to passing over the step edge yields negative horizontal values. The inferior heel may have a negative horizontal value if the foot is larger than the step tread or positioned such that the heel hangs off the step. 72

Figure 23. Resultant (A), horizontal (B & E), and vertical (C & D) clearance distances for the foot during descent (toe tip marker shown as an example for the forefoot). Marker positions prior to passing over the step edge have negative values. If any forefoot marker is positioned off of the step tread during stance the vertical distance will be negative and correspond to the instant of initial forefoot motion. 74

Figure 24. Typical sound limb inferior heel motion during stair descent. Red circles highlight heel-strike events. 75

Figure 25. Typical prosthetic foot toe tip marker trajectory during one gait cycle for all subjects. Zero and 100% of the gait cycle are identified by initial forefoot motion. 78

Figure 26. Typical sound foot toe tip marker trajectory during one gait cycle for all subjects. Zero and 100% of the gait cycle are identified by initial forefoot motion. 79

Figure 27. Comparison of mean toe tip trajectory across 3 steps for the sound foot and prosthetic foot of subject 1; dashed lines indicate standard deviation. Zero percent of the swing phase is identified by initial forefoot motion, 100% of the swing phase is identified by heel-strike..... 80

Figure 28. Comparison of mean toe tip trajectory across 3 steps for the sound foot and prosthetic foot of subject 2; dashed lines indicate standard deviation. Zero percent of the swing phase is identified by initial forefoot motion, 100% of the swing phase is identified by heel-strike..... 82

Figure 29. Comparison of mean toe tip trajectory across 3 steps for the sound foot and prosthetic foot of subject 3; dashed lines indicate standard deviation. Zero percent of the swing phase is identified by initial forefoot motion, 100% of the swing phase is identified by heel-strike..... 84

Figure 30. Comparison of mean toe tip trajectory across 3 steps for the sound foot and prosthetic foot of subject 4; dashed lines indicate standard deviation. Zero percent of the swing phase is identified by initial forefoot motion, 100% of the swing phase is identified by heel-strike..... 86

Figure 31. Comparison of the sound foot and prosthetic foot motion for subject 5. Note the sound foot heel rise in comparison to the vertical and forward motion of the prosthetic foot. This figure display is set to approximately one swing phase for each foot. 88

Figure 32. Sound limb forefoot marker trajectories for subject 5 during one swing phase..... 89

Figure 33. Prosthetic limb forefoot marker trajectories for subject 5 during one swing phase... 91

Figure 34. Comparison of the sound foot and prosthetic foot motion for subject 6 during one swing phase. This figure display is set to approximately one swing phase for each foot. 94

Figure 35. Sound limb forefoot marker trajectories for subject 6 during one swing phase..... 95

Figure 36. Prosthetic limb forefoot marker trajectories for subject 6 during one swing phase... 98

Figure 37. Subject 5 forefoot marker trajectories for the prosthetic limb during stair ascent. .. 103

Figure 38. Subject 5 forefoot marker trajectories for the sound limb during stair ascent. 103

Figure 39. Subject 6 forefoot marker trajectories for the prosthetic limb during stair ascent. A sliding technique was used to progress the foot up the step, where the toe tip slid up the riser. 105

Figure 40. Subject 6 forefoot marker trajectories for the sound limb during stair ascent. 105

Figure 41. Sagittal plane trunk angle during the stumble perturbation trial and during a baseline walking trial for subject 2. Initial contact with the obstacle and heel-strike of the prosthetic limb recovery step are identified by vertical lines. The sagittal plane trunk angle at initial contact is represented throughout the recovery phase by a dashed line..... 110

Figure 42. Frontal plane trunk angle during the stumble perturbation trial and during a baseline walking trial for subject 2. Initial foot-obstacle contact and heel-strike of the prosthetic limb recovery step are identified by vertical lines. The trunk angle at initial contact is represented throughout the recovery duration by a dashed line. 111

Figure 43. Trunk angular velocity during the stumble perturbation trial and during a baseline walking trial for subject 2. Initial foot-obstacle contact and heel-strike of the prosthetic limb recovery step are identified by vertical lines. The angular velocity at initial contact is represented throughout the recovery duration by a dashed line. 112

Figure 44. Sagittal plane trunk angle during the stumble perturbation trial and during a baseline walking trial for subject 4. Initial contact with the obstacle and heel-strike of the first recovered step are identified by vertical lines. The sagittal plane trunk angle at initial contact is represented throughout the recovery phase by a dashed line. 114

Figure 45. Frontal plane trunk angle during the stumble perturbation trial for subject 4. Initial foot-obstacle contact and heel-strike of the prosthetic limb recovery step are identified by vertical lines. The trunk angle at initial contact is represented throughout the recovery duration by a dashed line..... 115

Figure 46. Trunk angular velocity during the stumble perturbation trial for subject 4. Initial foot-obstacle contact and heel-strike of the prosthetic limb recovery step are identified by vertical lines. The angular velocity at initial contact is represented throughout the recovery duration by a dashed line. 116

Figure 47. Sagittal plane trunk angle during the stumble perturbation trial and during a baseline walking trial for subject 5. Initial contact with the obstacle and heel-strike of the prosthetic limb recovery step are identified by vertical lines. The sagittal plane trunk angle at initial contact is represented throughout the recovery duration by a dashed line. 117

Figure 48. Frontal plane trunk angle during the stumble perturbation trial and during a baseline walking trial for subject 5. Initial contact with the obstacle and heel-strike of the prosthetic limb recovery step are identified by vertical lines. The frontal plane trunk angle at initial contact is represented throughout the recovery duration by a dashed line. 118

Figure 49. Trunk angular velocity during the stumble perturbation trial and during a baseline walking trial for subject 5. Initial contact with the obstacle and heel-strike of the prosthetic limb recovery step are identified by vertical lines. The angular velocity at initial contact is represented throughout the recovery duration by a dashed line. 119

Figure 50. Example of the sliding technique used by subjects 3, 5, and 6 during stair descent with the prosthetic limb. The heel of the shoe was slid down the step riser to reach the step tread. 125

Figure 51. (A) Three-dimensional model of the foot segment using a series of stadium solids. (B) Cross-section of a stadium solid, defined as a rectangle with length $2t$ and width $2r$, adjoined by a semi-circle at each edge of the rectangle. The $2r$ distance is the measured superior-inferior distance. The measured medial-lateral distance is adjusted to yield the $2t$ distance. 130

Figure 52. Geometric model of the shank segment, modeled as a rectangular prism and two hollow cylinders..... 131

Figure 53. (A) Geometric model of the thigh segment. Both the socket and residual limb are modeled as a series of geometric shapes: proximal right-angled wedge (green), intermediate elliptical cylinders (white), distal elliptical paraboloid (blue), and socket adapter (red). (B) Cross-section of an elliptical cylinder..... 132

Figure 54. Subject 1 knee joint angles for the sound and prosthetic limb during level surface walking. Solid lines represent the mean knee angle across gait cycles; dashed lines show the standard deviation. Heel-strike occurs at zero and 100% of the gait cycle. 153

Figure 55. Subject 2 knee joint angles for the sound and prosthetic limbs during level surface walking. Solid lines represent the mean knee angle across gait cycles; dashed lines show the standard deviation. Heel-strike occurs at zero and 100% of the gait cycle. 154

Figure 56. Subject 3 knee joint angles for the sound and prosthetic limbs during level surface walking. Solid lines represent the mean knee angle across gait cycles; dashed lines show the standard deviation. Heel-strike occurs at zero and 100% of the gait cycle. 155

Figure 57. Subject 4 knee joint angles for the sound and prosthetic limbs during level surface walking. Solid lines represent the mean knee angle across gait cycles; dashed lines show the standard deviation. Heel-strike occurs at zero and 100% of the gait cycle. 156

Figure 58. Subject 5 knee joint angles for the sound and prosthetic limbs during level surface walking. Solid lines represent the mean knee angle across gait cycles; dashed lines show the standard deviation. Heel-strike occurs at zero and 100% of the gait cycle. 157

Figure 59. Subject 6 knee joint angles for the sound and prosthetic limbs during level surface walking. Solid lines represent the mean knee angle across gait cycles; dashed lines show the standard deviation. Heel-strike occurs at zero and 100% of the gait cycle. 158

Figure 60. Sagittal plane trunk angle during the stumble perturbation trial for subject 3. Initial contact with the obstacle and heel-strike of the first recovered step are identified by vertical lines. The sagittal plane trunk angle at initial contact is represented throughout the recovery duration by a dashed line..... 164

Figure 61. Frontal plane trunk angle during the stumble perturbation trial for subject 3. Initial contact with the obstacle and heel-strike of the first recovered step are identified by vertical lines. The frontal plane trunk angle at initial contact is represented throughout the recovery duration by a dashed line..... 165

Figure 62. Trunk angular velocity during the stumble perturbation trial for subject 3. Initial contact with the obstacle and heel-strike of the first recovered step are identified by vertical lines. The angular velocity at initial contact is represented throughout the recovery duration by a dashed line. 166

Figure 63. Sagittal plane trunk angle during the stumble perturbation trial for subject 6. Initial contact with the obstacle and heel-strike of the first recovered step are identified by vertical lines. The sagittal plane trunk angle at initial contact is represented throughout the recovery duration by a dashed line..... 168

Figure 64. Frontal plane trunk angle during the stumble perturbation trial for subject 6. Initial contact with the obstacle and heel-strike of the first recovered step are identified by vertical lines. The frontal plane trunk angle at initial contact is represented throughout the recovery duration by a dashed line..... 169

Figure 65. Trunk angular velocity during the stumble perturbation trial for subject 6. Initial contact with the obstacle and heel-strike of the first recovered step are identified by vertical lines. The angular velocity at initial contact is represented throughout the recovery duration by a dashed line. 170

NOMENCLATURE

The following abbreviations are used in this text:

AMP	Amputee Mobility Predictor
BW	Baseline Walking
COM	Center Of Mass
MFCL	Medicare Functional Classification Level
MPK	Microprocessor-controlled Prosthetic Knee
NMPK	Nonmicroprocessor-controlled Prosthetic Knee
PEQ	Prosthesis Evaluation Questionnaire
SAM	StepWatch Activity Monitor

PREFACE

First and foremost, I would like to thank my thesis advisor, Dr. Rakié Cham, for allowing me the opportunity to be exposed to the world of research and for guiding me along the way during this experience. Many thanks to my thesis committee members: Dr. Ray Burdett, Dr. April Chambers, and Dr. Mark Redfern. Your expertise and feedback have been instrumental in guiding me with my work and shaping the success of this research study, which will truly make an impact on the fields of lower limb prosthetics and geriatrics. Furthermore, a special thank you to all faculty, staff, and students at the Human Movement and Balance Laboratory. Over the past two years you have become my friends and support group here in Pittsburgh, and I am truly grateful for the time we have had together. To Alison Sukits, thank you for showing me the ropes when I first arrived. To Jenna Montgomery, thank you for your unyielding assistance in making this research a success. To Jarad Prinkey, thank you for brainstorming with me during the early stages of this study and for developing the electronic equipment. To Chris Sivi, thank you for assisting me in all aspects of this research project. To the many others who have contributed to my work, both directly and indirectly, a sincere thank you for your support. And lastly, to my family and friends who have supported me from afar, I could not have done this without your love and encouragement.

1.0 INTRODUCTION

1.1 THE SIGNIFICANCE OF FALLS

1.1.1 Impact of Falls in the Older Adult Population

Experiencing a fall at a later age in life can result in detrimental physical and psychological results for an individual. Each year approximately one in three adults age 65 and older will suffer a fall [1]. In the United States, falls are the number one cause of death for unintentional injuries among adults over 65 years of age [2]. In 2009, a total of 20,422 deaths resulting from a fall occurred, which corresponds to 52.2% of all unintentional injury deaths in this older adult population. Of the falls that caused these deaths, 48.7% were reported as an unspecified fall, while 6.8% occurred on stairs or steps and 3.5% occurred on a level surface due to a slip, trip or stumble.

Furthermore, 2.2 million non-fatal fall injuries occurred among the older adult population in 2009 with more than 26.4% of these patients needing hospitalization [3]. Older adults are hospitalized for fall injuries five times more often than they are for other causes, undeniably leading to a large economic burden for treating unintentional fall-related injuries [4]. In 2005, medical costs for unintentional fall-related injuries in older adults totaled \$6.3 billion dollars in the United States [5]. By 2020, this cost is estimated to increase to \$32.4 billion dollars in the

United States [1]. The total amount of associated medical costs will only continue to grow as the proportion of the population age 65 and older in the United States is projected to increase from approximately 35 million people in 2000 to an estimated 71 million people in 2030 [6]. Furthermore, as age increases, the probability of experiencing a fall increases. In 2009, the United States rate of fall injuries for adults over the age of 85 was almost four times that for adults ages 65 to 74 [3].

1.1.2 Causes for Falling in Older Able-Bodied Adults

An increase in age is associated with an increase in gait variability due to a loss of leg strength and passive range of motion in the lower limbs [7-8]. Previous research has found older adults who perform poorly in clinical gait evaluations are at an increased risk of falling [9]. Specifically, increased stride time variability has been shown to predict fall risk in older adults [10]. Stride time variability has also been significantly correlated with lower limb strength, balance, and gait speed.

In general, as age increases changes in the temporal and spatial parameters of gait occur. Previous gait research has found young adults have a self-selected gait speed of $1.48 \text{ m/s} \pm 0.18 \text{ m/s}$ while older adults who do not have a history of falling have a gait speed of $1.13 \text{ m/s} \pm 0.39 \text{ m/s}$ [11]. This shows a significant increase in gait speed variability with age, but furthermore, a history of falling among older adults increases to the variability to 0.42 m/s . Gait stride time also increases with age. Young adults were found to have a stride time of $1048 \text{ ms} \pm 73 \text{ ms}$ and older adults without a history of falling had a stride time of $1077 \text{ ms} \pm 85 \text{ ms}$. In terms of the stance phase of the gait cycle, young adults had a stance time of $651 \text{ ms} \pm 55 \text{ ms}$ while older adults who do not have a history of falling had a stance time of $690 \text{ ms} \pm 64 \text{ ms}$. Based on these stance

phase results, the percentage of stance during the gait cycle is significantly different between young and old adults. In terms of spatial gait parameters, an increase in age has been found to yield shorter step length with greater variability in comparison to younger adults [12]. Previous research has found step length variability (reported as a percentage of body height, %bh) for young adults to be $0.0078 \%bh \pm 0.006 \%bh$ while variability for older adults was $0.01 \%bh \pm 0.007 \%bh$. Similar results were seen for stride width variability: older adults had significantly larger stride width variability during gait than younger adults ($1.26 \text{ cm} \pm 0.35 \text{ cm}$ and $0.92 \text{ cm} \pm 0.32 \text{ cm}$, respectively).

As gait becomes more variable with age, it can become more difficult to complete tasks such as walking over an uneven surface, negotiating obstacles, or ascending and descending stairs [13]. However, these tasks can become even more challenging for an older adult when a fear of falling is present. For older adults who have a fear of falling or a history of falling, the spatial-temporal measures of gait show reduced gait speed, shorter stride length, increased stride width, and increased double-limb support time in comparison to non-fallers [14].

In addition to the variability in gait that occurs with an increase in age, older adults are more likely than the younger population to experience a fall due to tripping while walking. Tripping has been reported to account for up to 53% of falls among older adults, most often occurring while walking over a level floor or over an uneven floor [15]. Tripping while attempting to ambulate over a vertical change in level can also result in falls among older adults. Previous research found over a 2-year period a 23% risk for older adults to fall when there was a change in surface level, such as ambulating over stairs or a curb [16].

The risk of tripping while walking over a level surface can be understood by analyzing the minimum foot clearance of the foot as it passes over the flooring surface during swing.

Minimum foot clearance (MFC) has been defined for able-bodied individuals as the minimum vertical distance between the lowest point of the foot of the swing leg and the walking surface at the midswing location in the gait cycle [17]. The MFC value is found by identifying a local minimum point in the foot vertical displacement during the swing phase (Figure 1).

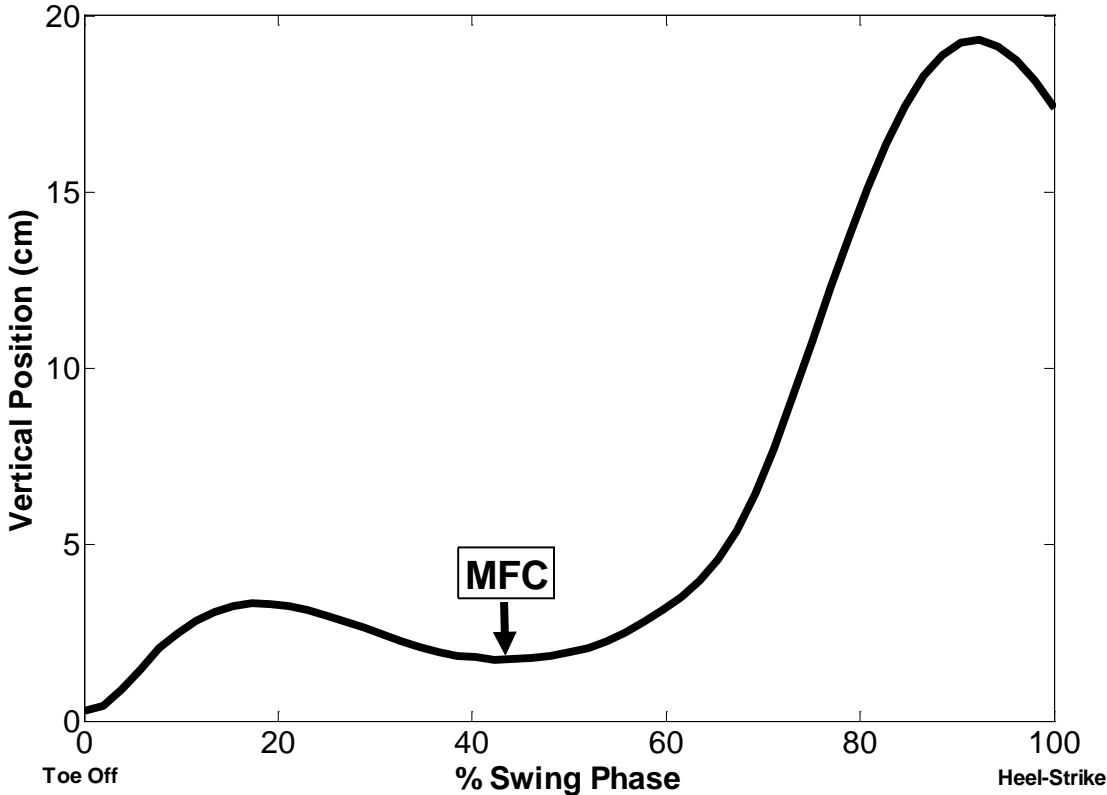


Figure 1. Trajectory of shoe toe tip for an able-bodied adult during the swing phase. Minimum foot clearance occurs at a visible local minimum point around midswing.

Comparison of MFC between healthy young adults and older adults has shown older adults are a greater risk of tripping when walking on level surfaces. The mean MFC reported for young adults is $1.29 \text{ cm} \pm 0.45 \text{ cm}$ [18]. For older adults, the MFC has been shown to decrease to a mean of $1.11 \text{ cm} \pm 0.53 \text{ cm}$ [19]. However, older adults who have a fear of falling or history of falling have been found to have MFC of $2.02 \text{ cm} \pm 0.51 \text{ cm}$ [20]. Minimum foot clearance variability has also been shown to be greater for older adults compared to younger adults and greater for older adult fallers compared to older non-fallers [15].

1.1.3 Lower Limb Loss and Falls in Older Adult Amputees

The number one cause for lower limb amputation in older adults is diabetes mellitus [21]. In 2010, the Centers for Disease Control and Prevention reported that 10.9 million Americans age 65 and older were affected by diabetes, which is 26.9% of this age group. The prevalence of diabetes in the United States is projected to nearly double by the year 2030, and those with living with diabetes and lower limb loss is projected to nearly triple by 2050 [22]. In 2005, there were 504,000 Americans who underwent a lower limb amputation either at a level above or below the knee, and 71% of these persons had a comorbidity of diabetes. Age also is a factor in lower limb amputation as evidence has shown an age-related increase in lower limb amputation secondary to vascular disease [23].

As of 1996 there was 1.2 million persons living with lower limb loss in the United States [24]. Of the amputations resulting from dysvascular causation (82% of all limb loss discharges), 25.8% of these amputations occurred at a level above the knee. Lower limb amputation has a large economic cost. Investigation into direct health-care costs associated with unilateral transfemoral amputation found in 2002 that the total 2-year cost associated with undergoing this

amputation, the rehabilitation process, and obtaining prosthetic equipment was \$110,039 [25]. For the 31 unilateral transfemoral patients included in this cost estimate, a new prosthesis was purchased every 2.3 years at an average cost of \$18,722 (2002 USD).

Currently, research by Miller et al. has reported that among community-dwelling adults with either a below knee or above knee amputation, 52% fell within the previous one-year period, 49% were afraid of falling, and 65% had low balance confidence scores [26]. Another study by Miller reported that for young and old adults who have a transfemoral amputation, approximately 66% experienced a fall within a one-year period [27]. A study by Gauthier-Gagnon found approximately 64% of community-dwelling transfemoral amputees reported falling over a one-month period [28]. In comparison to able-bodied older adults, where there is a 33% chance of experiencing a fall over a one-year period [1], the risk of falling is greatly increased following lower limb amputation in older adults.

1.1.4 Causes for Falling in Unilateral Transfemoral Amputees

Transfemoral amputees are at a significantly greater risk of falling due to the loss of the knee and ankle joints in the amputated limb. As a result of the amputation, gait will become more difficult regardless of age. Younger adult unilateral transfemoral amputees have been found to have reduced gait speed, increased postural sway during static standing or dynamic ambulation, increased energy expenditure when utilizing a prosthesis, asymmetrical step lengths, and asymmetrical stance durations between the prosthetic and sound limb [26, 29-30]. Furthermore, research investigating the vertical position of the shoe sole during the prosthetic limb swing phase of gait found average clearance over the walking surface to be $1.82 \text{ cm} \pm 1.20 \text{ cm}$ among younger subjects [31]. Based on knowledge regarding gait variability for spatial-temporal gait

parameters and MFC for able-bodied older adults, it can be inferred that these variations also hold true for the gait of older adult unilateral transfemoral amputees, and may even be increased due to the amputation. However, current literature has yet to focus solely on the older adult unilateral transfemoral amputee population. Furthermore, no biomechanics-based evidence has been published for understanding the fall risk for older adults with unilateral transfemoral amputation.

1.2 PROSTHETIC KNEE JOINTS

1.2.1 Prosthetic Knee Joint Technology

Over the last 50 years, prosthetic knee joint technology has advanced to provide transfemoral amputees with a device able to control the swing phase motion of the shank during gait [32]. These knees are known as mechanical, or nonmicroprocessor-controlled prosthetic knee joints (NMPK joints). The swing control of these knees is driven by either the mechanics of motion or a fluid-based system. The simplest NMPK joint uses constant friction and a single axis of rotation to provide a hinging motion at the knee, and is optimal for individuals walking at a single, fixed cadence [33]. A specific type of mechanical knee is the polycentric, or “four-bar” knee, which has four points of rotation each controlled by a linkage bar. The polycentric knee can provide greater toe clearance during swing and increased stance stability when the knee is in extension. This knee can be advantageous for a wide range of amputees who need added stability but are able to walk at a moderate or high pace [32]. The use of fluid flow control systems, such as hydraulic (fluid) or pneumatic (air) cylinders, use resistance to control the

flexion and extension speed of the knee during swing so that cadence can be varied. Some NMPK joints are able to offer stance phase control based on weight bearing activation during gait to keep the knee in extension. Manually locking knee joints can be given to feeble or unsteady amputees in order to provide more stability, but the result is a stiff-legged gait pattern where the knee is kept in extension. Mechanical knee joints require manual adjustment by a prosthetist to set the fluid flow resistance settings for the individual's optimal gait speed. Consequently, if the user wants to drastically alter their gait speed or make immediate changes to appropriately maneuver obstacles such as stairs or uneven terrain, they must alter their gait pattern and increase physical effort [34].

Advancements in technology during the late 1980's and early 1990's provided prosthetic manufacturers with the opportunity to introduce a new type of prosthetic knee joint to the market [35]. This new prosthesis included the addition of a microprocessor within the knee to allow for real-time control of the joint during both the swing and stance phases. The microprocessor-controlled prosthetic knee joint (MPK joint) uses a series of sensors to monitor and analyze the knee position and gait pattern, allowing for immediate changes in flexion and extension resistance to be made for maintaining optimal control during various ambulatory situations. This improvement has been shown to increase prosthetic limb stability during normal gait and increase functionality while ambulating over stairs and ramps, walking with a variable cadence, or walking over an uneven terrain [35-38].

The first set of sensors in the MPK joint monitor the knee flexion angle to determine the current flexion or extension [35]. The second set of sensors measure the amount of rotational stress applied below the knee joint during gait. Data collection ranges from a rate of 50 to 1,000 times per second, and the microprocessor analyzes the data using gait assessment algorithms to

determine if the knee angle and force are appropriate for the stance or swing phase of gait. Within 1/100th of a second, changes can be applied to the resistance level in order to provide optimal stability. When stance resistance is activated, the microprocessor sets the resistance for knee flexion at a high level so the knee does not collapse during stance on the prosthetic limb side. A MPK joint can also detect interruptions to normal gait, activating higher resistance to flexion in order to help prevent an uncontrollable fall should loss of balance occur.

1.2.2 Research Comparing Prosthetic Knee Joints

Over the past few years there has been an increase in the percentage of gait research focusing on persons with unilateral transfemoral amputation who are using different types of prosthetic knee joints. Most often unilateral transfemoral amputee research has attempted to make gait performance comparisons between different types of prosthetic knee joints by using biomechanics-based outcome measures or self-reported clinical measures. While these studies have used a wide range of subjects, no study has focused on how age affects the gait of transfemoral amputees who are using prosthetic knee joints. This section presents a summary of results for a few of the aforementioned studies.

A study by Segal and colleagues presented a kinematic and kinetic comparison using two opposing knee types with eight subjects ranging from 28 to 60 years of age [39]. Subjects were randomly assigned to use either a MPK joint or NMPK joint over a three-month acclimation period. After data collection with this prosthesis the knee was switched to the opposing type, and another three-month acclimation period was given before the final data collection occurred. Results showed an increase in self-selected walking speed with the MPK joint. To control for differences in kinematic and kinetic variables that may arise due to walking speed, subjects were

instructed to walk at a controlled speed of $1.11 \text{ m/s} \pm 0.11 \text{ m/s}$. At this speed, the prosthetic limb step length decreased for the MPK joint compared to the NMPK joint, making the MPK joint step length closer to that of the sound limb step length. Knee flexion angles in the sagittal plane were determined at multiple points in the gait cycle. The peak knee flexion angle during stance phase and the angle at the instant of opposite foot heel-strike were not significantly different for the two knee joint types for either the prosthetic or sound limb. During swing phase with the MPK joint, the prosthetic limb peak knee flexion angle was significantly decreased compared to the NMPK joint, but not significantly different compared to the sound limb. These results imply knee type has more impact on the swing phase rather than the stance phase of gait with regards to peak knee flexion. The prosthetic limb peak knee flexion moment in the sagittal plane during early stance was significantly increased for the MPK joint compared to the NMPK joint. This increase in peak knee flexion moment for the MPK joint may allow for controlled stance phase knee flexion to occur. However, both prosthetic knee flexion moments were significantly decreased compared to the sound limb.

Research by Berry et al. utilized a before-and-after study through a self-reported assessment of 50 questions with 368 unilateral transfemoral amputees ranging from 15 to 85 years of age [33]. The pre-survey was conducted when subjects entered the study while they were wearing their personal NMPK joint. The post-survey was conducted after six to nine months of using a MPK joint. The questions were grouped into six subsets: socket fit, confidence and security during ambulation, gait and maneuverability with the prosthesis, physical attributes of the prosthesis, physical effects of the prosthesis, and safety and negative attributes of the prosthesis. For all six categories, the post-survey mean scores were statistically significantly higher than the pre-survey mean scores. These results show unilateral transfemoral

amputees perceived the MPK joint to offer functional improvements over the NMPK joint. Particular attributes associated with this improvement were increased comfort, decreased pain or fatigue, stance phase stability, ability to alter gait speed, greater agility, confidence in walking down stairs and ramps with a step-over-step method, and ability to negotiate uneven surfaces.

A study by Bellmann and colleagues made comparisons on the functionality of four different MPK joints while walking, descending stairs and a ramp, and undergoing a stumbling perturbation during swing phase of the prosthetic limb [38]. Nine subjects who normally wore a MPK joint participated in the study and subject age ranged from 24 to 46 years. All knee joints were able to increase the peak knee flexion angle as gait speed increased. At the slowest walking speed (approximately 1.1 m/s) the knee flexion angles ranged from approximately 56 – 65 degrees. At fast walking speeds (between 1.53 m/s and 1.66 m/s) the knee flexion angles increased to approximately 62 – 75 degrees. During stair descent all but one MPK joint were found to be slightly flexed prior to stair contact. While using some MPK joints during stair descent, there were significant differences in the maximum vertical ground reaction force between the prosthetic and sound limb, but the differences seen during ramp descent were not significant. The stumbling condition found only one MPK joint was able to prevent a fall if the swing phase of the prosthetic limb was interrupted between 10 – 35 degrees of knee flexion.

Another crossover-designed study, conducted by Kaufman and colleagues, tested the gait of 15 unilateral transfemoral amputees ranging in age from 26 to 57, whose personal prosthesis was the NMPK joint [40]. After data collection with this knee joint, all subjects were switched to a MPK joint and given an acclimation period as needed (range 10 – 39 weeks). The study found improvements in gait with the MPK joint. When subjects walked with the NMPK joint, the ground reaction force was maintained anterior to the knee joint center, resulting in knee

hyperextension and locking of the knee in extension to maintain stability during stance. From this ground reaction force pattern, an internal knee flexion moment was also found while subjects wore the NMPK joint. With the MPK joint, there was a statistically significant change to a more normal knee flexion loading response and an internal knee extension moment. This increase in internal knee extension moment shows that more demand was placed on the prosthesis by the subjects, as MPK joints are capable of providing knee flexion resistance to prevent knee collapse. A second publication by Kaufman et al. for the same set of 15 subjects examined kinematic and kinetic symmetry during gait with two knee joint types [41]. Overall, no significant differences were found for the hip, knee, and ankle joint sagittal plane kinematic symmetry of the prosthetic limb when comparing between the two different types of prosthetic knee joints. Comparing the prosthetic limb to the sound limb did reveal some discrepancies when focusing on the swing and stance phases of gait; however, the hip sagittal plane motion displayed good symmetry for both the stance and swing phases of gait with each knee joint. There was a significant difference in symmetry at the knee joint for the stance and swing phases. This kinematic asymmetry at the knee joint was due to differences in knee position during initial stance, as most subjects displayed symmetry between the prosthetic and sound knee joints during the swing phase. The ankle joint was near symmetric during the stance phase but the swing phase had large kinematic asymmetry. In terms of kinetic joint symmetry, for both types of prosthetic knee joints, all prosthetic limb joints except the knee during stance phase exhibited a symmetrical pattern. The hip moment symmetry was better during stance phase while the knee and ankle moments were more symmetrical during the swing phase. Overall, there was a significant improvement in kinetic symmetry when using the MPK joint.

The long term goal of the research study this thesis is a product of is to effectively identify functional differences and similarities between MPK joints and NMPK joint when used by older adult unilateral transfemoral amputees as they perform various ambulatory tasks. These results will provide evidence to fill the current void in the literature regarding older adult unilateral transfemoral amputee gait. Comparisons between the knee joint types will allow for a better understanding of their overall functionality and help ascertain the impact knee joint type may have on the fall risk within this age group.

1.2.3 Classifying Older Adult Amputees Based on Functional Status

For older adult amputees the additional real-time feedback provided by a microprocessor-controlled prosthetic knee joint may be very beneficial, as an increase in age is associated with a decrease in gait stability and muscle strength, with an increased risk for falls [7, 10, 13]. The type of prosthetic knee joint an individual will be fitted with is determined by a clinical assessment conducted by a physician or prosthetist during the initial consultation for the prosthetic limb post-surgery. Difficulties may arise when determining the appropriate prosthesis to fit an individual with because generally re-assessment does not occur after this initial evaluation. A number of factors influence what type of prosthesis will be chosen: age, weight, cause of amputation, physical ability, overall health, medical history, functional goals, personal motivation, and medical coverage [30].

The U.S. Department of Health and Human Services' Centers for Medicare and Medicaid Services adopted a coding system in 1995 that is also used by the U.S. Health Care Financing Administration to describe individuals with lower limb amputation [30]. This classification system is known as the Medicare Functional Classification Level (MFCL) system. This system

describes a patient’s functional status so appropriate prosthetic components are chosen that will be covered by Medicare and Medicaid services. An overview of the MFCL system and the K-levels used to describe patient functional status is provided in Table 1. Based on Medicare and Medicaid coverage, prosthetic devices available to those at a higher K-level may not be available to those at a lower K-level. This limitation is especially significant for older adults because they may not be able to receive a MPK joint at the time of their initial fitting due to a lower activity level and associated K-level. After rehabilitation, older adults may be limited in the recovery they can achieve due to their prosthesis, and it may be difficult to convince third-party payers to cover a more expensive knee.

Table 1. Coding system modifiers and Medicare Functional Classification Level descriptions used by the U.S. Health Care Financing Administration [30].

<i>Modifier</i>	<i>Description</i>
K0	Does not have the ability or potential to ambulate or transfer safely with or without assistance, and a prosthesis does not enhance quality of life or mobility.
K1	Has the ability or potential to use a prosthesis for transfers or ambulation on level surfaces at fixed cadence. Typical of the limited and unlimited household ambulator.
K2	Has the ability or potential for ambulation with the ability to transverse low-level environmental barriers such as curbs, stairs, or uneven surfaces. Typical of the limited community ambulator.
K3	Has the ability or potential for ambulation with variable cadence. Typical of the community ambulator who has the ability to transverse most environmental barriers and may have vocational, therapeutic, or exercise activity that demands prosthetic utilization beyond simple locomotion.
K4	Has the ability or potential for prosthetic ambulation that exceeds the basic ambulation skills, exhibiting high impact, stress, or energy levels, typical of the prosthetic demands of the child, active adult, or athlete.

An evaluation known as the Amputee Mobility Predictor (AMP) assessment has been shown to be a reliable and valid measure for differentiating among MFCL categories in lower limb amputees [42]. The AMP assessment is able to measure an amputee's functional capabilities with or without a prosthesis, thus providing the ability to predict a patient's ability to ambulate before receiving a prosthesis. The AMP assessment also assists in assigning a MFCL K-level for Medicare and Medicaid patients. To conduct the AMP assessment, patients are asked to complete a short series of tasks focusing on the following: sitting and standing balance, transfers, gait, and traversing low-level environmental barriers (see Appendix A for a full description of the AMP tasks).

Based on a patient's ability to complete each task, and taking into consideration the use of any assistive devices, a total score is assigned at the end of the AMP assessment [42]. The tasks are organized with an increasing level of difficulty, so if a patient is unable to complete independent sitting and sitting-reach tasks, then the possibility of prosthesis use is very limited and a MFCL level of K0 would be assigned. A K1 level patient would be able to complete the aforementioned tasks as well as simple transfers and standing tasks. A K2 level patient is able to complete more challenging tasks associated with balance, such as single-limb balance, eyes-closed balance, and the ability to control postural movement when perturbed. For a K3 level patient the ability to vary cadence, step over an obstacle, and negotiate stairs is present to some degree. A K4 level patient requires no additional skills or prosthetic devices than a K3 level patient, however, in theory this is the maximum level an amputee can achieve and is marked by the ability to perform all tasks on the AMP assessment with greater ease.

Reliability testing of the AMP assessment has found excellent reliability for assessments conducted with or without a prosthesis [42]. Intra-rater reliability was tested using a test-retest

method at an average of 2.86 weeks apart. Correlation coefficients for the raters were 0.96 and 0.98 when testing patients with a prosthesis, and 0.97 and 0.86 when testing patients prior to prosthesis use. Inter-rater reliability had a correlation of 0.99 for both AMP assessments. Validity testing of the AMP assessment with and without a prosthesis showed a strong positive correlation between AMP scores and scores for the Amputee Activity Survey, which is a self-reported measure of function. A strong correlation was also seen between the AMP scores and the 6-Minute Walk test, which is a physical performance measure for identifying ambulation ability.

Activity levels for lower limb amputees following prosthetic fitting have also been evaluated using a StepWatch Activity Monitor (SAM). The SAM is a light-weight device attached to the prosthetic limb around ankle height, and it is used to evaluate activity outside of a laboratory setting over a long period of time, such as a few weeks or a few months [43]. Motion is detected using an internal accelerometer that has an accuracy exceeding 99% for normal walking [44]. The SAM is also able to record the number of steps taken at different cadences. Previous research has found lower limb amputees are unable to accurately self-report their activity level in comparison to the SAM measured results [43]. Of 77 unilateral lower limb amputees who documented their activity level in 15-minute intervals over a one-week period, only 34% of subjects were able to accurately report their activity between the hours of 9 am and 9 pm. Overall, agreement between the SAM and the self-reported activity was greater during a 24-hour period than it was during the 9 am to 9 pm period.

1.3 THE BIOMECHANICS OF GAIT AND STAIR AMBULATION

This section begins with a comprehensive comparison between the gait cycle of able-bodied individuals and those with a transfemoral amputation. The gait of transfemoral amputees differs from normal gait because of adaptive strategies employed to compensate for a loss of sensory motor function in the knee, ankle and foot [45]. The hip musculature is not directly connected to the prosthetic knee joint, so forces must be transferred to the prosthesis by the residual limb in order to create movement. The geometry and volume of hip musculature within the residual limb is different for all individuals as a result of the amputation level and the amount of atrophy within the intact hip flexors and abductors on the prosthetic limb side. All of these factors result in an absence of natural muscle control for stabilization of the prosthetic knee and ankle joints, leaving only the pelvic and hip musculature as a source of support.

1.3.1 Normal Gait

The gait cycle for an able-bodied individual consists of the stance and swing phases, constituting 60% and 40% of the gait cycle, respectively [33]. Figure 2 provides a visual of the gait cycle for the right leg and details for associated events within the gait cycle. Stance phase begins at the instant the heel contacts the ground, continues as body weight is rotated over a flat-foot, and ends when the body propels forward enough for the toe to come off the ground [46]. At heel-strike, forward momentum of the body and rotational forces acting on the knee and foot naturally force the knee into flexion [35]. Normal knee flexion is 5-7 degrees, but can reach up to 20 degrees of flexion in order to provide shock absorption and a smooth transition from the swing phase to the stance phase. The flexion moment at the knee is countered by contraction of the quadriceps to

prevent the knee joint from collapsing. Double-limb support occurs while both feet are in contact with the ground and the body's center of mass moves to its lowest point during the gait cycle [46].

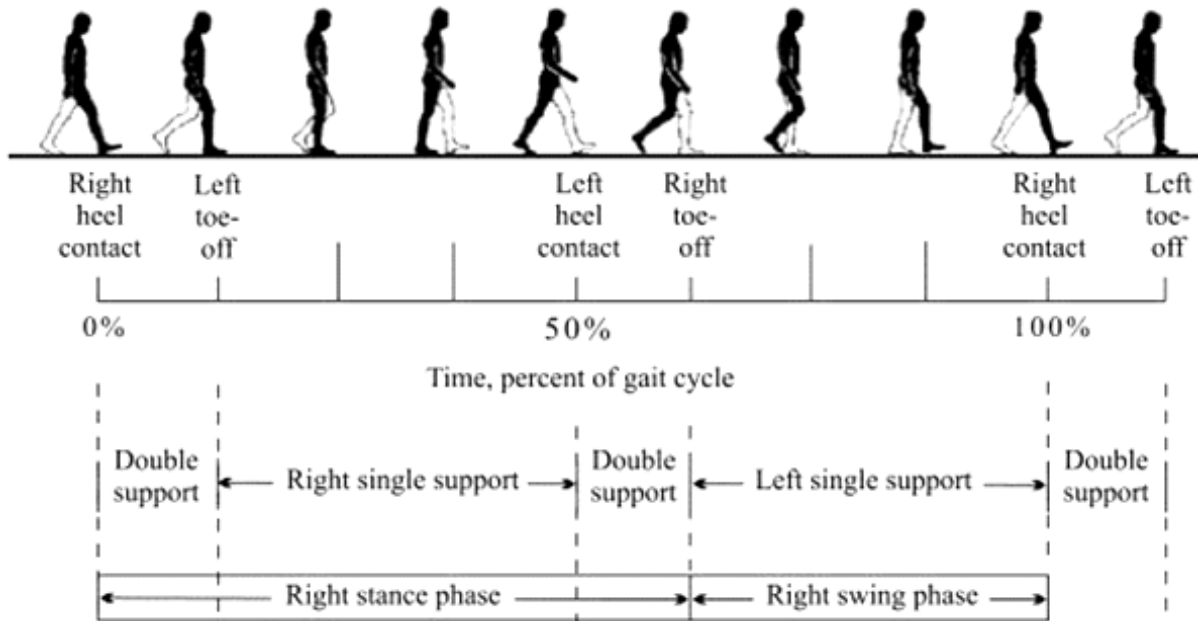


Figure 2. Example gait cycle for the right limb, with phases and temporal variables labeled [47].

Continuing forward, the center of mass is elevated to its highest point during single-limb support as the hip and knee extend in midstance. Knee extension continues to occur while the trunk moves over the supporting limb by contraction of the quadriceps. The rate of progression of the center of mass is controlled through eccentric contraction of the ankle plantar flexors, shifting to concentric contraction during late single-limb support as the trunk is accelerated forward. Once the swing limb has made contact with the ground a second period of double-limb support occurs, as the hip flexors of the prior stance limb contract to lift the limb off of the ground and accelerate it forward. The ankle plantar flexors contribute to the forward

acceleration of the limb as well by providing push-off. Immediately prior to the toe leaving the ground (referred to as toe-off), the hip and knee begin to flex as the knee extensors eccentrically contract to control the rate and extent of knee flexion.

During the swing phase, the limb is initially accelerated forward by concentric contraction of the hip flexors and the effect of gravity [46]. Eccentric contraction of the quadriceps continues during the first half of the swing phase to control the rate and extent of knee flexion. The degree of knee flexion at toe-off and the resulting heel rise are directly related to gait speed [35]. The normal maximum knee flexion reached during swing is approximately 60 degrees. During the later portion of the swing phase, the limb is decelerated and positioned to accept weight for transfer to stance phase. Extension of the knee occurs through concentric contraction of the hip extensors, and eccentric contraction of the hamstring muscles decelerates the foot and shank until the knee is in its extended position [46]. The quadriceps maintain contraction to prevent rapid knee flexion upon heel-strike [35]. Continued forward movement of the trunk is facilitated by the transfer of energy from the swing limb to the trunk, providing an impulse for forward acceleration [46]. The gait cycle repeats once the swing limb has contacted the ground.

1.3.2 Unilateral Transfemoral Amputee Gait

The loss of sensory motor function at the knee, ankle, and foot results in overall decreased stance phase stability [46]. Some degree of knee stability can be achieved through prosthetic alignment and the type of prosthetic knee joint used, however alteration of the gait cycle biomechanics will still occur. During stance phase on the prosthetic limb, transfemoral amputees typically do not allow knee flexion to occur during the first 30-40 percent of stance phase. To prepare the knee

for weight acceptance at heel-strike, the individual secures the knee by contracting the hip extensors to pull back and extend the residual limb within the socket, thereby forcing the prosthetic knee into extension [35]. This helps to ensure the knee joint remains extended in order to reduce the opportunity for knee buckling to occur while the prosthetic limb is the supporting limb, and also eliminates the stance flexion motion that is present within the sound knee joint to provide shock absorption at initial contact. However, some MPK joints are able to adjust the knee flexion resistance at the instant of heel-strike to provide 5-7 degrees of controlled knee stance flexion, before ramping up the resistance to prevent the knee from collapsing.

As the prosthetic limb enters the swing phase, it must generate the same amount of power as the sound limb in order to accelerate the prosthetic limb forward at an equal pace [46]. The lack of ankle plantar flexors to assist with this motion at toe-off places greater demand on the hip flexors to create enough power to produce limb progression. To assist with this, the sound limb increases energy generation from the hip extensors and ankle plantar flexors to compensate for the reduced push-off of the prosthetic limb as it transitions from stance to swing phase. Once the prosthetic limb is in swing phase there are few muscular differences from that of normal gait. Fluid flow control of knee flexion during swing allows for similar reproduction of the quadriceps function during early swing phase and the hamstrings during late swing phase. Common adaptations seen in transfemoral amputee gait are vaulting or hip hiking, in order to compensate for the inability to reduce the length of the advancing prosthetic limb and obtain appropriate foot clearance during swing. At the end of swing phase, the lack of muscle input at the knee is replaced by the microprocessor for individuals using a MPK joint, while individuals using a NMPK joint must actively prepare for heel-strike by ensuring the knee reaches full extension.

Common spatial and temporal parameters used to assess gait have been investigated for unilateral transfemoral amputees. Gait speed is used to identify how fast an individual walks, while cadence is used to describe how many steps per minute the individual achieves during gait. Stride duration is the time it takes to complete one gait cycle [48]. Stride length is the anterior-posterior distance between two consecutive heel-strikes of the same foot, and stride width is the medial-lateral distance between two consecutive heel-strikes of opposing feet. Research by Jaegers et al. has identified differences between the spatial-temporal gait parameters for normal gait and unilateral transfemoral amputee gait for male adults ranging in age from 20 to 56 years (Table 2) [45]. This research also provided comparisons between the prosthetic and sound limb regarding the percentage of the gait cycle devoted to stance phase, swing phase, and double-limb support (Table 3).

Table 2. Comparison of mean spatial-temporal gait parameters for normal gait and unilateral transfemoral amputee gait in adults (age range 20-56 years) [45].

Gait Parameter	Normal Gait	Unilateral Transfemoral Amputee Gait
Gait speed (m/s)	0.95	1.01
Cadence (steps/min)	90.0	89.4
Stride duration (s)	1.34	1.36
Stride length (m)	1.28	1.33
Stride width (cm)	18.0	24.7

Table 3. Comparison of the mean (standard deviation) values between the sound and prosthetic limb for the phases of gait in unilateral transfemoral amputees (age range 20-56 years) [45].

Gait Parameter	Sound Limb	Prosthetic Limb
Stance phase (%)	63.4 (3.14)	58.4 (2.38)
Swing phase (%)	36.9 (3.15)	41.6 (2.38)
Double-limb support (%)	11.5 (3.14)	10.3 (2.53)

Knee kinematics has also been examined for normal gait in comparison to unilateral transfemoral amputee gait during the swing and stance phases, as well as between the sound and prosthetic limb. Research by James and colleague examined the maximal knee flexion for 10 unilateral transfemoral amputees ranging in age from 27-62 years, and made comparisons to previous results for 30 able-bodied adults of similar age reported by Murray et al. (Table 4) [49].

Table 4. Comparison of mean (standard deviation) maximal knee flexion values between middle-aged able-bodied and unilateral transfemoral amputee adults [49].

Maximal Knee Flexion (deg)			
Phase	Able-Bodied	Sound Limb	Prosthetic Limb
Stance phase	20	22 (6)	N/A
Swing phase	71	64 (6)	56 (13)

1.3.3 Stair Ascent and Descent in Able-Bodied Individuals

Stair ascent is divided into two phases just like gait: stance and swing. For able-bodied adults, the average stance phase lasts for 65% of the stair ascent cycle, with 31% of this time in single-limb support and 34% in double-limb support [50]. The stance phase begins when the foot contacts the step. The first portion of the stance phase is known as weight acceptance, generally consuming the first 17% of the stance phase. During this time, load on the stance limb increases until the contralateral limb is no longer in contact with the floor. Some vertical thrust motion is present during the weight acceptance period in order to “pull-up” the body center of mass, but the majority of the vertical thrust period occurs once single-limb support has been achieved. During vertical thrust, lasting from 17-37% of the stance phase, the body’s center of mass is displaced vertically, with maximum displacement occurring at midstance. Next, a period of

forward continuance occurs within the single-limb stance phase. During this time no further vertical displacement of the center of mass occurs. Instead, the weight begins to transfer back to the contralateral limb as foot contact is made on the step and the double-limb support is re-established.

Following toe-off near 65% of the stair ascent cycle, the swing phase begins. This phase consists of foot clearance as the swing limb foot clears the edge of the next step, followed by foot placement onto the next step. Throughout stair ascent the body's center of mass is displaced anteriorly.

During stair descent, the stance phase on average consumes 68% of the total cycle duration, with 39% devoted to single-limb support and 29% double-limb support [50]. During the stance phase, weight acceptance occurs as the contralateral limb moves out of double-limb support and into swing. The single-limb support period begins with forward continuance, during which time the center of mass is progressed forward but does not undergo any vertical displacement. Next, during a period of controlled lowering, the body center of mass is lowered until transition to the swing phase occurs at approximately 68% of the stair descent cycle. The first half of the swing phase is focused on pulling the leg through and over the edge of the step. The remainder of the swing phase is associated with foot placement on the next step.

Kinetic analysis of stair ascent and descent has found the maximum external knee flexion moment during stair ascent to be 3 times greater than that for level surface walking, and the maximum hip flexion moment during stair descent is 1.5 times greater [51]. Further analysis found an average knee flexion of 93.9 degrees during stair ascent and 90.5 degrees of knee flexion during stair descent. Stair ascent has been shown to last longer than stair descent, with mean velocities of 0.49 m/s and 0.56 m/s, respectively, in healthy adults.

Comparison of the stair ascent and stair descent cycles reveals that stair ascent requires greater stability based on longer double-limb support durations and shorter single-limb stance durations [50]. However, previous research has found that falls during stair descent occur three times more often than during stair ascent [52]. Additionally, 55% of falls during stair descent were due to misjudging foot placement on the lower step. For healthy young adults, the resultant distance between the inferior position of the heel and the step edge was on average 45.88 mm. Research by Hamel et al. with 10 older adults undergoing stair descent found that 7% of all clearance values over the step edge were below 5 mm [53]. Furthermore, a trend during stair descent occurred: as subjects progressed over a set of five steps, the minimum clearance between the foot and the step edge decreased. The mean overall difference in clearance between the first step and last step was a decrease of 5 mm.

As age increases, the risk of falling during stair descent also increases. Age-related changes such as loss of muscle strength, decreased visual performance and osteoarthritis may contribute to the increased fall risk, as well as environmental factors such as lighting and step rise and tread dimensions [53]. In terms of spatial-temporal gait parameters during stair descent, research by Mian et al. compared young and old adults during descent (Table 5) [54].

Table 5. Comparison of mean (standard deviation) spatial-temporal gait parameters during stair descent for young and old adults [54].

Parameter	Young Adults	Older Adults
Stride Time (s)	0.96 (0.12)	1.10 (0.16)
Single-Limb Support Time (s)	0.72 (0.08)	0.84 (0.12)
Step Width (cm)	20.7 (3.1)	19.9 (3.0)

1.3.4 Stair Ascent and Descent in Unilateral Transfemoral Amputees

Unilateral transfemoral amputees prefer to use a step-to-step method during stair ascent [55]. With this method, the prosthetic limb is “pulled-up” the step after the sound limb has become the supporting limb on the higher step. From the instant of sound limb contact with the step, the prosthetic limb remains in full extension until prosthetic limb toe-off and progression to the next step. During the swing phase of the prosthetic limb, the sound limb ankle and knee joints have been found to rapidly flex and extend in order to provide power for movement of the prosthetic limb. Strong plantar flexion in the sound limb ankle joint is commonly seen at the end of stance phase for assisting in weight transfer onto the prosthetic limb.

During stair descent a transfemoral amputee must initiate a controlled fall. To complete this, while the sound limb is being advanced, the prosthetic knee quickly flexes such that the sound limb must stop downward momentum when contact with the lower step is made [35]. With a MPK joint, the individual initiates descent by placing the prosthetic toe over the edge of the step. The microprocessor sensors identify the lack of resistance at the toe and determines the maximum knee resistance needed to enable descent in a safe, controlled manner. With a NMPK joint it is difficult achieve knee flexion during stair descent. The knee must remain in extension to provide stance support, which requires more muscle strength and control of momentum from the individual. Consequently, negotiating stairs can be difficult task and is a likely situation for falls to occur.

Previous research studies have used clinical assessments and self-reported measures to determine the occurrence of falls during stair ambulation in unilateral transfemoral amputees [36-37, 56]. However, these studies rate the quality of stair ambulation to provide a numerical score for assessing stair performance or use a questionnaire-based approach for assessing the risk

of falling. Therefore, a current void in the literature exists in evaluating stair ascent and descent using biomechanics-based analysis to understand the risk of tripping among older adult unilateral transfemoral amputees.

1.3.5 Responses to Stumbling in Older Adults

In order to recover from a trip, an individual must be able to quickly apply an appropriate recovery response, control forward momentum of the trunk, and execute a recovery step that will be sufficient for obtaining a new base of support [57]. The unperturbed limb is the initial support limb, and it provides support in slowing the body's momentum down which is crucial for successful recovery from a trip. Three common strategies employed during recovery from a stumble are: lowering, elevating, and reaching. The lowering strategy involves immediately lowering the obstructed foot to the ground so it will become the support limb while the contralateral limb clears the obstacle. The elevating strategy consists of the obstructed foot continuing over the obstacle to complete the original step. Support from the stance limb is important for successful execution of the elevating strategy. Since the obstructed limb flexes at the ankle, knee and hip joints, the contralateral ankle must assist in providing appropriate body height for vertical clearance over the obstacle. The reaching strategy is similar to the elevating strategy expect flexion of obstructed limb is limited primarily to the hip joint. Overall, the lowering strategy has been found to be best suited for recovering from trips that occur during late swing, and it is the strategy preferred by older adults [58].

Faster response time has also been shown to be more important than slower gait speed for successful recovery from a stumble in older adults [58]. Research by Grabiner and colleagues examined the trunk flexion responses to tripping in both young and old adults [59]. Following

an unannounced tripping perturbation, young adults had on average a 27 ± 9 degree post-trip trunk flexion angle in the sagittal plane at recovery foot contact. The peak trunk flexion velocity was approximately 140 deg/s and occurred less than 300 ms after the trip was induced. The results for older adults showed increased trunk flexion. Older adults who fell following the induced trip had a trunk flexion angle averaging 42% larger than the older adults who were able to recover, which corresponded to a flexion angle approximately twice as large as the young adult flexion angle. Relating these trunk flexion responses to gait speed prior to the trip, young adults had a gait speed of $1.46 \text{ m/s} \pm 0.24 \text{ m/s}$ while the gait speed of older adults who fell was $1.39 \text{ m/s} \pm 0.31 \text{ m/s}$. Older adults who were able to recover following the induced trip had a reduced gait speed in comparison to the other two groups, averaging $1.13 \text{ m/s} \pm 0.19 \text{ m/s}$. Thus, while reduced gait speed can aid in successful recovery from a stumble in older adults, appropriately responding to time to sudden changes in trunk angle is very important.

1.3.6 Responses to Stumbling in Unilateral Transfemoral Amputees

Reduced gait speed promotes decreased knee flexion among transfemoral amputees and can be used as an adaptive strategy to minimize adverse effects should a stumble occur while traversing an obstacle [60]. Crossing an obstacle with the sound limb first is another adaptive strategy seen among transfemoral amputees because the sound limb is able to provide more knee flexion and can provide more support for balance recovery should a stumble occur while the center of mass is moving away from the stance foot. Since the sound limb has improved proprioception and ability to maneuver obstacles compared to the prosthetic limb, this strategy provides a better opportunity for recovery from a stumble.

Research by Crenshaw et al. found that when obstruction of the prosthetic limb occurs during swing, transfemoral amputees tend to use a lowering strategy for recovery of balance [61]. For transfemoral amputees there is still a risk of falling when using the lowering strategy to recover if knee flexion in the prosthesis occurs after it becomes the supporting limb. Especially for NMPK joints, the knee must be kept in full extension or have stance resistance activated if sufficient support to recover from the stumble is to occur [62]. Microprocessor-controlled prosthetic knee joints have been shown to provide some improved recovery during a stumble, depending on the specific knee joint's stance resistance activation process. For example, if stance resistance is reactivated when the knee stops flexing at the end of initial swing, then contact with the obstacle during midswing or terminal swing may result in recovered balance.

Research investigating the recovery response following a stumbling perturbation in unilateral transfemoral amputees is currently very limited. Previous studies have focused on whether or not a prosthetic knee joint can help reduce the chance of falling following a stumble or trip. However, there is no biomechanics-based research evaluating trunk kinematics in this subject population so comparisons cannot be made to able-bodied adults in order to understand how transfemoral amputation impacts the recovery response following a stumble or trip.

1.4 INERTIAL PROPERTIES OF THE PROSTHETIC LIMB

Knee collapse, also known as knee buckling, refers to the prosthetic knee flexing when the individual is not anticipating or attempting to flex the knee joint. This event is a serious concern for many unilateral transfemoral amputees as it can lead to an uncontrollable fall. In order to determine from a biomechanics viewpoint when a prosthetic knee may buckle, the lower limb

joint moments need to be analyzed to determine when a flexion moment about the knee joint is likely to occur during an individual's gait cycle. To determine the lower limb joint moments the inertial properties of mass, center of mass location, and mass moment of inertial for each segment of the lower limb (thigh, shank, and foot) need to be known. For able-bodied individuals, previous research using regression equations has shown the inertial properties of all human body segments can be predicted based on an individual's total body mass and the specific segment length, for both males and females [63-65]. The segment mass is based on a percentage of the total body mass, and the center of mass location and the moment of inertial are based on segment length. Geometric modeling has also been used for determining body segment inertial properties in able-bodied individuals [66-68].

For the lower limb unilateral amputee population, the inertial property information for males and females is not readily available as it is for able-bodied individuals. Transfemoral amputees have an altered total body mass due to the amputation; therefore, the published percentages for determining the mass, center of mass, and moment of inertia for able-bodied individuals cannot be utilized. As research involving lower limb amputees has increased over the past decade, some studies have addressed how to determine inertial properties for both the prosthetic and sound limb segments [69-75]. The prosthetic limb is disassembled into three segments: socket, prosthetic knee and pylon, and prosthetic foot. All of these studies have found the mass for each segment by weighing it on a scale. The center of mass location has been found by using a straight edge or reaction board. Moments of inertia have been calculated from measured periods of oscillation determined using a pendulum technique. The following moment of inertia (MOI) equation is used, where T is the period of oscillation, m is the segment mass, g is gravitational acceleration, and d is the distance from the axis of rotation to center of mass [75].

$$MOI = \frac{T^2 mgd}{2\pi^2}$$

Residual limb inertial properties have been found using various techniques. Work by Gitter and colleagues modeled the residual limb as a cylinder with uniform mass, from which the moment of inertia was determined [70]. A study by Mattes et al. modeled the residual limb as a frustum of a right circular cone and calculated the volume using a uniform tissue density of 1.10 g/cm³ [73]. The COM location of the residual limb was assumed to be coincident with the center of the frustum. Research by Selles et al. [74] used a geometric modeling approach with a series of stadium solids (Figure 3), based on the prior work of Kingma and Yeadon [66-67].

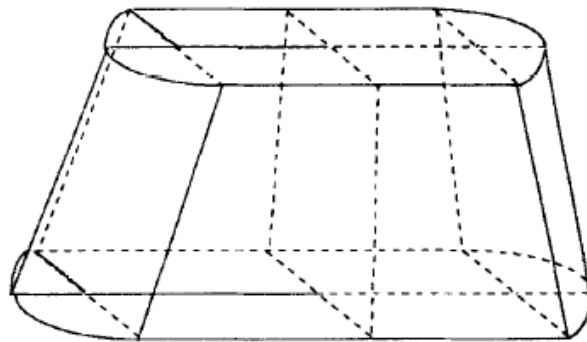


Figure 3. Stadium solid geometry used by Kingma and Yeadon [67].

Work by Fowler and Goldberg modeled the residual limb using a cylinder at the proximal end, followed by a series of frustum and a distal paraboloid (Figure 4) [71, 75]. Circumference measurements were taken along the length, every 5 cm by Fowler and every 3 cm by Goldberg. Residual limb volume was calculated using an assumed density of 1.0 g/mL. Using the residual limb segment mass and volume, the COM location and moment of inertia were calculated.

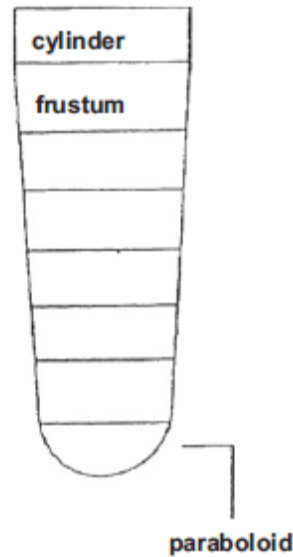


Figure 4. Geometric model of the residual limb used by Fowler and Goldberg. Design consists of a proximal cylinder followed by a series of frustum and a distal paraboloid [75].

Research by Goldberg also determined prosthetic limb inertial properties using the regression equations of Dempster [76], assuming the prosthetic limb anthropometries were the same as the sound limb [75]. Kinematic and kinetic results of this study showed the symmetric anthropometry method was reliable for stance phase analysis but did not accurately assess the prosthetic limb during swing phase.

The sound limb inertial properties were also determined using various techniques. The method used by Gitter and colleagues followed the prior technique reported by Winter that utilized regression equations [77]. The research by Mattes et al. estimated the sound limb segment inertial properties using the anthropometric measures published by de Leva [64]. The total body mass was also adjusted to reflect a symmetrical lower extremity structure since the prosthetic limb mass was less than the sound limb mass, but specific details regarding the technique are not provided in the publication [73]. The study by Selles et al. used the subject

height, mass, and lengths of the thigh, shank and foot segments for calculation of the masses, COM locations, and moments of inertia based on previous work published by Winter [17]. Research by van der Linden and colleagues found the mass and COM location of the sound limb segments by using the data of Drillis and Contini [78]. The moments of inertia for the sound limb segments were calculated using equations from McConville [79]. Work by Fowler et al. determined the sound limb segment inertial properties using the regression equations developed by Dempster [76] based on measured body mass and segment lengths [71]. Research by Goldberg and colleagues also calculated the sound limb segment masses and center of masses from the regression equations derived by Dempster [75]. The moments of inertia were calculated using a reference mass and height (73.44 kg and 1.76 m) multiplied by a ratio of the segment mass times segment height squared to the reference mass times reference height squared. This method was used to make adjustments because the subjects were children and the technique developed by Dempster used young adult subjects.

Only the work of Goldberg has published inertial property results for the segments of the prosthetic limb, in order to compare the direct measurement and symmetric anthropometry techniques that were used. The four subjects analyzed in this work were children with an average age of 13.5 ± 1.5 years [75]. As a result, there is a current gap in the literature regarding inertial properties of the prosthetic limb segments in older adult unilateral transfemoral amputees.

1.5 IMPORTANCE OF UNILATERAL TRANSFEMORAL AMPUTEE GAIT RESEARCH IN OLDER ADULTS

As the provided background information has shown, there is a variety of current literature addressing the gait mechanics of unilateral transfemoral amputees. However, there are still major voids in this literature regarding the gait of older adults and the risk of falls among this population, as no study has focused solely on the relationship between prosthetic knee joint type, gait and aging. The research presented in this thesis intends to provide a foundation for future unilateral transfemoral amputee gait research, with a particular focus placed on older adults.

Among current unilateral transfemoral amputee research, for subjects of any age, there is a lack of evidence for minimum foot clearance while walking over a level surface or while ascending and descending stairs. Minimum foot clearance while walking over a level surface has been reported for unilateral transfemoral amputees but the methodology for analyzing this measure varies between studies. Further, biomechanics-based methods have not been used to identify MFC during stair ambulation. Only clinical assessments have been used to provide qualitative data about stair ascent and descent abilities in unilateral transfemoral amputees.

A lack of evidence also exists for the response to stumbling among unilateral transfemoral amputees. Studies that have investigated stumbling or tripping have looked only at the ability of prosthetic knee joints to provide successful recovery from a fall, and the subjects used in these studies were young adults. The results from these studies cannot be transferred directly to the older adult unilateral transfemoral amputee population due to age differences that are already seen between young and old able-bodied adults. Further, no study has yet to examine the trunk kinematics of unilateral transfemoral amputees during recovery from a stumble or trip.

Despite the number of studies that have reported findings comparing moments in the prosthetic and sound limb joints, there is no standard method for determining the inertial properties of the prosthetic limb or the sound limb. Additionally, these studies have provided limited details about the methodology used and none have reported the resulting inertial properties values for the subjects.

Following a thorough understanding of unilateral transfemoral amputee gait in older adults, and undeniably the large amount of variation occurring within this population, recommendations regarding safe ambulation should be provided to physical therapists and amputee rehabilitation programs. Given this information, individual patient programs should be altered to account for the patient's age, physical ability, prosthetic knee type, use of assistive device, etc. in order to provide an opportunity for reducing the fall risk in older adults who have undergone a unilateral transfemoral amputation.

2.0 SPECIFIC AIMS

The purpose of this thesis is to describe gait analysis methods used to quantitatively and qualitatively assess fall risk in older adults with unilateral transfemoral amputation. Only a few prior studies have reported the fall risk for older adult unilateral transfemoral amputees based on self-reported measures. The first focus of this thesis is the development of gait analysis methods to identify the risk of tripping while walking on a level surface and while ascending and descending stairs. Minimum foot clearance is a common gait measure used to understand the risk of tripping for able-bodied adults, but the methodology used for determining this measure is not suitable for analyzing unilateral transfemoral amputee gait based on preliminary analysis for this thesis and the range of gait styles seen among unilateral transfemoral amputees. In this thesis, specific outcome measures to assess the risk of tripping while walking over a level surface will include minimum foot clearance and gait speed, with supporting evidence regarding gait stability and symmetry from knee angles and spatial-temporal measures. Specific outcome measures to assess the risk of tripping during stair ambulation will include minimum foot clearance, with supporting evidence from foot placement measures. The first specific aim of this thesis is:

Specific Aim 1: To compare the kinematics of the prosthetic foot and sound foot in older adult unilateral transfemoral amputees while walking on a level surface and during stair ambulation.

The second focus of this thesis is the recovery response after experiencing a stumbling perturbation on the prosthetic limb side during the midswing phase of gait. Interruption of the prosthetic foot during swing can lead to collapse of the prosthetic knee joint upon heel-strike of the recovery step if the individual is not able to recover appropriate knee extension by this time. Specific outcome measures to describe the response to stumbling will include maximum trunk flexion angle in the sagittal and frontal planes, maximum trunk angular velocity, the recovery response duration, and the recovery method utilized. The second specific aim of this thesis is:

Specific Aim 2: To describe the response to stumbling while walking on a level surface in older adult unilateral transfemoral amputees.

The third focus of this thesis is to develop a method for determining the inertial properties of the prosthetic limb segments, in order to correctly quantify the joint moments about the ankle, knee, and hip during gait in future analysis. Lower limb moments are important for understanding from a biomechanics viewpoint when a prosthetic knee may collapse, as knee collapse is likely to result in a fall. Previous research to determine inertial properties for able-bodied individuals does not hold true for amputees as their anthropometry has been altered by the amputation. The inertial properties of interest include mass, the center of mass location, and the mass moment of inertia for the thigh, shank, and foot segments of the prosthetic limb. The third specific aim of this thesis is:

Specific Aim 3: To develop a geometric modeling approach for calculation of the inertial properties of the prosthetic limb segments.

3.0 METHODS FOR ASSESSING MINIMUM FOOT CLEARANCE AND STUMBLE RECOVERY IN OLDER ADULTS WITH UNILATERAL TRANSFEMORAL AMPUTATION

3.1 STUDY PARTICIPANTS

3.1.1 Subject Recruitment

The results presented in this thesis are the initial findings of a larger, on-going research study. Four of the six subjects included in this thesis were part of a pilot study to prepare for the full research study. The pilot study recruited subjects between the ages of 50 and 80 years. The full study will recruit 50 unilateral transfemoral amputees between the ages of 65 and 90 years. A sample size of 50 subjects is based on previous laboratory experience with the biomechanical outcome measures that will be derived in this study [80-83].

Subjects are recruited from local clinical practitioners and amputee support groups. Recruitment is carried out to match the demographics of Allegheny County in Pennsylvania, USA. Eligibility for participation in the study is initially assessed via a phone screening questionnaire after a waiver of signed written informed consent is obtained, to determine whether the potential subject is healthy enough to carry out all tasks involved in the study. Inclusion and exclusion criteria for the study are displayed in Table 6.

Table 6. Inclusion and exclusion criteria for participation in the research study.

<i>Inclusion Criteria</i>	<i>Exclusion Criteria</i>
50-90 years old	Chronic skin issues
Unilateral transfemoral amputee using either a MPK or NMPK	Inconsistent limb volume
At least 2 years post-amputation	Secondary health issues precluding completion of the study protocol (i.e. heart, peripheral, or pulmonary issues)
MFCL K2 or K3	MFCL K1

A Medicare Functional Classification Level of K2 or K3 is necessary in order to be considered a subject in the study. Distinguishing characteristics of a MFCL K2 amputee include the ability to transverse low-level environmental barriers, such as curbs, stairs, and uneven terrain, while a MFCL K3 amputee is also able to vary cadence during gait [30].

3.1.2 Subject Overviews

This thesis presents results for the first six subjects who completed a gait biomechanics visit at the laboratory. The mean age of the subjects was 64 years (range 55-73 years) and amputation had been performed an average of 11.2 years prior to the visit (range 3-30 years). Two NMPK joints and four MPK joints were tested in total. Details for each subject are presented in Table 7. Subjects 1 and 4 are the same individual; the first visit was completed while using the NMPK joint and the second visit occurred approximately 1 month later while using the MPK joint. The remainder of this section provides an overview for each subject in order to describe the way they walked over a level surface, ascended and descended stairs, and responded to a stumbling perturbation based on video and motion capture recordings. Specific quantitative results will be presented in the results section.

Table 7. Overview of the subjects presented in the results of this thesis. Subjects 1 and 4 are the same individual but a different prosthetic knee joint was used at each visit. Full study participation refers to those who were involved in the on-going research study.

<i>Subject</i>	<i>Age</i>	<i>Gender</i>	<i>Prosthetic Knee Type</i>	<i>Years Since Amputation</i>	<i>Side of Amputation</i>	<i>Etiology</i>	<i>MFCL</i>	<i>Study Participation</i>
1	55	Male	NMPK	5	Right	Vascular	K3	Pilot
2	56	Male	MPK	3	Right	Vascular	K2	Pilot
3	73	Female	MPK	13	Right	Trauma	K3	Pilot
4	55	Male	MPK	5	Right	Vascular	K2	Pilot
5	71	Male	NMPK	30	Right	Vascular	K2	Full
6	65	Female	MPK	5	Left	Vascular	K2	Full

Subject 1 was a 55-year-old male with a right side amputation who used a nonmicroprocessor-controlled prosthetic knee joint. No assistive device was needed to walk over the level surface. This subject's typical walking pattern on the level flooring surface appeared to produce slight trunk lean toward the prosthetic side during stance on the prosthetic limb. Visually, the prosthetic and sound limb step lengths were approximately equal. The prosthetic limb mechanics during the swing phase showed weight shift over the prosthetic toe during toe-off that led to knee flexion during swing. The prosthetic knee appeared to remain extended during the prosthetic limb stance phase. During stair ascent, this subject used the staircase handrail on the prosthetic limb side and progressed by stepping up with the sound limb first. The prosthetic knee was near full extension during ascent and circumduction was used to move the prosthetic limb up to the same step the sound limb was on. During stair descent the subject did not use the handrail. The prosthetic knee was kept approximately fully extended and was advanced down the step first before the sound limb was moved to the same step. For the stumbling perturbation, this subject's prosthetic foot clearance was higher than the height of the perturbation obstacle that was elevated from concealment under the flooring surface, so a stumbling perturbation was not induced.

Subject 2 was a 56-year-old male with a right side amputation who used a microprocessor-controlled prosthetic knee joint while walking with a cane in each hand. This subject also wore a foot-ankle orthosis on the sound limb side. While walking over a level surface, the stance phase appeared to receive stability from the cane in contact with the floor, which was held in the swing limb side hand. Visually, prosthetic limb step length and foot clearance were greater than the sound limb. The prosthetic limb mechanics were such that prosthetic knee flexion occurred during the prosthetic limb swing phase while the prosthetic knee remained in extension during the stance phase. For stair ascent, the subject used the handrails on both sides of the staircase. The sound limb was advanced up each step first, followed by movement of the prosthetic limb to the same step while keeping the prosthetic knee near full extension. During stair descent, the sound limb was moved to the lower step first with concentration and deliberate movement such that the sound foot was held out past the step edge for a short period of time before weight was shifted over the sound limb and descent occurred. Both handrails were used during stair descent. When the prosthetic limb was advanced down to the same step, flexion of the prosthetic knee was visible. The stumbling perturbation was induced during midswing on the prosthetic limb side. Due to the use of two canes supporting body weight and the subject's slower gait speed, the stumble did not appear to significantly alter the gait cycle. When the prosthetic foot hit the obstacle an elevating strategy was used by the subject to continue walking forward without much deviation of the trunk or loss of balance.

Subject 3 was a 73-year-old female with a right side amputation who used a microprocessor-controlled prosthetic knee joint and walked holding a cane in the sound limb side hand to gain support during prosthetic limb stance. Step length was visually equal between the prosthetic and sound limb sides. Step width appeared asymmetric due to prosthetic limb

placement slightly outside of the base of support. This led to an apparent correction during gait in order to remain walking in a straight line. Prosthetic limb gait mechanics yielded prosthetic knee flexion during swing. The prosthetic limb stance phase showed very slight knee flexion. During stair ascent, the subject continued to use the cane in the sound limb side hand and used the staircase handrail on the prosthetic limb side. The sound limb was advanced up the step first, followed by circumduction of the prosthetic limb to advance the limb up to the same step the sound limb; the prosthetic knee visually remained in extension at all times. During stair descent, the prosthetic limb was advanced downward first by sliding the back of the foot down the step riser while keeping the knee in extension. The sound limb was then moved down to the step the prosthetic limb was on. For the stumbling perturbation, contact with the obstacle occurred during late swing and the force upon contact caused the obstacle to be dislodged from the slot within the walkway. The subject did not notice the obstacle until the dislodged piece slid out in front of the subject such that the following step with the sound foot landed on part of the piece. The subject quickly tried to alter the gait cycle to avoid fully stepping on the piece, which resulted in reduced gait speed and trunk deviation to maintain balance.

Subject 4 was a 55-year-old male with a right side amputation who used a microprocessor-controlled prosthetic knee joint and did not use an assistive device to walk over the level flooring surface. Again, this subject was the same individual as subject 1 but a different prosthetic knee joint was used after an approximate 1 month acclimation period (the subject had used the MPK joint in the past). The level surface walking pattern continued to have a slight increase in trunk lean toward the prosthetic limb side during prosthetic limb stance. Step length appeared approximately equal and prosthetic limb mechanics promoted clear knee flexion during the swing phase. The prosthetic knee appeared to be in extension during prosthetic limb stance.

During stair ascent, the handrail on prosthetic limb side was used and the sound limb was advanced up step first, followed by circumduction of the prosthetic limb up to the same step the sound limb was on. During stair descent, the subject attempted to use a step-over-step method while holding both handrails. The prosthetic limb was advanced down the first step, followed by advancement of the sound limb toward the second step but the foot caught the edge of the step above. A slight pause was seen in the subject's progression as balance was regained following the unexpected interruption in foot movement. Then, the sound limb continued down to the third step and the prosthetic limb was flexed in order to advance over this step to the floor. Last, the sound limb was progressed down to the floor. The stumbling perturbation was induced during early swing phase of the prosthetic limb. When the foot contacted the obstacle, the obstacle moved slightly forward within its slot in the walkway. However, contact with the obstacle still interrupted the gait cycle such that an elevating strategy was used in response to the perturbation. Clearance of the obstructed foot over the obstacle occurred with assistance from the sound limb plantar flexors to elevate body center of mass height, and overall very little trunk deviation resulted.

Subject 5 was a 71-year-old male with a right side amputation who used a nonmicroprocessor-controlled prosthetic knee joint and walked with a cane held in the sound side hand. This subject appeared to have a very stiff prosthetic knee joint, resulting in no visual knee flexion during prosthetic limb swing phase. It is unclear whether the subject preferred to walk straight-legged on the prosthetic side or if the flexion resistance increase was set by the subject's personal prosthetist. The prosthetic limb mechanics led to visible trunk lean toward the sound limb side during prosthetic limb swing phase and the cane was advanced as the prosthetic limb stepped forward. The prosthetic limb step length was visibly larger than the sound limb

side. Toe-off for the prosthetic foot was not very clear as the subject appeared to pick the foot off of the floor and progress it forward instead of a more natural swing motion of the foot. During prosthetic limb stance phase the knee was also kept in full extension. For stair ascent, the subject used the cane in the prosthetic limb side hand and used the staircase handrail on the sound limb side. The sound limb was advanced up the step first, followed by movement of the prosthetic limb up to the same step with circumduction while keeping the prosthetic knee joint in full extension. During stair descent, the prosthetic limb was advanced down the step first and placed such that the heel hit the back edge of the step before weight-shifting onto the prosthetic limb occurred. The prosthetic knee joint was kept in full extension during descent. The sound limb was then advanced to the same step as the prosthetic limb and the motion repeated for the remaining two steps. The stumbling perturbation was induced during midswing of the prosthetic limb. The subject implemented a lowering strategy with the obstructed foot and then stepped over the obstacle with the sound limb. Due to the subject's inability to flex the prosthetic knee, excessive clearance with this limb over the obstacle resulted in a forward-falling motion toward the prosthetic limb side. The subject planted the prosthetic limb and was caught by the harness as trunk deviation reached a maximum position approximately parallel to the floor. After returning to the upright position the subject was able to recover balance and continue walking.

Subject 6 was a 65-year-old female with a left side amputation who used a microprocessor-controlled prosthetic knee joint and walked with a wheeled-walker. This subject's gait pattern over the level surface was very deliberate, with the subject appearing to be focused on gait progression with the prosthetic limb. The prosthetic limb clearly flexed during the swing phase. Visually, there was a small degree of prosthetic knee flexion during the stance phase, but this may have been influenced by the prosthesis alignment. Step length for both limbs

appeared approximately equal, with a clear increase in foot clearance over the flooring surface on the prosthetic side. For stair ascent, the subject used the both staircase handrails. The sound limb was advanced up each step first, followed by the prosthetic limb which appeared to be kept in extension during the entire duration of stair ascent. Additionally, the subject appeared to use a large amount of upper body strength to pull the body upwards during prosthetic limb advancement. The toe tip of the prosthetic foot appeared slide along part of the step riser during ascent as well. For stair decent, the subject advanced the prosthetic limb down to the next step first by internally rotating the limb during decent such that the entire pelvis was at an angle to the progression line toward the sound limb side. Also, the back of the prosthetic foot heel was placed up against the step riser before weight was slowly shifted onto the prosthetic side and sliding the foot down to the next step tread occurred. Slight flexion of the prosthetic knee may have occurred during the transition to the next step but the subject did appear to try to keep the knee in extension. The sound limb was then moved to the same step as the prosthetic limb and this pattern was repeated for the remainder of the steps. During the stumbling perturbation, the subject experienced contact with the obstacle during midswing of the sound limb due to misalignment of the subject within the walkway. Given the subject's use of a wheeled walker for support and a slow gait speed with deliberate stepping, the subject was able to utilize an elevating strategy to clear the obstacle. The walker appeared to help reduce forward and lateral trunk deviation during stumble recovery.

3.2 METHODS

3.2.1 Experimental Protocol

The following protocol is used for the full, on-going research study. A total of four laboratory visits are used to assess a subject's performance using both their personal prosthesis and an opposing knee joint type that will be provided to them by the laboratory staff. Four of the six subjects used for the analysis in this thesis were part of a pilot study which involved a modified laboratory visit 2 protocol.

3.2.1.1 Laboratory Visit 1

Subjects who qualified for inclusion in the study based on a phone screening questionnaire were instructed to visit the laboratory for evaluation of their activity level with their personal prosthesis. When subjects arrived, they provided signed consent to be involved in the study. During this first visit subjects completed the Amputee Mobility Predictor (AMP) assessment, which was designed to measure ambulatory potential of lower limb amputees while using their prosthesis [42]. As part of the evaluation, subjects were asked to complete a short series of tasks involving sitting balance, standing balance, gait, negotiating an obstacle, and ascending and descending stairs (see Appendix A for a full description and scoring of the AMP assessment). A score was given for each task based on ability and/or quality of completing of the task. Following completion of the AMP assessment subjects were assigned a K-level; the classification levels were determined based on the descriptions in Table 8. Only subjects who were assigned a K2 or K3 level could be included in the research study.

Table 8. Criteria for determining K-level after performing the AMP evaluation [42].

K-Level Classification	Key AMP Tasks
K1	Able to maintain balance during simple tasks (i.e. chair to chair transfer) and stand unchallenged. Focus placed on Items 3-7.
K2	Able to perform balance tasks, maintain step continuity, complete 3-step turn without intervention, transverse low-level barriers (curbs, stairs, uneven surfaces). Focus placed on Items 8-13.
K3	Able to ambulate with variable cadence, evaluate quality of gait (i.e. initiation without hesitation, able to organize simple planned movement), able to negotiate specific obstacles and stairs. Focus placed on Items 14-20.

Also during this visit subjects completed a demographics survey and the Prosthesis Evaluation Questionnaire (PEQ). The purpose of the PEQ was to help evaluate prosthesis use and functional ability [84]. At the end of visit 1, subjects were given a falls log to maintain until their next visit. The falls log consisted of a standard month-format calendar on which subjects recorded a description of any loss of balance events (stumbles, falls, slips, etc.) [85]. Additionally, a StepWatch Activity Monitor (Orthocare Innovations, Oklahoma City, OK) was placed on the subject's prosthesis at ankle height in order to collect functional activity data (e.g. number of steps taken throughout the day, cadence, etc.) before the next laboratory visit. The StepWatch Activity Monitor was setup for the subjects in the laboratory, thus no action needed to be taken while wearing it. Upon leaving the lab subjects were asked to continue their normal daily lifestyle for a period of 4 weeks before returning to the laboratory for a second visit. During this 4-week span, a staff member from the laboratory contacted the subject via phone to ensure the activity monitor and falls log were being maintained, and to discuss any loss of balance events that may have occurred as well as address any additional concerns.

3.2.1.2 Laboratory Visit 2

The second visit to the laboratory consisted of a biomechanical analysis as the subject performed various ambulatory tasks and experienced a stumbling perturbation. When subjects arrived to the laboratory, activity data from the StepWatch Activity Monitor was uploaded from the device and the falls log entries were copied. A total of 69 passive reflective spherical markers were placed on the subject based on a custom marker set used in the Human Movement and Balance Laboratory (Figure 5). Each shoe had 6 markers placed on the forefoot for the static trial only; these markers were recreated virtually during post-processing to model the bottom of the shoe sole [86]. The marker set used during the pilot study had a modified foot that only included the superior heel, toe, and toe tip markers for both the static and dynamic trials. The following anthropometric measurements were taken to create subject-specific motion capture models: leg length, knee width, ankle width, shoulder offset, elbow width, wrist width, hand thickness, and inter-anterior superior iliac spine distance.

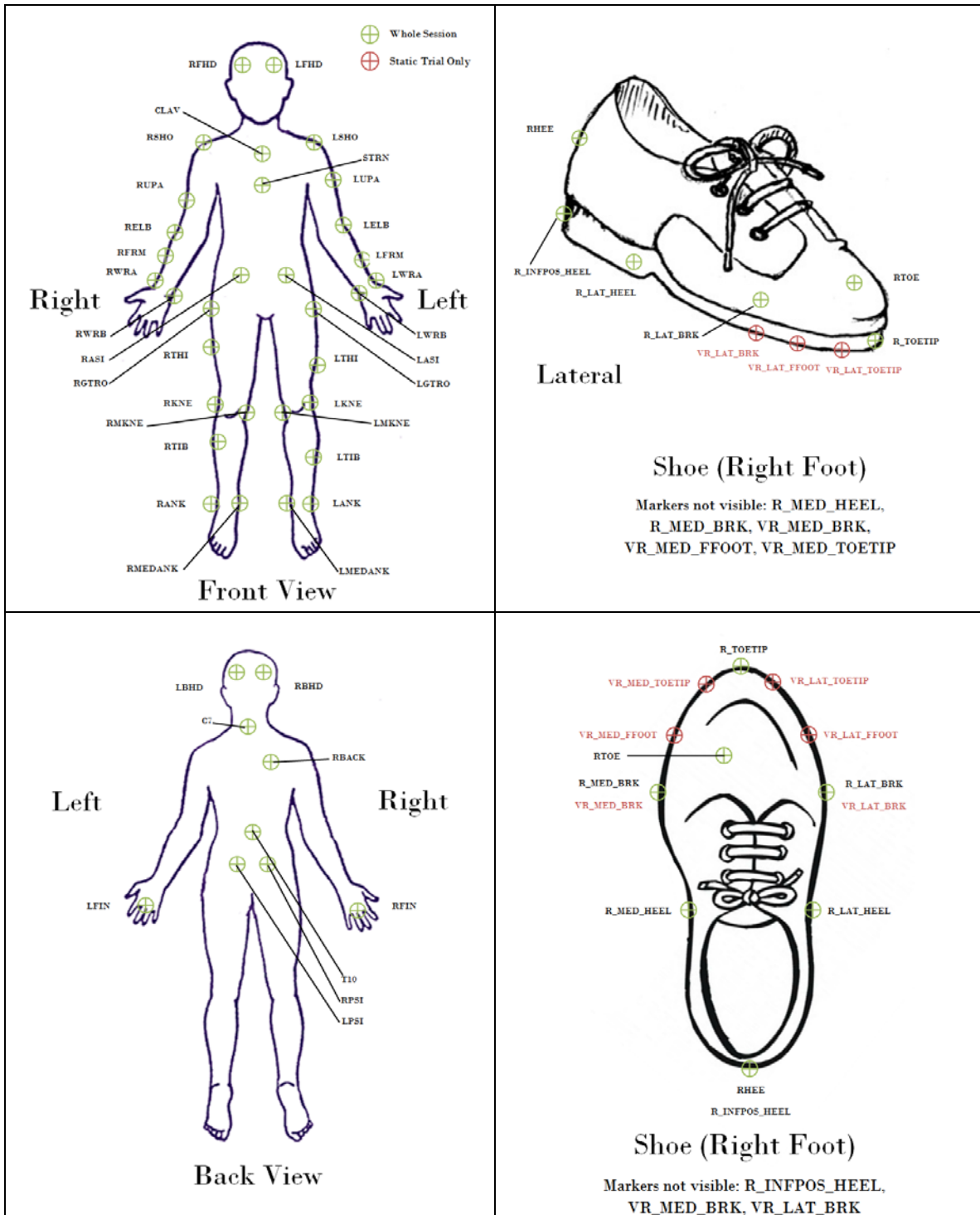


Figure 5. Diagrams of marker placement for the full research study marker set. The pilot study marker set did not include markers on the forefoot of the shoe (the static trial only markers), medial and lateral break markers, medial and lateral heel markers, or inferior heel markers.

During the second laboratory visit subjects were asked to walk at a comfortable pace for six experimental conditions; three trials were collected for each condition except the stumbling perturbation, which was only induced once. The six experimental conditions are summarized in Table 9. Recall, the results of this thesis will only focus on experimental conditions for level surface walking, stair ascent and descent, and the stumbling perturbation. The level surface walking trials provide a baseline measure of the subjects' gait pattern; baseline walking is abbreviated as BW.

Table 9. Experimental conditions for biomechanical analysis during laboratory visits 2 and 4. Pilot study experimental conditions are noted with an asterisk.

<i>Experimental Condition</i>	<i>Flooring Surface / Contaminant</i>	<i>Number of Trials</i>
Level Surface Walking (BW)*	Level surface / Dry floor	3
Up & Down Ramp*	5° incline / Dry floor	3 per direction
Up & Down Uneven Ramp	5° incline with uneven surface / Carpet	3 per direction
Uneven Walking	Uneven surface with Carpet	3
Up & Down Stairs*	Stairs / Dry steps	3 per direction
Stumble*	Level surface / Dry floor	1 perturbation

The first condition was walking over a level, dry floor in order to collect a measure of baseline walking for the subjects while using their personal prostheses. A 14-camera Vicon T40S motion analysis system (Vicon, Oxford, UK) with a sampling rate of 120 Hz was used to record the individual marker movement as the subjects walked across a 5.5 m long walkway in the middle of the laboratory (Figures 6-7). Two Bertec force plates (Bertec, Columbus, OH) were embedded within the walkway to record ground reaction forces at a sampling rate of 1080 Hz. The force plates were positioned one right after the other in the walkway such that the first force plate was contacted with the right foot and the second force plate was contacted with left

foot. At all times subjects were secured in a harness connected to a ceiling mounted track and trolley system (Solo-Step, Sioux Falls, SD) in order to prevent contact with the floor in the event that an irrecoverable loss of balance occurred. Motion capture and force plate data were collected for three level surface walking trials. Subjects were positioned to start walking approximately 1.5 m before the beginning of the walkway in order to obtain normal gait speed before reaching the walkway. Subjects were not specifically instructed to contact the force plates while walking; the laboratory staff attempted to adjust the subject starting position so contact would occur naturally, and a clean force plate hit was recorded if only one foot came in contact with an individual force plate during the trial.

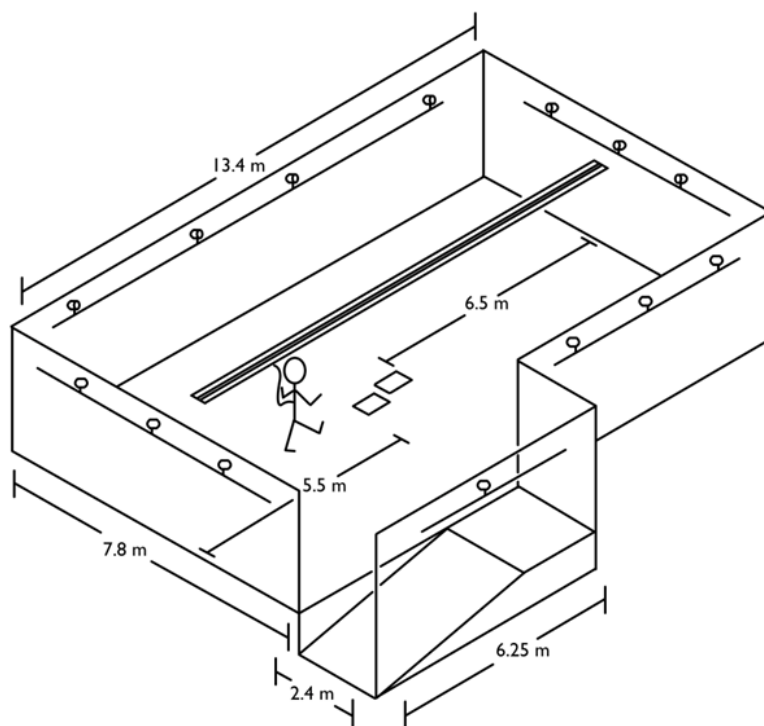


Figure 6. Schematic of the laboratory area, instrumented with 14-Vicon motion capture cameras, 2-Bertec force plates embedded in a level surface walkway, and a Solo-Step ceiling mounted harness system.

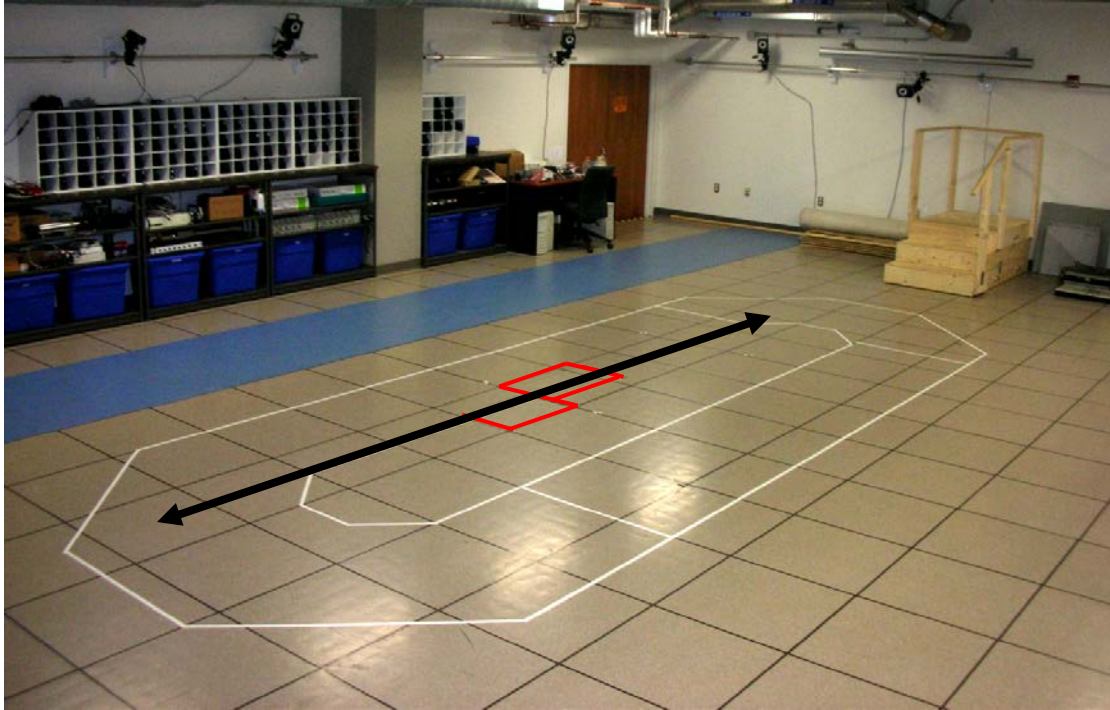


Figure 7. View of the level surface walkway and the two embedded force plates. The black line spans the length of the walkway; the two force plates are outlined.

The ramp used in this study was set at a 5-degree incline, based on previous findings and safety recommendations [87-90]. The inclined portion of the ramp was 306.07 cm long with a width of 91.5 cm (Figure 8). A handrail was provided on one side of the ramp at a height of 92.7 cm above the ramp surface. One Bertec force plate (Bertec, Columbus, OH) was embedded in the ramp, centered at 106.5 cm from the toe of the ramp and 55.5 cm from the handrail side of the ramp. The landing at the top of the ramp was 130 cm long. The ramp's inclined walking area and embedded force plate were covered in the same floor tile as the lab floor in order to keep flooring properties constant between experimental conditions (3.2 mm Imperial Texture Standard Excelon Vinyl Compression Tile; Armstrong, Lancaster, PA).

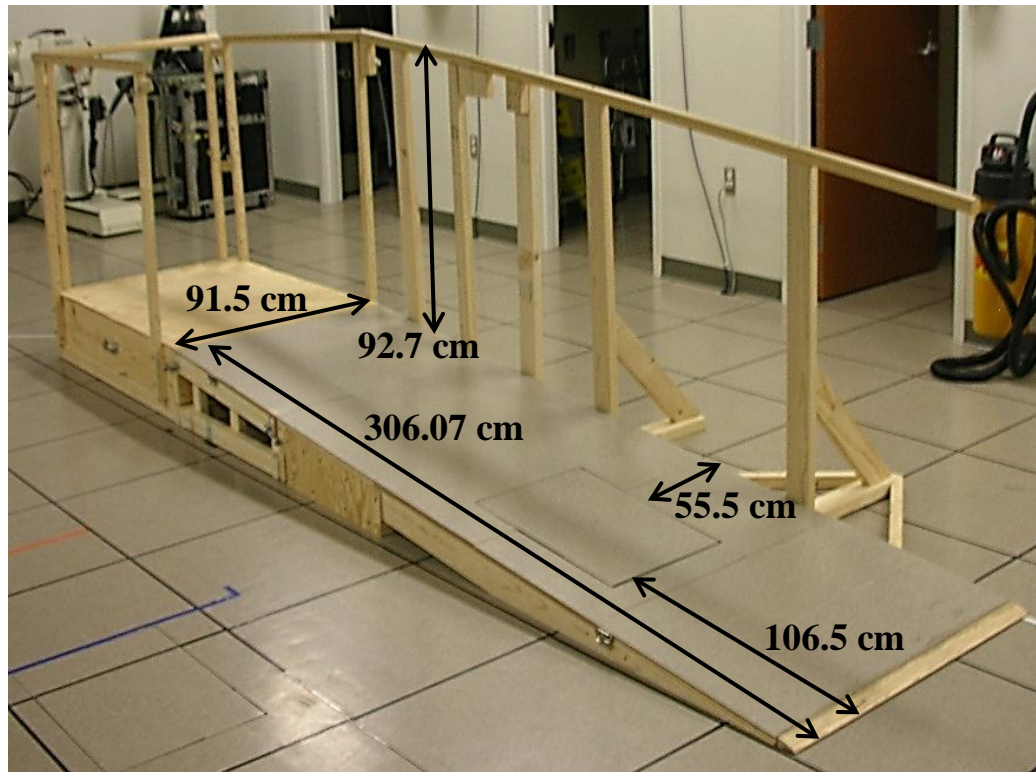


Figure 8. Ramp with a 5-degree incline and embedded Bertec force plate.

To ascend the ramp, subjects stood approximately 1.5 m in front of the ramp on the level floor and then walked up the ramp to the top platform. A clean force plate hit was recorded when one foot contacted the force plate while walking up the ramp. The use of any personal assistive device or the ramp handrail was permitted and the laboratory staff recorded usage. Subjects were secured in the harness at all times during the ramp trials and the lanyard connecting the harness to the ceiling mounted track was adjusted to account for the vertical change surface height prior to ascent. After reaching the top platform, subjects waited to descend until instruction was given to return to the starting position on the level floor. Subjects repeated this ascent and descent procedure while motion capture data and force plate data were collected for three ascent and three descent trials.

The next experimental condition was walking up and down the ramp while it had an uneven surface placed on it. The uneven surface was constructed from triangular wooden prisms with a height of 1.5 cm, width of 3.5 cm, and length ranging from 6-16 cm in 1 cm increments [91-92]. Twenty wooden prisms were distributed randomly over an area of 0.74 meter squared and secured to 1.4 cm thick plywood to match the distribution used in previous research. The entire ramp was covered with one layer of 1.27 cm high 100% nylon pile carpet (Figure 9).



Figure 9. Ramp with a 5-degree incline and an uneven surface.

The next experimental condition involved placing an uneven surface walkway over the level floor. The uneven surface walkway was 304.8 cm long with an irregular surface constructed in the same way as the ramp uneven walkway [91-92]. The entire walkway was covered with one layer of 2.54 cm high 100% nylon pile carpet, 365 cm in length. Figure 10 shows the uneven surface walkway with the triangular wooden prisms underneath the carpet displayed. To pass over the uneven surface walkway, subjects were instructed to stand approximately 1 m in front of the carpet. Motion capture data was collected as they progressed over the uneven surface walkway. Subjects were secured in the harness during all uneven surface walking trials. After passing over the uneven surface walkway, subjects were instructed to return back to the starting position, again starting approximately 1 m in front of the carpet. Subjects completed a total of three trials across the uneven walkway.



Figure 10. Walkway with an uneven surface.

A three-step staircase was used to collect motion capture data while the subjects ascended and descended the steps (Figure 11). The stairs were constructed to comply with the Americans with Disabilities Act Accessibility Guidelines [87]. Each step had a rise of 19 cm, tread of 28 cm, and the staircase had a width of 91.5 cm. Handrails were provided on both sides of the staircase at a height of 92 cm above each step. The top landing area was 130 cm long.

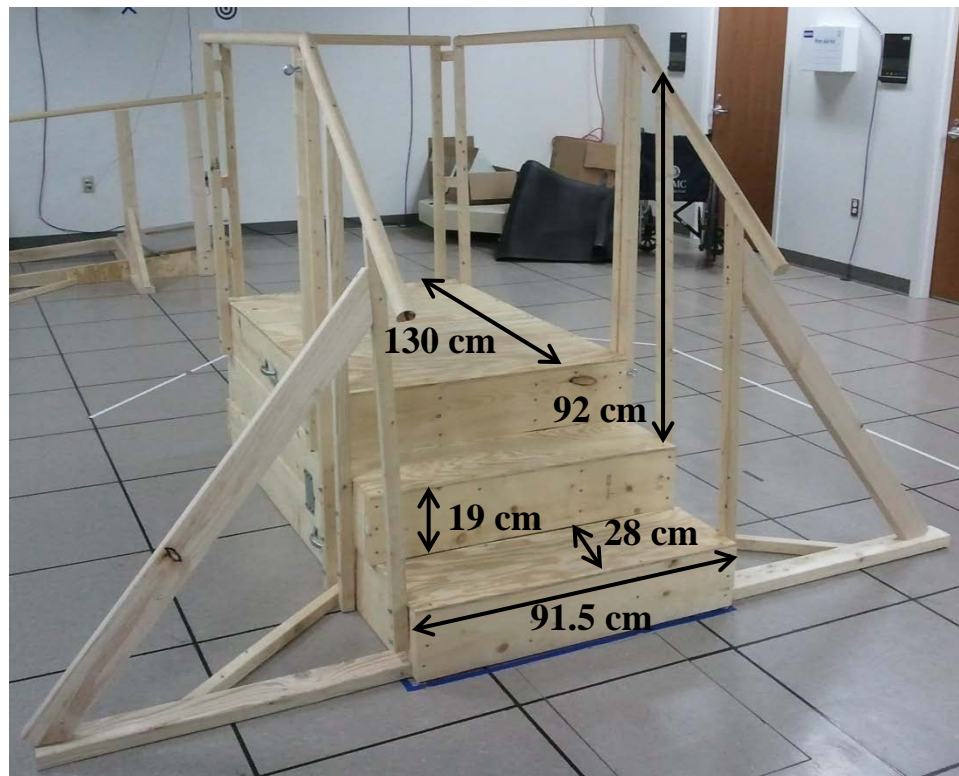


Figure 11. Staircase used for stair ascent and descent trials.

To ascend the stairs, subjects were allowed to position themselves as desired near the black line on the floor in front of the first step. This position allowed for possible force plate data to be collected during the push-off phase of the first step. Subjects were instructed to use the handrails or their personal assistive device if necessary to complete the task as they normally

would outside of the lab. Additionally, subjects were secured in the harness during all trials on the stairs and the harness was adjusted to account for increased slack in the lanyard during ascent. Subjects ascend the steps to the landing at the top of the staircase using either a step-over-step or step-to-step progression method depending on their preference. After reaching the top platform subjects waited until instructed to descend the staircase. Prior to descent, subjects were allowed to align themselves as desired behind the landing edge. Subjects completed three ascent trials and three descent trials.

For the stumbling condition, subjects were unaware that they would experience the perturbation. At the time of the trial they were instructed to complete additional trials in the same manner as the level surface walking condition. Subjects were secured in the harness at all times during this experimental condition. Two level surface walking trials were collected before the laboratory staff prepared to induce the stumble. To deploy a stumble to the prosthetic limb at approximately midswing, a laboratory staff member chose when to deploy a rapidly elevating obstacle that was concealed underneath the flooring surface [61, 93]. The staff member was able to choose one of three obstacles to elevate, depending on the location at which the obstacle needed to be placed to obstruct the foot at midswing.

The three obstacles were spaced approximately 16 cm apart over a length of 40 cm before the first force plate. The obstacles were concealed within the raised flooring structure in the laboratory, and they were held in place flush with the surface of the walkway via electromagnets (Figure 12). When the obstacles were hidden below the floor, springs were depressed; thus, when power to an individual electromagnet was turned off the springs were free to decompress and raise the obstacle out of the floor and into the walkway (Figure 13).

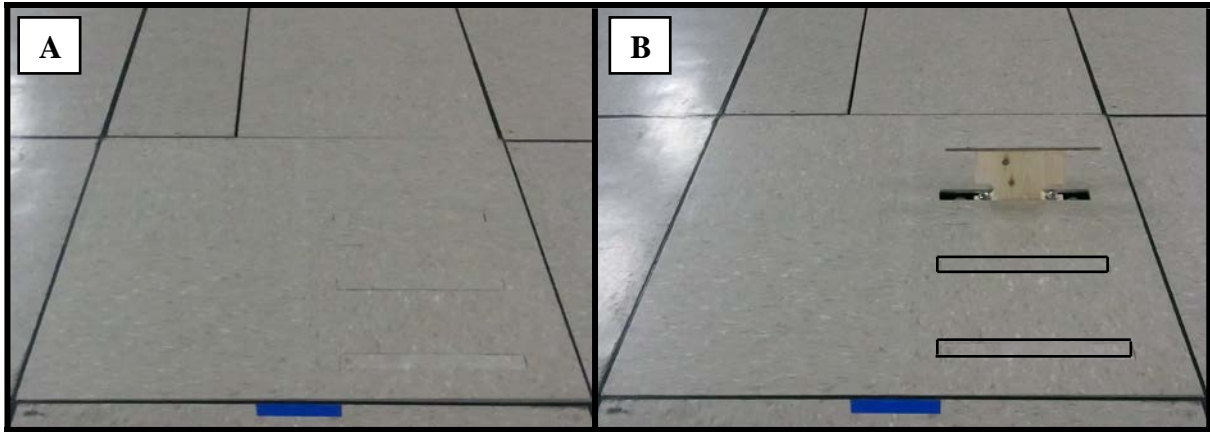


Figure 12. (A) The stumbling condition obstacles in the lowered position. (B) One obstacle in the raised position with the remaining two obstacle slots outlined.

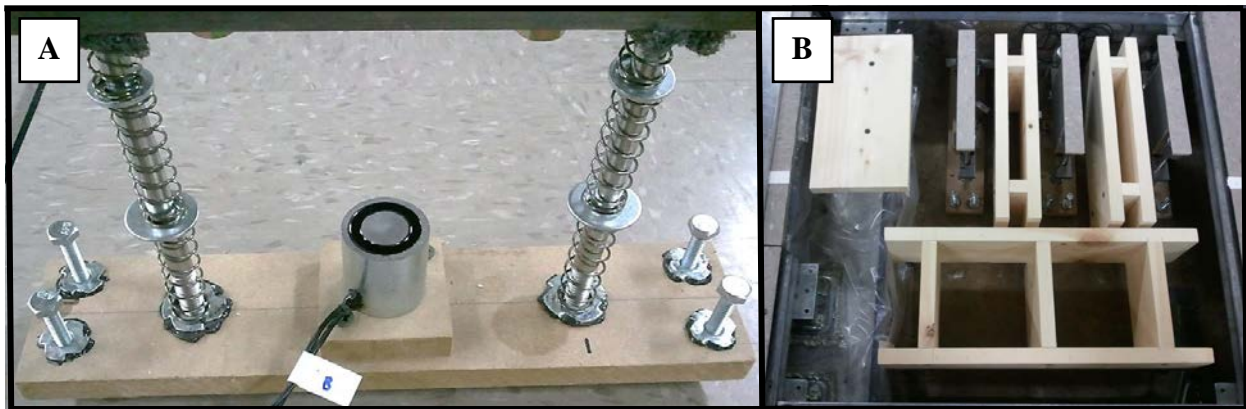


Figure 13. (A) One of three stumbling device mechanisms housed underneath the laboratory flooring structure. When the springs are decompressed, the electromagnet holds the steel platform down so the top of the obstacle is flush with the walkway floor. Bolts in the four corners of the mechanism allow for fine-tuning the height of the obstacle within its slot in the walkway. (B) Set up of the stumbling device underneath the flooring structure.

The obstacles were fabricated from wood, with a top piece made from the same floor tile as the walkway to aid in concealing the pieces within the floor. The width of the wooden portion of all of the obstacles was 12 cm, and the floor tile piece had a length of 20.3 cm and a width of 2.8 cm. Each obstacle was fastened to a steel platform using a nut/bolt attachment so the

obstacle piece could not be dislodged from its slot within the walkway upon contact with the prosthetic foot. The raised heights of the obstacles were 7.8 cm for the first position (furthest from the force plate) and 8.2 cm for the remaining two positions; this was due to space constraints within the raised flooring structure. Adjustments were made to the stumbling device construction as necessary during the duration of the pilot study, based upon results seen from each stumbling perturbation trial. First, the height of the obstacles was increased from 5 cm in height above the flooring surface, as subject 1's prosthetic foot clearance was larger than this. Next, the attachment for the obstacle pieces to the platforms was changed from a Velcro system to a nut/bolt system, in order to provide a more permanent attachment to the device. Lastly, the construction of the obstacles was changed to a solid wood design. During the pilot study, the obstacles were constructed of a polycarbonate center piece surrounded by foam (the obstacles and tile top piece had same the same dimensions as described above). These foam pieces were unable provide a consistent stumble perturbation across all subjects, as the foam obstacle sometimes bent forward within the walkway slot upon foot contact. No changes have been made to the stumbling device since the full research study began.

Also during visit 2 subjects completed the following assessments: Activities-Specific Balance Confidence Scale [94], European Quality of Life Instrument [95-98], and Locomotor Capabilities Index [99-100]. These functional assessments were collected to help provide further details regarding ambulation ability and comfort using a prosthesis. Upon completion of visit 2, the activity monitor was replaced on the prosthesis and the falls log was provided to the subject.

3.2.1.3 Laboratory Visit 3

Within a one-week period of visit 2, subjects returned to the laboratory to have their knee exchanged to an opposing knee type by the study’s certified prosthetist. The knee joints used in this study are listed in Table 10. The same socket, suspension, and prosthetic foot were used throughout the study.

Table 10. Prosthetic knee joint models used in the study.

<i>Microprocessor-controlled</i>	<i>Nonmicroprocessor-controlled</i>
Orion ^a	Mercury Hi Activity with CatTech SNS ^a
Plie ^b	Total Knee Hydraulic ^c
Rheo ^c	Mauch SNS ^c
C-Leg ^d	3R80 Hydraulic ^d

a) Endolite, Miamisburg, OH; b) Freedom Innovations, Irvine, CA; c) Ossur, Reykjavik, Iceland; d) Otto Bock, Duderstadt, Germany

The prosthetist ensured proper alignment of the prosthetic limb and settings in the prosthetic knee joint, as well as provided subjects with training on how to use the knee effectively. A physical therapist worked with the subjects to make sure they were able to safely ambulate over various flooring conditions with the new prosthesis before leaving the laboratory. Also before leaving the laboratory, subjects were provided with the StepWatch Activity Monitor and falls log. One week following the knee exchange the subjects were contacted via phone to make sure the knee was still fitting properly and no medical or functional issues had arisen. Following visit 3 an 8-week acclimation period was given, during which time the subjects were asked to continue their daily routine. Over this period a weekly phone call was made to subjects by a laboratory staff member to ensure the activity monitor was still being worn, and to discuss any events recorded in the falls log or address any concerns that may have developed.

3.2.1.4 Laboratory Visit 4

Following the 8-week acclimation period subjects returned to the laboratory for the final visit. Upon arrival, activity monitor data was uploaded from the device and the falls log entries were obtained. Subjects were prepared for motion capture data collection by attaching the 69 markers used during visit 2. Data collection started with re-evaluation of the subjects' activity level while wearing the opposing knee type by using the AMP assessment. Next, all of the six experimental conditions performed during visit 2 were repeated. Also during this visit subjects completed the functional assessments again, in order to evaluate their functional abilities and comfort with the opposing knee type (assessments included: Prosthesis Evaluations Questionnaire, Activities-Specific Balance Confidence Scale, European Quality of Life Instrument, and Locomotor Capabilities Index).

After all trials and assessments were completed, subjects were re-fitted with their personal knee by the prosthetist. Proper alignment and fit were verified by the prosthetist and a safety checklist was conducted by the physical therapist. A one-week follow-up phone call was made by the laboratory staff to ensure no medical or functional issues had arisen following the knee fitting. In the event that there was an issue, the prosthetist met with the subject.

3.2.2 Method for Minimum Foot Clearance during Level Surface Walking

The motion capture trajectories for all markers placed on the shoes during the static trial (Figure 14), and all markers remaining on the shoes during the dynamic trials were exported to MATLAB for post-processing. Motion capture data was collected at 120 Hz. The forefoot markers which were on the shoes only during the static trial were recreated virtually in MATLAB by transforming the local coordinates of these markers with respect to each shoe, to

the corresponding global coordinates within the motion capture volume. These virtual markers were used to determine the position along the bottom of the shoe sole, since markers cannot be physically placed under the shoe [86, 101]. The position of these virtual markers was adjusted in the vertical direction based on marker radius, and the center point of a line connecting each medial marker to its respective lateral marker was used to identify the bottom of the shoe sole. The toe tip marker was included as one of the forefoot markers in order to complete the sole geometry, but this marker remained in place during the dynamic trials and its position was not adjusted during post-processing. For the pilot study subjects, only the toe tip marker was available for use in the minimum foot clearance analysis due to a different marker set being used at that time.

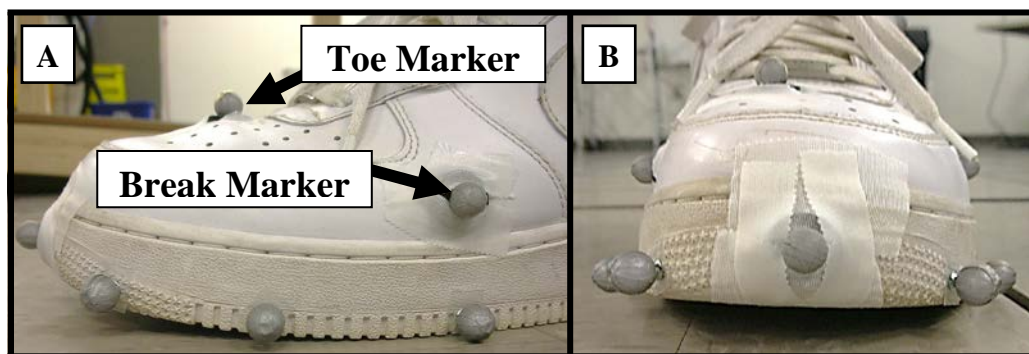


Figure 14. (A) Forefoot markers along the shoe sole, from left to right: toe tip, front forefoot, middle forefoot, and break forefoot; the break and toe markers are labeled. (B) Anterior view of the shoe; forefoot markers on the lateral side of the shoe sole are shadowed on the medial side.

For both the pilot study and full study level surface walking trials, key events during the gait cycle were identified to determine individual swing phases within each trial. Swing phase is commonly referred to as the time elapsing from shoe toe-off to shoe heel-strike for the same foot [48]. Due to the variations in amputee gait style and the impact a rigid prosthetic foot has on the

motion of the commonly identified toe-off event, the definition for toe-off was redefined in this thesis. Since the heel of the prosthetic foot cannot rotate over the forefoot as the foot is leaving the ground, such as the sound limb does, initial motion of the forefoot into swing phase occurs before the shoe physically leaves the ground. Consequently, the starting point of the swing phase for the analysis presented in this thesis was identified by initial forefoot motion. To determine this point within the gait cycle, the vertical trajectory component of the toe marker was used; initial forefoot motion was the point when the toe marker began to move upward (Figure 15). The use of trajectory data was verified against force plate data to understand the physical relation between initial forefoot motion and when the shoe actually left the ground (Figure 16). Across all subjects, initial forefoot motion found using the trajectory data occurred before the force plate data identified the shoe leaving the ground. Generally there was an approximate 167 ms difference between initial forefoot motion and when the shoe departed from the force plate. To identify the end of swing phase the heel-strike of the foot was used; this point was identified using the vertical trajectory component of the superior heel marker (Figure 17) [102-103]. Each swing phase was normalized to 100% so comparisons could be made between multiple swing phases.

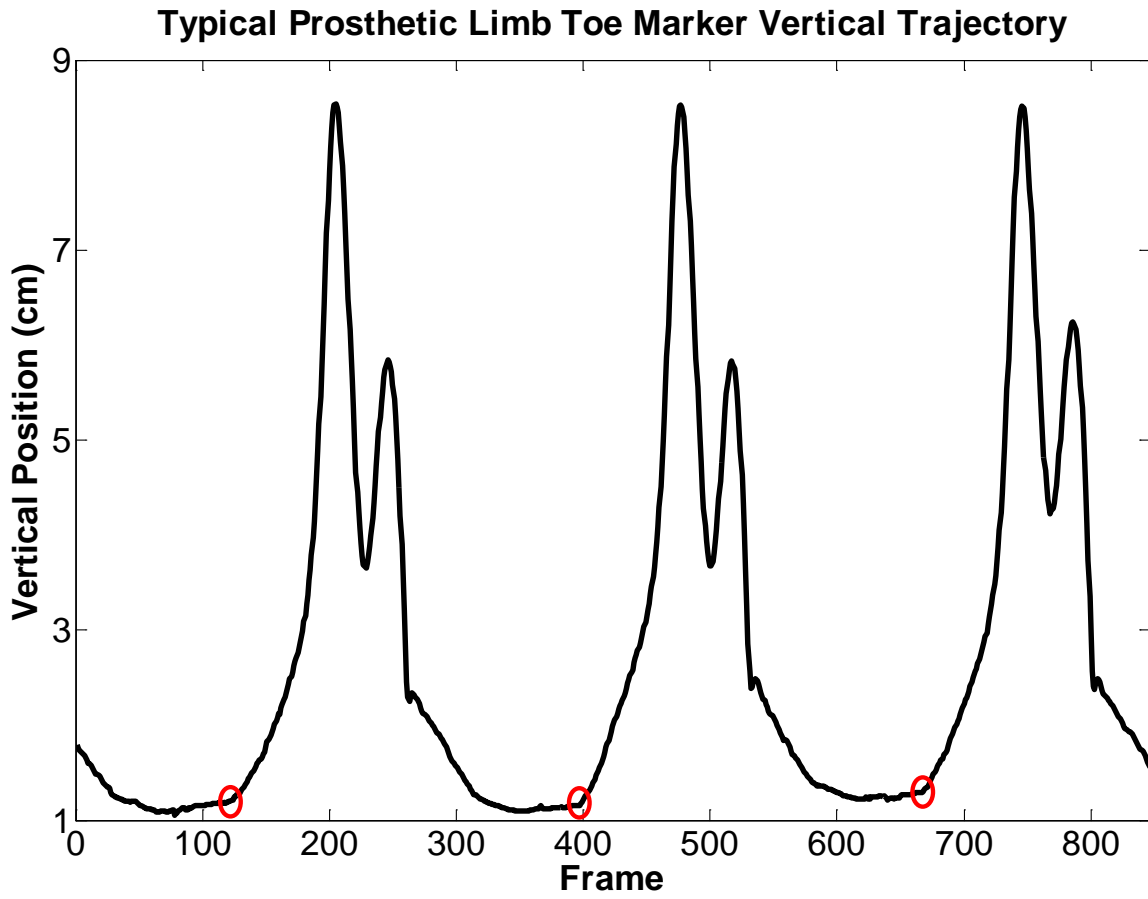


Figure 15. Typical toe marker vertical trajectory for the prosthetic limb. Initial forefoot motion points are circled.

Comparison of Force Plate and Trajectory Data for Determining Gait Events

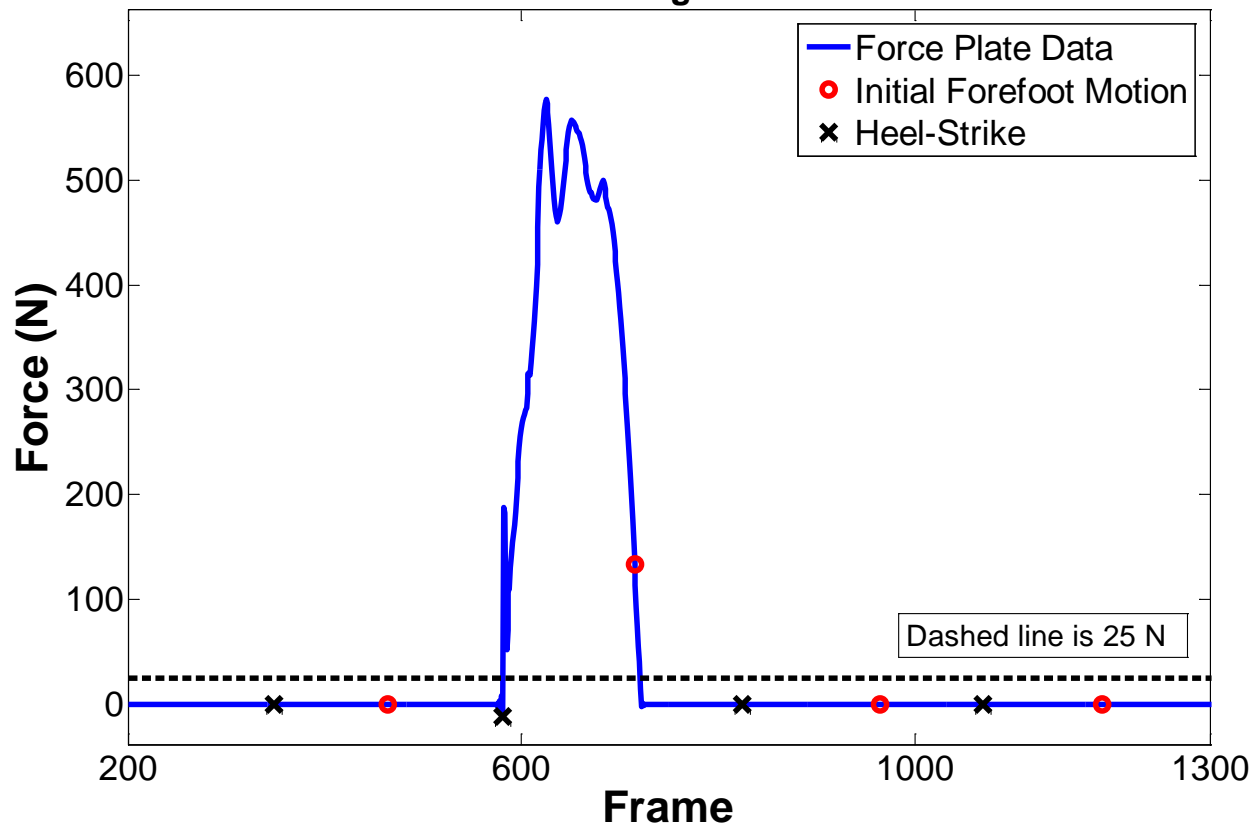


Figure 16. Typical prosthetic limb force plate contact. Initial forefoot motion and heel-strike events found using vertical trajectories of the toe and superior heel markers, respectively, are identified. Heel-strike events were accurately identified using trajectory data and an approximate 167 ms difference was seen between initial forefoot motion and physical toe-off of the shoe leaving the floor.

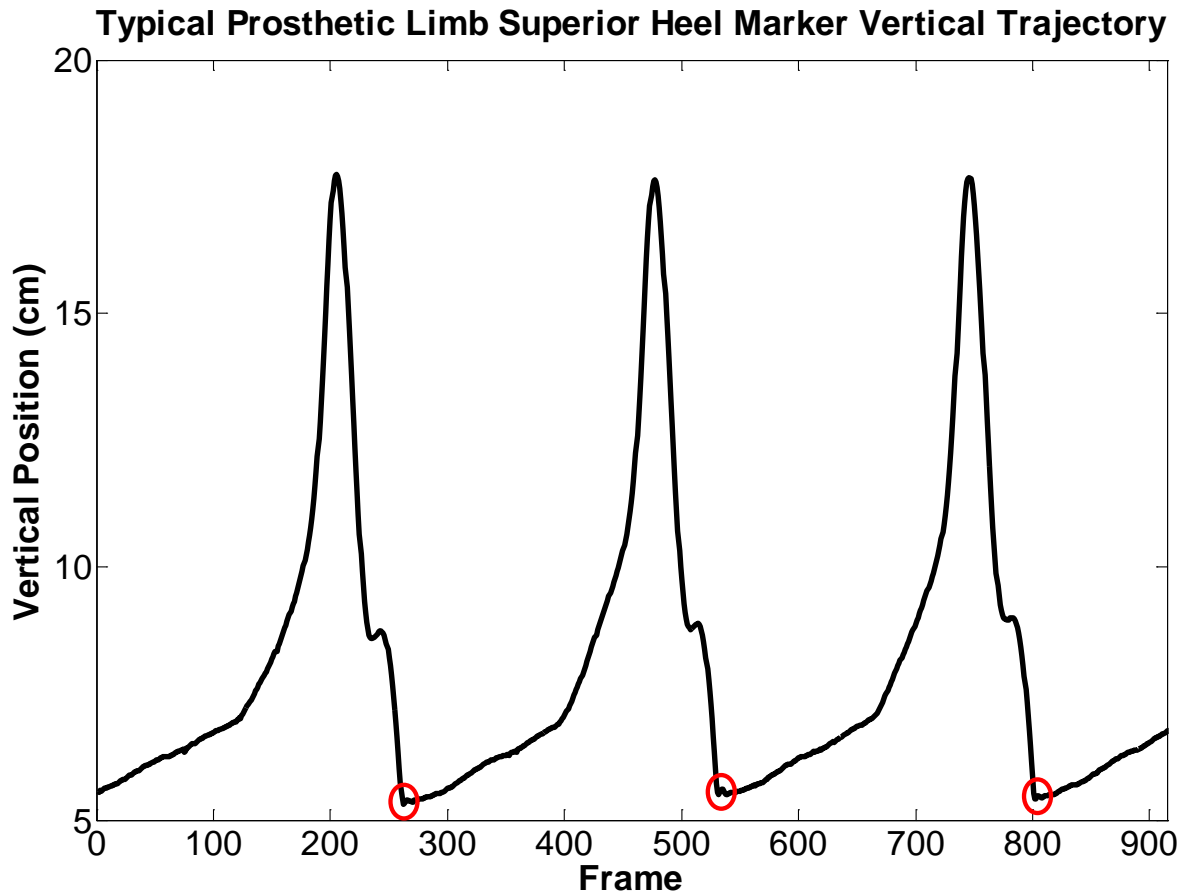


Figure 17. Typical superior heel marker vertical trajectory for the prosthetic limb. Heel-strike points are circled.

Minimum foot clearance (MFC) is defined as the minimum vertical distance between the walking surface and the lowest point of the sole of the forefoot during the swing phase [101, 104]. In able-bodied individuals the MFC value is identified by a clear local minimum point occurring at approximately 51% of the swing phase [104]. The MFC location during the swing phase has been reported as the instant within the gait cycle when the risk for stumbling is the highest. Anatomically, for able-bodied individuals this local minimum point occurs just before the ankle returns to its neutral position during the swing phase [31]. Toe clearance for able-bodied subjects has also been shown to be very sensitive to small angular changes in the swing

ankle and knee joints [18]. Therefore, unilateral transfemoral amputees are likely to display a different vertical displacement pattern of the forefoot during swing due to gait adaptations for obtaining adequate foot clearance during gait (Figure 18). As a result, the minimum foot clearance method presented in this thesis was developed specifically for unilateral transfemoral amputee gait analysis.

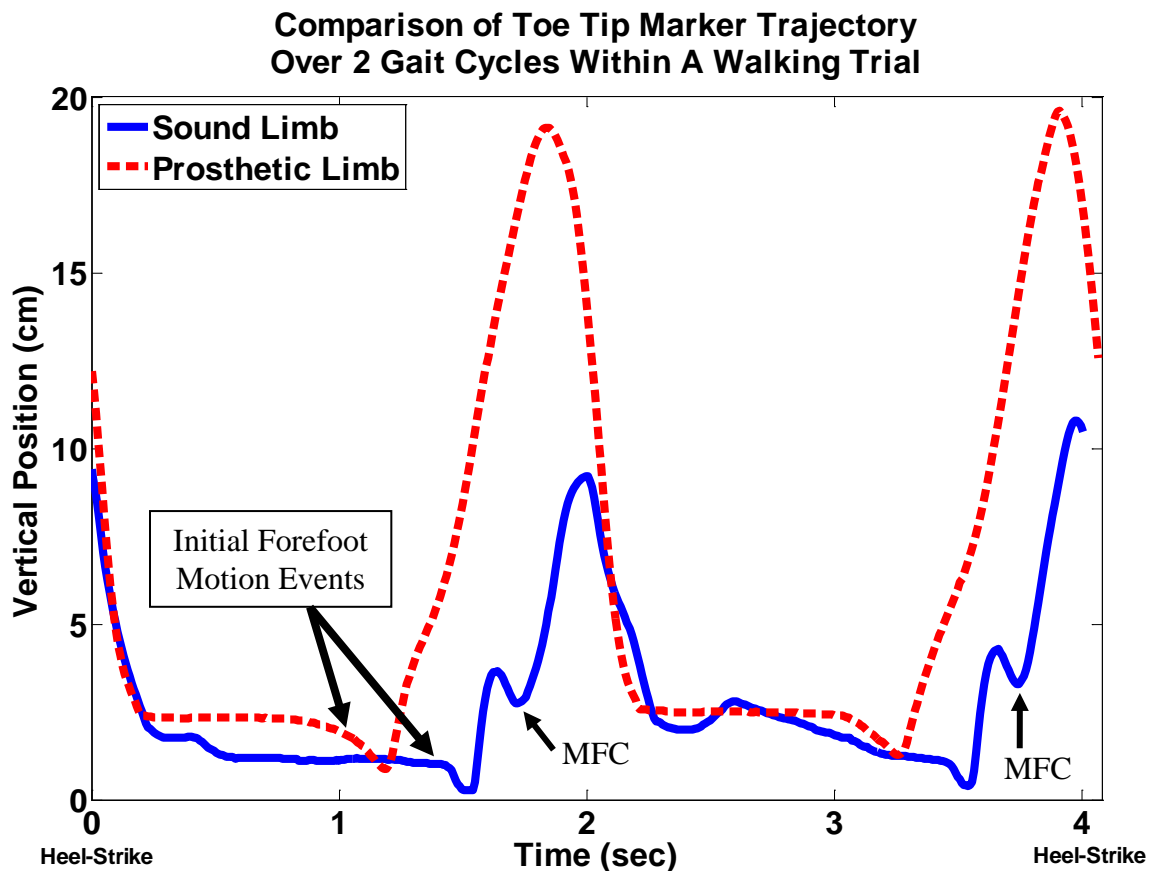


Figure 18. Example of different sound limb and prosthetic limb toe tip patterns during gait. The sound limb toe tip trajectory has a local minimum point as the foot moves through the swing phase while the prosthetic limb does not have a minimum foot clearance point.

As the example in Figure 18 shows, the trajectory of the forefoot may not result in a clear local minimum point during the swing phase in unilateral transfemoral amputee gait. It is also

possible that the sound limb forefoot trajectory does not produce a local minimum point during swing as there is a wide variation in amputee gait styles. To address this issue, the methodology for identifying MFC was altered for this subject population. If a clear local minimum point signifying MFC was not identified during the swing phase for either the prosthetic limb or the sound limb, the minimum clearance at two distinct points during the swing phase was reported. If MFC could be identified during swing, this minimum clearance value was reported along with the clearance value at each distinct point, in order to provide comparison to swing phases where MFC was not found. The distinct points were determined by dividing the swing phase up into three sub-phases: initial swing, midswing, and terminal swing (Figure 19). Initial swing begins at initial forefoot motion and lasts until 32.5% of the swing phase has been reached. Continuing from this point, midswing lasts until 67.5% of the swing phase has been reached, and terminal swing is the final period until heel-strike occurs [105]. Therefore, if a forefoot marker trajectory did not yield a clear local minimum point during swing, the clearance values at 32.5% and 67.5% were reported.

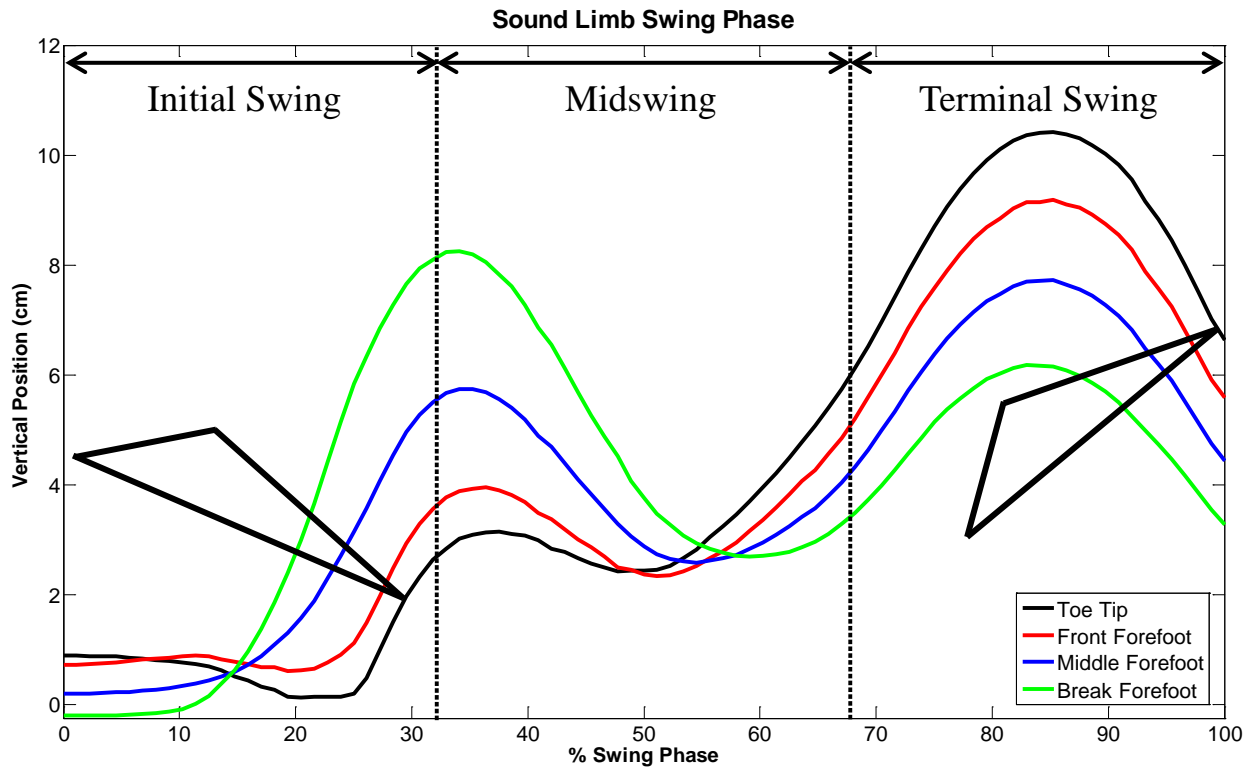


Figure 19. Example of the forefoot marker trajectories of the sound limb during swing phase (shoe figures included for visual identification of foot position during swing; not drawn to scale). The toe tip MFC occurs at approximately 50% of the swing phase while the break forefoot MFC occurs at approximately 60%.

If the any of the forefoot marker trajectories revealed a plateau during the swing phase, only the clearances at 32.5% and 67.5% were reported (Figure 20). A plateau region was not used to identify MFC because it did not fully satisfy the definition of “occurring at a local minimum point” during swing, and temporally, a specific time point was not identifiable.

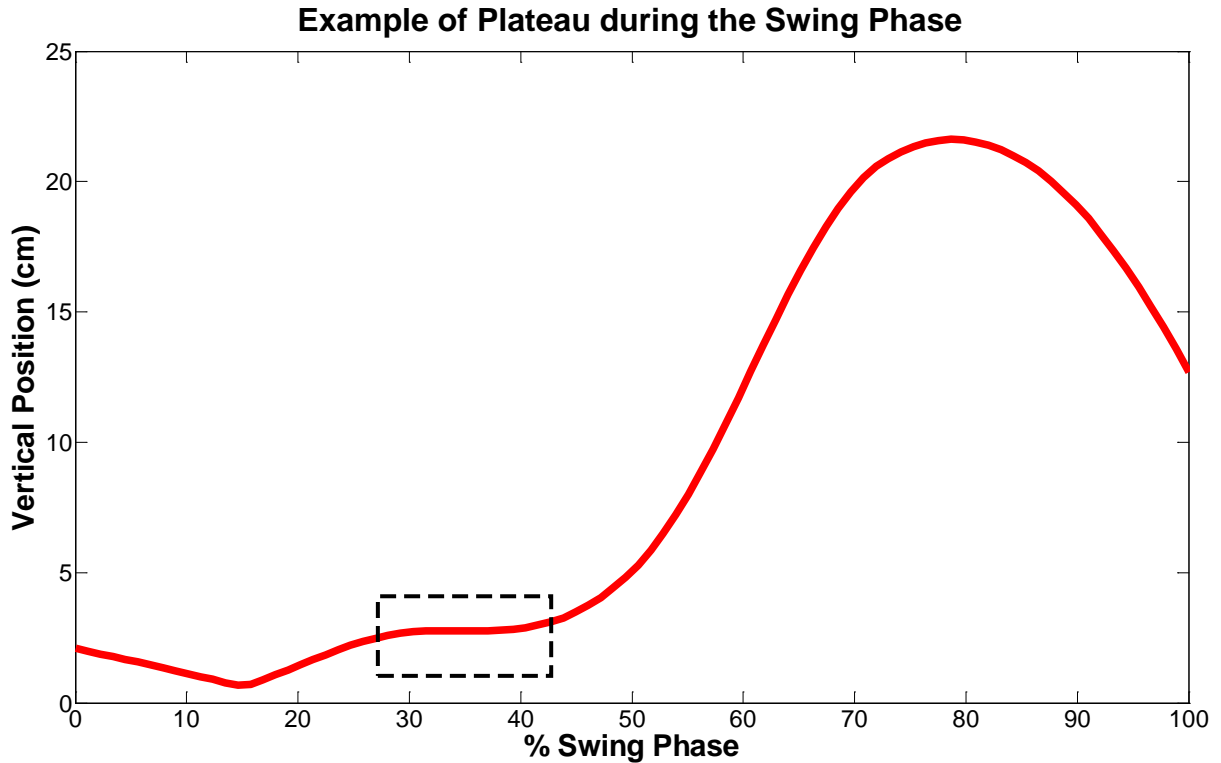


Figure 20. Typical swing phase displaying a plateau instead of a clear local minimum point. When this occurred, MFC was evaluated based on the clearance values found at 32.5% and 67.5% of swing.

Three level surface walking trials were analyzed for each subject. Within each trial, three swing phases for each limb were evaluated to determine the minimum foot clearance values during swing. For each swing phase where the MFC was identified for all forefoot markers, the overall smallest value was reported with its associated marker position, along with the overall smallest 32.5% and 67.5% clearance values. For each swing phase where the MFC was not identified for all forefoot markers, only the overall smallest 32.5% and 67.5% values were reported with the associated marker position.

3.2.3 Method for Foot Clearance during Stair Ascent

The shoe marker trajectories collected during the static trial and during the stair ascent trials were exported to MATLAB for post-processing. For the subjects enrolled in the full study, the forefoot markers used during the static trial were recreated virtually using the local coordinates and a transformation matrix to obtain the global marker trajectories in the motion capture volume during the dynamic trials. These virtual markers were used to determine the bottom edge of the shoe sole for the forefoot of the foot [86, 101]. Initial forefoot motion and heel-strike events were determined using the toe and superior heel markers, respectively, in order to determine the swing phase for each step [102-103]. For the pilot study subjects, only the superior heel, toe, and toe tip markers were used on the foot. Again, the toe and heel markers were used to identify the initial forefoot motion (Figure 21) and heel-strike events. The position of the stairs during the full study was recorded prior to the stair ascent trials by using markers to pin-point the step edges. This step placement information was not collected during the pilot study sessions, but the stairs were set up in the same spot within the capture volume.

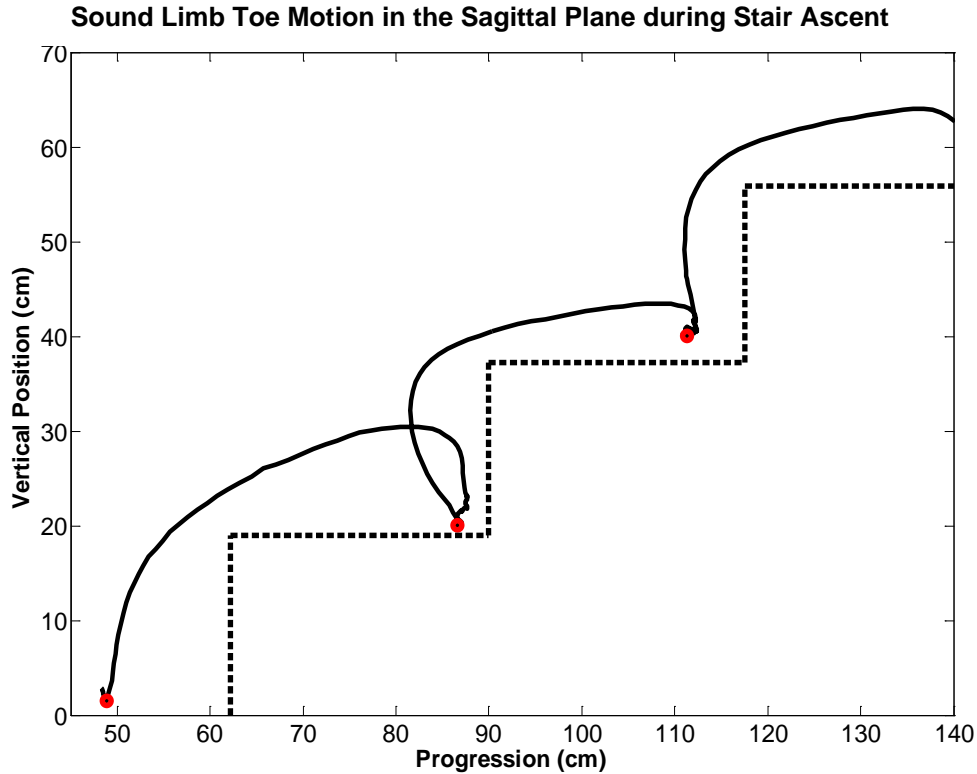


Figure 21. Typical sound limb toe motion during stair ascent. Red circles highlight initial forefoot motion points for each step.

Five variables were examined for each foot as it passed over each step, in order to gain an understanding of the foot clearance and placement strategies used by unilateral transfemoral amputees during stair ascent [52, 106]. Figure 22 shows the position of the foot for each variable measured. The resultant distance (A) for all forefoot markers was calculated for all time points between consecutive initial forefoot motion and heel-strike points, then the overall minimum resultant distance was found to identify which forefoot marker position had the minimum clearance. The forefoot horizontal distances (B) were found when each marker was at the same vertical height as the step edge during swing. The forefoot vertical distances (C) were found when each marker was passing over the step edge. The inferior heel vertical distance (D) was

found when this marker passed over the step edge. If a subject's shoe size resulted in the heel hanging off the back of the step during stance, then this variable was only able to be calculated during swing over the top step. The inferior heel horizontal distance (E) was found while the foot was flat on the step during stance immediately following heel-strike.

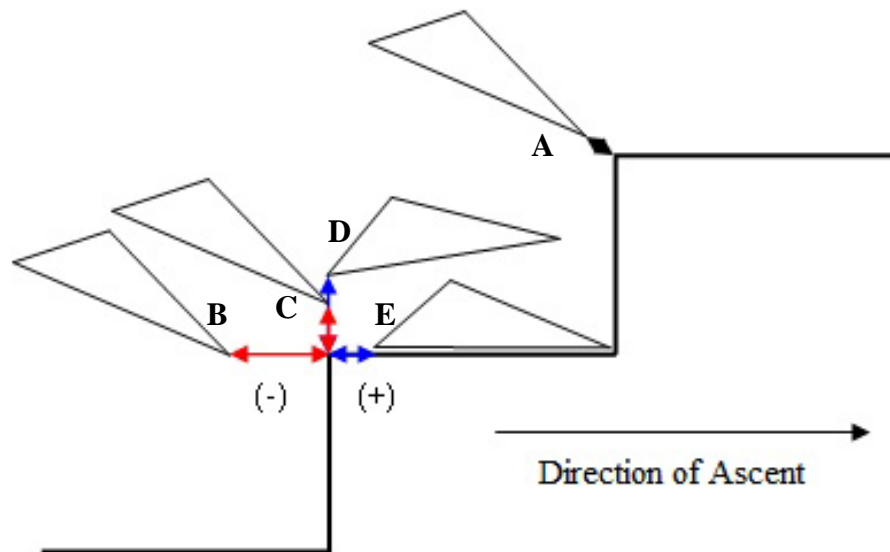


Figure 22. Resultant (A), horizontal (B & E), and vertical (C & D) clearance distances for the foot during ascent (toe tip marker shown as an example for the forefoot). Prior to passing over the step edge yields negative horizontal values. The inferior heel may have a negative horizontal value if the foot is larger than the step tread or positioned such that the heel hangs off the step.

Of these variables, those specifically examined to assess the risk of tripping during stair ascent include the overall minimum horizontal distance in front of the step for the forefoot markers, the overall minimum vertical distance over the step for the forefoot markers, and the overall minimum resultant distance between the forefoot and the step edge. For subjects in the full study, three stair ascent trials were collected. The pilot study subjects completed only one stair ascent trial. For each subject the mean and standard deviation of each variable was calculated using all steps for each foot.

3.2.4 Method for Foot Clearance during Stair Descent

All shoe marker trajectories for the static and stair descent trials were exported to MATLAB for post-processing. The static trial only forefoot markers were recreated virtually by transforming the local coordinates to the appropriate global coordinates within the motion capture volume. These virtual markers allowed for the forefoot position of the bottom of the shoe sole to be used when assessing clearance during descent [86, 101]. The initial forefoot motion and heel-strike events during stair descent were determined using the toe and superior heel marker vertical trajectories [102-103]. During the full study, the position of the stairs was recorded during data collection by using markers to pin-point the step edges; despite this data not being collected during the pilot study sessions, the stairs were set up in the same location in the capture volume.

Five variables were identified for each foot as it passed over a step in order to show the foot clearance and placement strategies during stair descent [52, 106]. Figure 23 shows the position of the foot when each variable was measured. The resultant distance (A) for the inferior heel marker was calculated for all time points between consecutive initial forefoot motion and heel-strike points. The forefoot horizontal distances (B) were found while the foot was flat on the step during stance immediately prior to initial forefoot motion. Due to differences in starting position at the top of the stairs, these horizontal distances for the first step were not included in the analysis. The forefoot vertical distances (C) were found when each marker was passing over the step edge. The inferior heel vertical distance (D) was found when this marker passed over the step edge. The inferior heel horizontal distance (E) was found when the inferior heel marker was at the same vertical height as the step during swing.

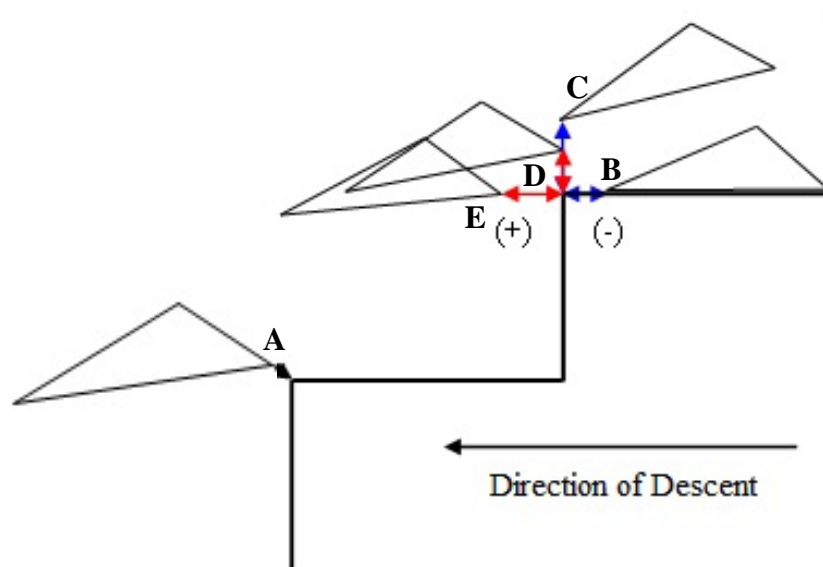


Figure 23. Resultant (A), horizontal (B & E), and vertical (C & D) clearance distances for the foot during descent (toe tip marker shown as an example for the forefoot). Marker positions prior to passing over the step edge have negative values. If any forefoot marker is positioned off of the step tread during stance the vertical distance will be negative and correspond to the instant of initial forefoot motion.

The variables used to specifically assess the risk of tripping during stair descent include the minimum vertical distance of the inferior heel over the step edge, the minimum horizontal distance of the inferior heel in front of the step edge, and the minimum resultant distance between the inferior heel and the step edge. An example of inferior heel motion during descent is provided in Figure 24. Subjects in the full study completed a series of three stair descent trials while the pilot study subjects only completed one stair descent trial. For each subject the mean and standard deviation were found for each variable using all of the steps taken with each foot.

Sound Limb Inferior Heel Motion in the Sagittal Plane During Stair Descent

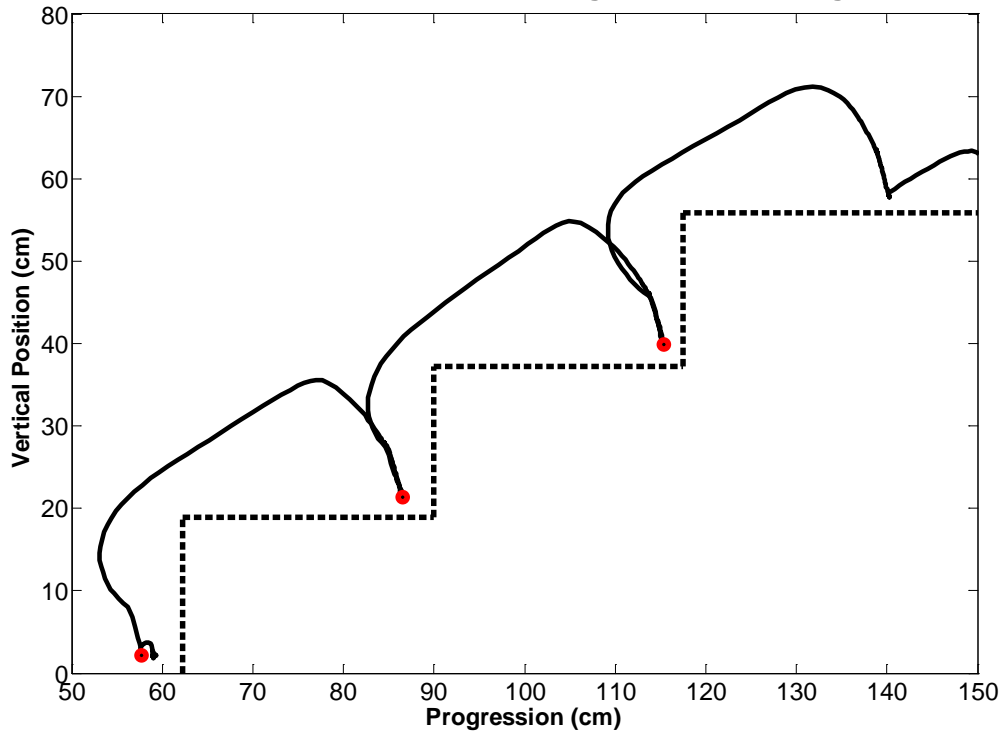


Figure 24. Typical sound limb inferior heel motion during stair descent. Red circles highlight heel-strike events.

3.2.5 Method for Stumbling Perturbation Outcome Measures

Motion capture trajectories for the shoe markers, shoulder markers, and pelvis markers from the static and stumbling perturbation trials were exported to MATLAB for post-processing. A fourth-order Butterworth filter with a cutoff frequency of 6 Hz was used to filter the stumbling trial trajectory data. The initial forefoot motion and heel-strike points for each foot during the trial were identified using the toe and superior heel markers, respectively [102-103]. The outcome measures to be examined for the stumbling perturbation trial include the recovery strategy utilized, the stumble recovery duration, trunk flexion deviation in the sagittal and frontal planes, and trunk angular velocity during the recovery period. There is a current void in the

literature identifying these measures specifically for unilateral transfemoral amputees; therefore, the methods in this thesis adapted those used for evaluating falls in able-bodied adults and the transtibial amputee population [57, 107-110].

The recovery strategy utilized by the subjects will be based upon the response of the prosthetic limb immediately following contact with the obstacle. Previous research has identified three distinct strategies for recovering from a stumbling perturbation [57]. A lowering strategy occurs when the obstructed limb is immediately lowered to the ground on the near side of the obstacle to become the stance limb while the contralateral limb initiates clearance over the obstacle. An elevating strategy occurs when the obstructed limb is flexed at multiple joints to clear the obstacle while the contralateral limb remains as the stance limb. Generally the stance limb displays some degree of plantar flexion to aide in elevating the body over the obstacle. A reaching strategy is similar to the elevating strategy, except the increase in prosthetic limb flexion to clear the obstacle occurs primarily at the hip joint of the obstructed swing limb.

The stumble recovery duration was defined as the period of time from foot-obstacle contact until heel-strike of the prosthetic limb recovery step [57, 93, 109-110]. For the lowering recovery strategy, the prosthetic limb recovery step was the first step taken with the obstructed prosthetic foot after it had acted as the supporting limb. For the elevating strategy, the prosthetic limb recovery step heel-strike occurred when the obstructed foot made contact with the ground following clearance of the obstacle.

The trunk angle in the sagittal and frontal planes was assessed during the stumble perturbation recovery. The trunk was defined as a segment from the shoulder medial-lateral midpoint to the posterior superior iliac spine medial-lateral midpoint [107]. The trunk angle was found with respect to vertical for both the sagittal and frontal planes [57, 111]. The maximum

and minimum angles during the stumble recovery duration were used to evaluate the magnitude of the stumble response with respect to the angles at the instant of contact with the obstacle. Average trunk maximum and minimum angles were also found for one level surface walking trial to determine a baseline range for comparison with the stumbling response. Angular velocity in the sagittal and frontal planes was calculated using the first derivative of the trunk angle data with respect to time. The resultant of the angular velocities yielded the trunk angular velocity [112]. The trunk angular velocity at the instant of contact with the obstacle was determined along with the maximum and minimum values during the recovery duration and the average trunk angular velocity during one level surface walking trial.

3.3 RESULTS

3.3.1 Minimum Foot Clearance during Level Surface Walking

A typical gait cycle for each subject is shown in Figures 25 and 26 in order to compare all prosthetic limb toe tip marker trajectories and all sound limb toe tip marker trajectories, respectively. These figures show a wide range of swing phase patterns and maximum toe tip height during terminal swing. Minimum foot clearance results found 4 of 6 subjects had smaller MFC with the prosthetic limb in comparison to the sound limb. Across all subjects, the largest MFC value for prosthetic limb was 7.95 cm (subject 1) when the MFC point was able to be identified by a clear local minimum point in the swing phase, and the largest MFC value for the sound limb was 4.84 cm (subject 2). Additional spatial-temporal gait parameters during the gait cycle and knee joint angles during the swing phase are reported for each subject in Appendix B.

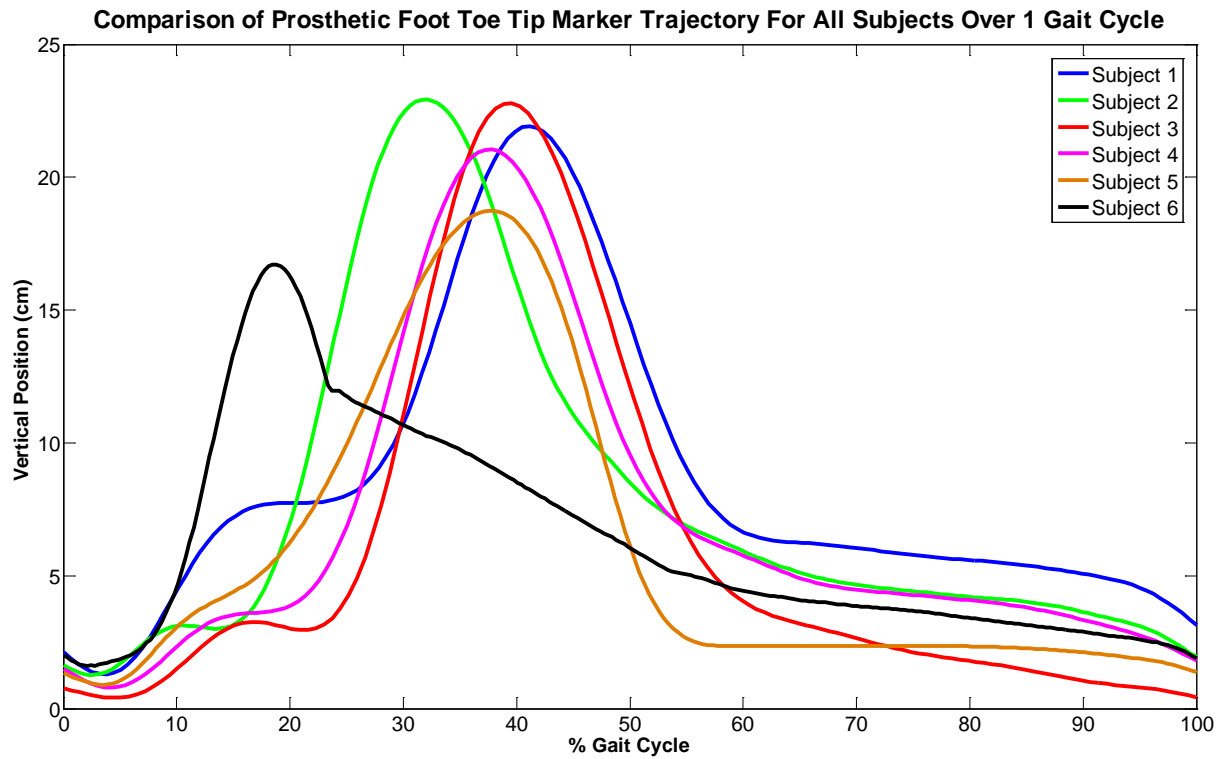


Figure 25. Typical prosthetic foot toe tip marker trajectory during one gait cycle for all subjects. Zero and 100% of the gait cycle are identified by initial forefoot motion.

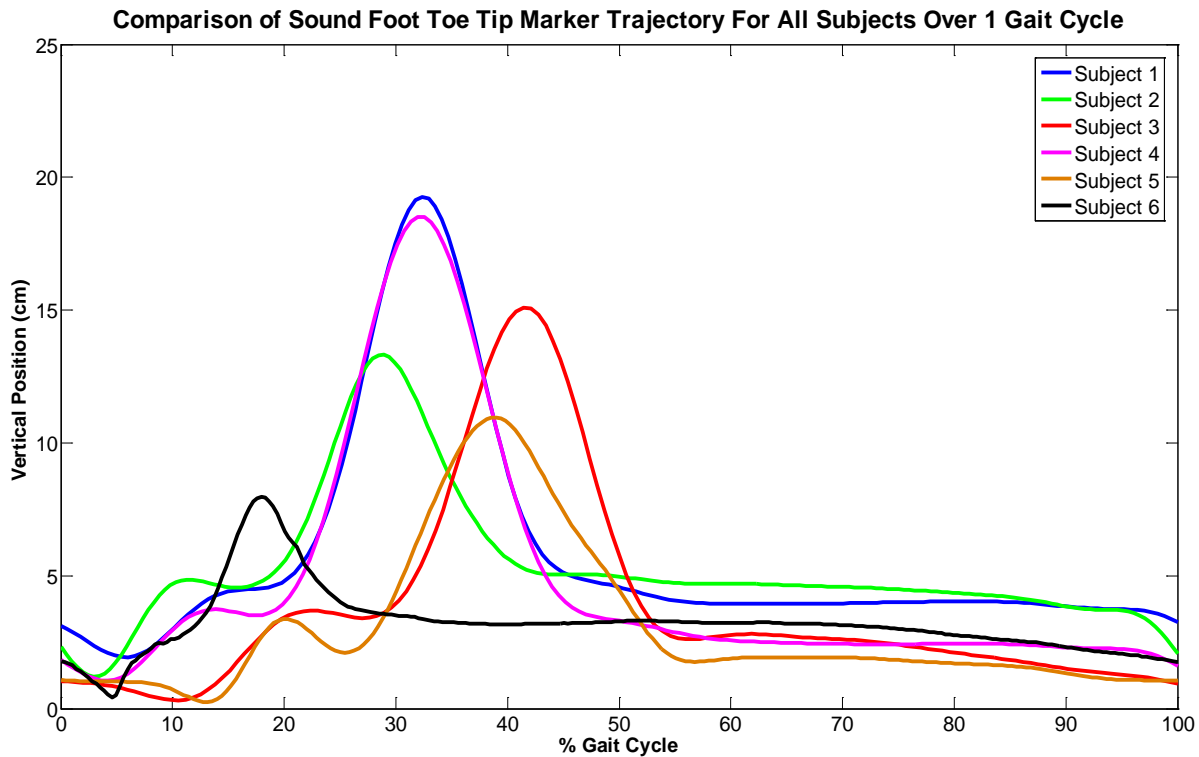


Figure 26. Typical sound foot toe tip marker trajectory during one gait cycle for all subjects. Zero and 100% of the gait cycle are identified by initial forefoot motion.

Minimum foot clearance of the toe tip for subject 1 on the sound limb side was found within 43-47% of the swing phase, with the MFC value ranging between 2.00 cm and 3.26 cm for the four swing phases where a clear local minimum point was identified (Figure 27 and Table 11). The prosthetic limb MFC values were higher than the sound limb. For the prosthetic limb toe tip, MFC occurred at approximately 46-50% of the swing phase and resulted in clearance values ranging from 6.98 cm to 7.95 cm. The swing phases without a clear MFC point were analyzed at 32.5% and 67.5% of the swing phase (the transition points between initial swing and midswing, and midswing and terminal swing, respectively). Results for the prosthetic limb toe tip show an average height of $7.44 \text{ cm} \pm 0.71 \text{ cm}$ at 32.5% of the swing phase, across all

nine swing phases. At 67.5% of the swing phase the prosthetic limb toe tip reached a height of $15.27 \text{ cm} \pm 2.65 \text{ cm}$. At 32.5% and 67.5% of the swing phase the sound limb toe tip reached an average clearance of $4.09 \text{ cm} \pm 0.47 \text{ cm}$ and $8.13 \text{ cm} \pm 1.21 \text{ cm}$, respectively.

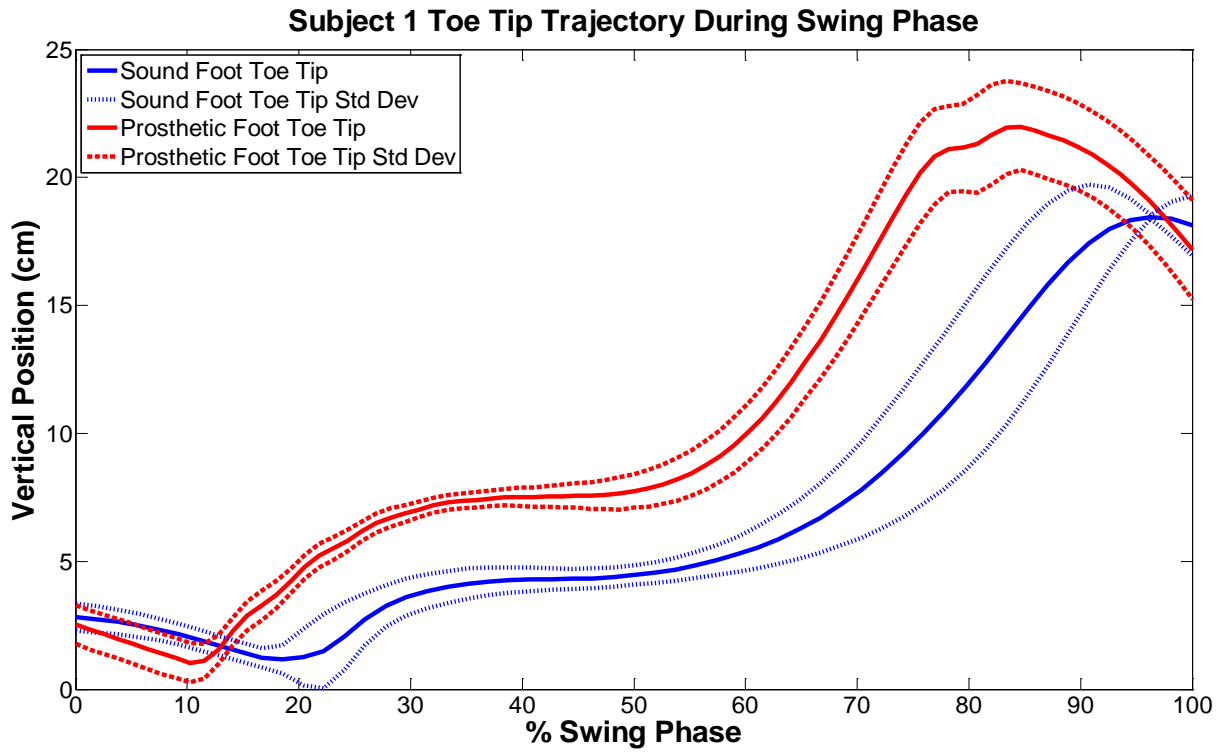


Figure 27. Comparison of mean toe tip trajectory across 3 steps for the sound foot and prosthetic foot of subject 1; dashed lines indicate standard deviation. Zero percent of the swing phase is identified by initial forefoot motion, 100% of the swing phase is identified by heel-strike.

Table 11. Subject 1 MFC values during the swing phase. Highlighted values are the MFC events identified by a clear local minimum point during the swing phase.

Prosthetic Limb and Sound Limb Minimum Foot Clearance Values (cm)				
Swing Phase	Prosthetic Limb Toe Tip	Location in Swing Phase	Sound Limb Toe Tip	Location in Swing Phase
1	6.86	32.5%	3.63	32.5%
	7.91	47%	N/A	MFC
	13.10	67.5%	7.23	67.5%
2	7.59	32.5%	4.11	32.5%
	N/A	MFC	2.75	43%
	18.29	67.5%	8.35	67.5%
3	7.43	32.5%	4.69	32.5%
	6.98	46%	2.99	46%
	15.13	67.5%	8.27	67.5%
4	6.49	32.5%	3.31	32.5%
	7.33	49%	N/A	MFC
	12.38	67.5%	7.43	67.5%
5	7.15	32.5%	3.99	32.5%
	N/A	MFC	N/A	MFC
	14.08	67.5%	8.20	67.5%
6	7.92	32.5%	3.97	32.5%
	N/A	MFC	2.00	47%
	18.58	67.5%	7.73	67.5%
7	7.29	32.5%	3.98	32.5%
	7.95	50%	3.26	46%
	11.73	67.5%	6.14	67.5%
8	8.98	32.5%	4.71	32.5%
	N/A	MFC	N/A	MFC
	15.95	67.5%	10.06	67.5%
9	7.25	32.5%	4.45	32.5%
	N/A	MFC	N/A	MFC
	18.22	67.5%	9.73	67.5%

Minimum foot clearance for the toe tip of subject 2 on the sound limb side occurred between 42-53% of the swing phase, with the clearance value ranging from 3.50 cm to 4.84 cm (Figure 28 and Table 12). The prosthetic limb MFC values were smaller than the sound limb, ranging from 1.79 cm to 3.12 cm. For these MFC values, the corresponding location was during initial swing, ranging from 29-31% of the swing phase. Only two swing phases for the prosthetic limb and two swing phases for the sound limb did not have identifiable MFC values. Across all nine swing phases, the prosthetic limb had a smaller clearance at 32.5% of the swing phase compared to the sound limb: $2.87 \text{ cm} \pm 0.51 \text{ cm}$ and $4.98 \pm 0.61 \text{ cm}$, respectively. An opposing pattern was seen at 67.5% of the swing phase, as the prosthetic limb toe tip height was $21.76 \text{ cm} \pm 1.65 \text{ cm}$ and the sound limb toe tip height was $7.81 \text{ cm} \pm 1.03 \text{ cm}$.

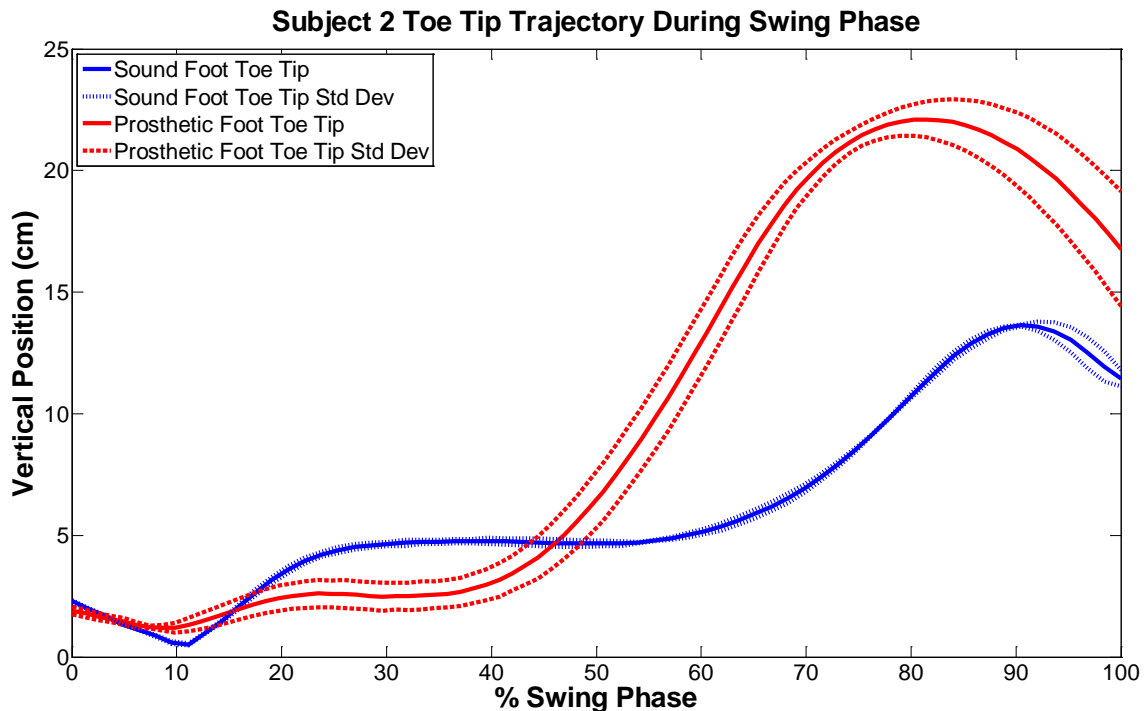


Figure 28. Comparison of mean toe tip trajectory across 3 steps for the sound foot and prosthetic foot of subject 2; dashed lines indicate standard deviation. Zero percent of the swing phase is identified by initial forefoot motion, 100% of the swing phase is identified by heel-strike.

Table 12. Subject 2 MFC values during the swing phase. Highlighted values are the MFC events identified by a clear local minimum point during the swing phase.

Prosthetic Limb and Sound Limb Minimum Foot Clearance Values (cm)				
Swing Phase	Prosthetic Limb Toe Tip	Location in Swing Phase	Sound Limb Toe Tip	Location in Swing Phase
1	3.84	32.5%	5.11	32.5%
	N/A	MFC	N/A	MFC
	23.74	67.5%	7.85	67.5%
2	3.18	32.5%	4.94	32.5%
	3.12	29%	N/A	MFC
	22.71	67.5%	9.69	67.5%
3	3.01	32.5%	4.76	32.5%
	2.52	30%	4.06	46%
	22.63	67.5%	8.46	67.5%
4	2.66	32.5%	4.61	32.5%
	2.65	31%	4.16	42%
	20.24	67.5%	8.40	67.5%
5	1.95	32.5%	4.88	32.5%
	1.79	31%	4.50	51%
	20.20	67.5%	8.26	67.5%
6	2.98	32.5%	4.77	32.5%
	2.77	31%	4.35	52%
	20.56	67.5%	6.45	67.5%
7	2.65	32.5%	5.20	32.5%
	2.57	31%	4.84	53%
	19.52	67.5%	6.62	67.5%
8	2.62	32.5%	6.39	32.5%
	N/A	MFC	4.01	47%
	22.34	67.5%	7.51	67.5%
9	2.90	32.5%	4.13	32.5%
	2.76	29%	3.50	45%
	23.89	67.5%	7.04	67.5%

Subject 3 had a clearly defined local minimum point within all swing phases for identifying the toe tip MFC. For the sound limb, the MFC value ranged from 2.60 cm to 3.45 cm, occurring between 43-57% of the swing phase (Figure 29 and Table 13). The prosthetic limb MFC values were smaller than those for the sound limb. The range of MFC values for the prosthetic limb was 0.73 cm to 2.39 cm, and the location within the swing phase for these values was 45-49%. For the transition points within the swing phase, the prosthetic limb toe tip average clearance at 32.5% was 2.56 cm \pm 0.36 cm, and 16.01 cm \pm 1.88 cm at 67.5%. For the sound limb, the toe tip height at 32.5% of the swing phase was 3.69 cm \pm 0.48 cm, and 5.55 cm \pm 1.23 cm at 67.5%.

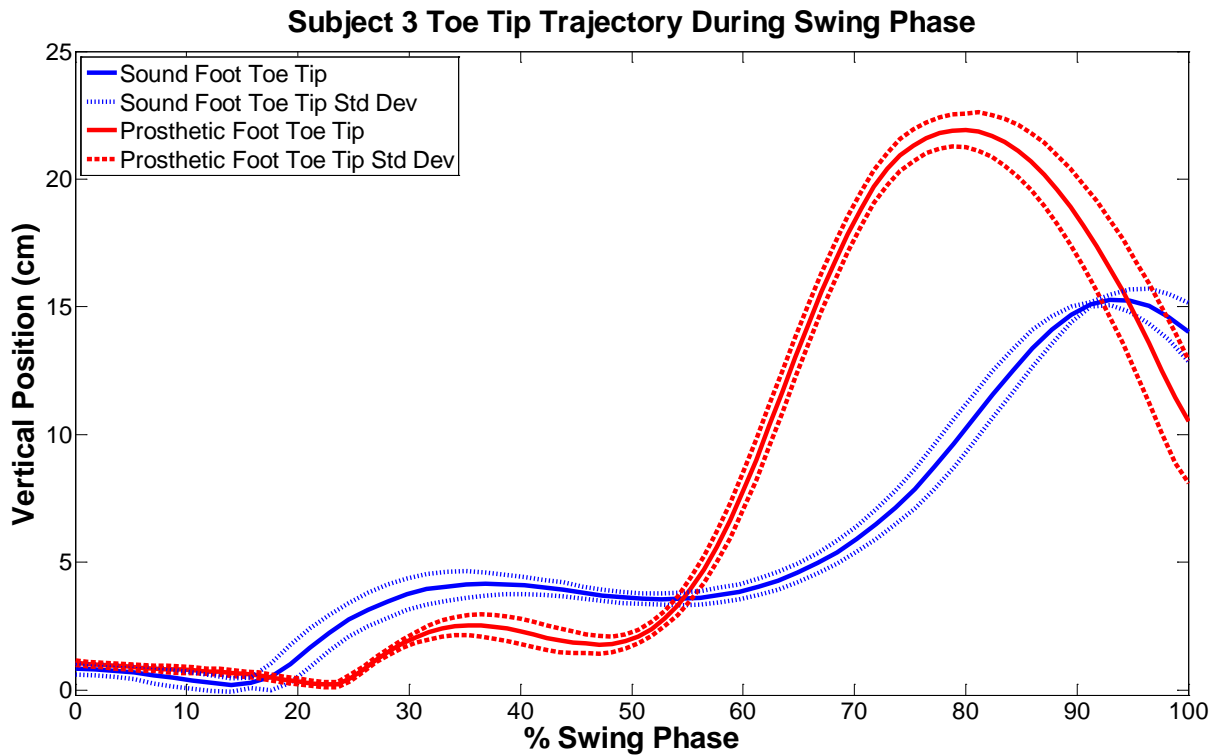


Figure 29. Comparison of mean toe tip trajectory across 3 steps for the sound foot and prosthetic foot of subject 3; dashed lines indicate standard deviation. Zero percent of the swing phase is identified by initial forefoot motion, 100% of the swing phase is identified by heel-strike.

Table 13. Subject 3 MFC values during the swing phase. Highlighted values are the MFC events identified by a clear local minimum point during the swing phase.

Prosthetic Limb and Sound Limb Minimum Foot Clearance Values (cm)				
Swing Phase	Prosthetic Limb Toe Tip	Location in Swing Phase	Sound Limb Toe Tip	Location in Swing Phase
1	1.94	32.5%	3.33	32.5%
	1.03	47%	2.60	57%
	16.10	67.5%	4.09	67.5%
2	2.47	32.5%	4.04	32.5%
	1.68	49%	3.22	43%
	13.88	67.5%	7.68	67.5%
3	3.05	32.5%	3.32	32.5%
	2.39	47%	2.84	50%
	15.09	67.5%	5.60	67.5%
4	2.60	32.5%	3.11	32.5%
	1.68	49%	2.67	55%
	14.32	67.5%	4.56	67.5%
5	2.94	32.5%	3.56	32.5%
	2.23	46%	2.97	48%
	18.49	67.5%	6.50	67.5%
6	2.72	32.5%	3.51	32.5%
	1.54	47%	2.87	56%
	16.33	67.5%	3.87	67.5%
7	2.69	32.5%	4.69	32.5%
	1.22	49%	3.45	54%
	14.95	67.5%	5.35	67.5%
8	2.47	32.5%	3.77	32.5%
	1.12	48%	3.16	49%
	15.41	67.5%	6.22	67.5%
9	2.12	32.5%	3.90	32.5%
	0.73	45%	2.96	53%
	19.51	67.5%	6.12	67.5%

The minimum foot clearance of the toe tip for subject 4 on the sound limb side ranged from 2.12 cm to 3.11 cm, located between 43-52% of the swing phase (Figure 30 and Table 14). No MFC points were able to be identified in the prosthetic limb toe tip trajectory due to a plateau pattern consistently present during swing. While clearly identifiable MFC points cannot be compared between the prosthetic and sound limb, the toe tip clearances at 32.5% and 67.5% of the swing phase can be compared in order to understand differences between limbs during swing. At 32.5% of the swing phase, the height of the toe tip was very similar between limbs, with an average of 3.23 cm \pm 0.46 cm for the prosthetic limb and an average of 3.25 cm \pm 0.57 cm for the sound limb. The prosthetic limb toe tip height at 67.5% of the swing phase was 17.42 cm \pm 1.90 cm while the sound limb toe tip height was only 6.68 cm \pm 0.92 cm.

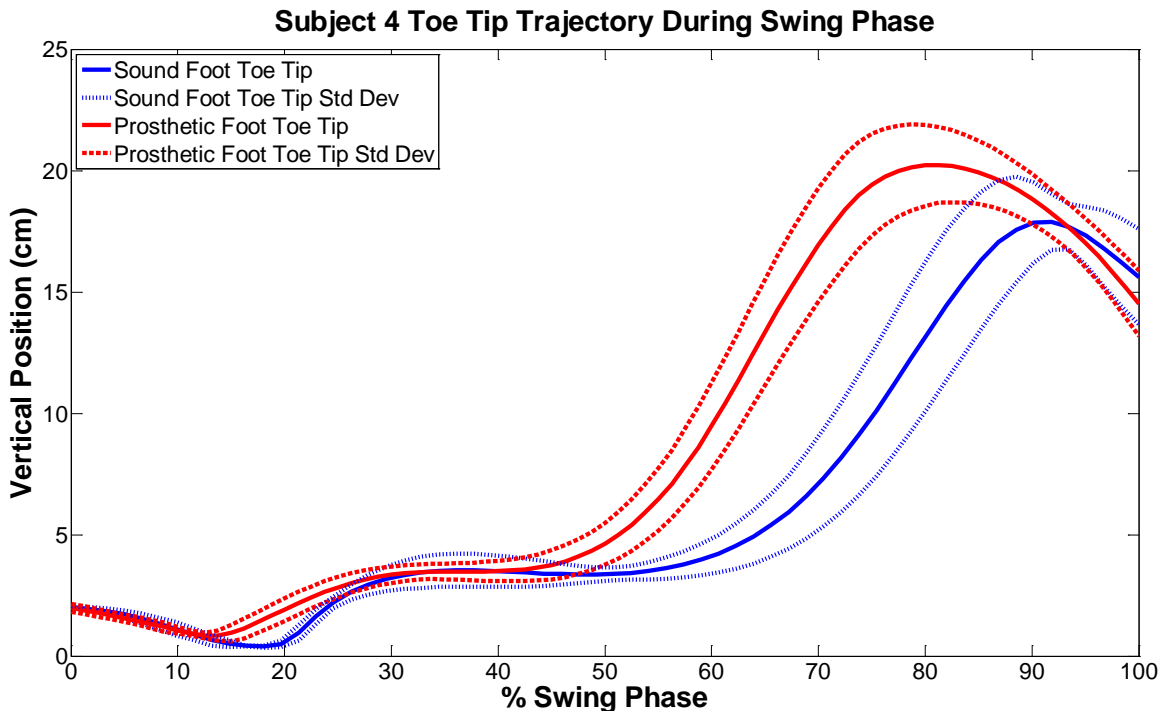


Figure 30. Comparison of mean toe tip trajectory across 3 steps for the sound foot and prosthetic foot of subject 4; dashed lines indicate standard deviation. Zero percent of the swing phase is identified by initial forefoot motion, 100% of the swing phase is identified by heel-strike.

Table 14. Subject 4 MFC values during the swing phase. Highlighted values are the MFC events identified by a clear local minimum point during the swing phase.

Prosthetic Limb and Sound Limb Minimum Foot Clearance Values (cm)				
Swing Phase	Prosthetic Limb Toe Tip	Location in Swing Phase	Sound Limb Toe Tip	Location in Swing Phase
1	3.80	32.5%	2.38	32.5%
	N/A	MFC	N/A	MFC
	18.37	67.5%	7.09	67.5%
2	3.51	32.5%	2.93	32.5%
	N/A	MFC	2.12	43%
	17.48	67.5%	7.73	67.5%
3	2.67	32.5%	3.69	32.5%
	N/A	MFC	2.32	52%
	18.41	67.5%	5.27	67.5%
4	2.77	32.5%	3.86	32.5%
	N/A	MFC	N/A	MFC
	18.26	67.5%	7.86	67.5%
5	3.29	32.5%	2.97	32.5%
	N/A	MFC	2.33	47%
	19.81	67.5%	5.90	67.5%
6	2.60	32.5%	3.03	32.5%
	N/A	MFC	2.62	49%
	13.80	67.5%	5.73	67.5%
7	3.14	32.5%	2.72	32.5%
	N/A	MFC	N/A	MFC
	15.04	67.5%	7.19	67.5%
8	3.72	32.5%	3.88	32.5%
	N/A	MFC	3.11	52%
	18.71	67.5%	7.10	67.5%
9	3.61	32.5%	3.83	32.5%
	N/A	MFC	2.86	51%
	16.94	67.5%	6.29	67.5%

The MFC analysis for subject 5 was able to utilize the marker set developed in this thesis for identifying the bottom of the shoe sole. As a result, variations were seen in which forefoot marker had the overall smallest MFC value. Figure 31 provides a comparison between the sound foot and prosthetic foot motion during gait, with focus set on one swing phase. Since this subject kept the prosthetic knee extended during the swing phase the prosthetic limb foot motion was very flat. There was minimal heel rise in the prosthetic foot which led to an increase in toe tip height until the foot began to move down toward the floor immediately prior to heel-strike.

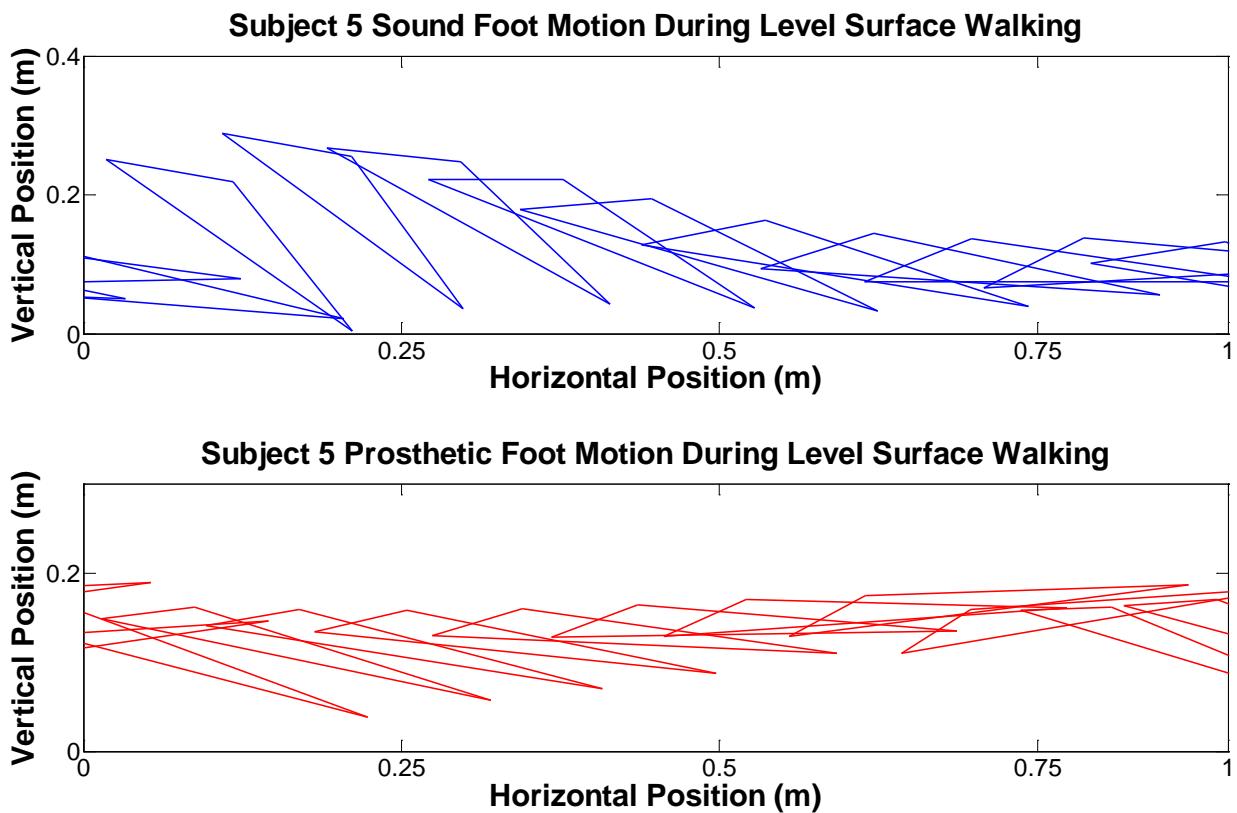


Figure 31. Comparison of the sound foot and prosthetic foot motion for subject 5. Note the sound foot heel rise in comparison to the vertical and forward motion of the prosthetic foot. This figure display is set to approximately one swing phase for each foot.

Subject 5 had a definitive MFC point within the swing motion of the sound foot for all of the forefoot markers (Figure 32 and Table 15). The front forefoot marker had the smallest MFC value out of all of the forefoot markers the most often among the nine swing phases analyzed, with values ranging from 1.80 cm to 3.21 cm within 62-65% of the swing phase. In terms of the 32.5% and 67.5% transition points between initial swing, midswing, and terminal swing, across all swing phases the sound limb clearance at 32.5% was $0.35 \text{ cm} \pm 0.17 \text{ cm}$, and $2.45 \text{ cm} \pm 0.41 \text{ cm}$ at 67.5%. As seen in Table 15, the toe tip position always had the smallest clearance at 32.5% of the swing phase, while either the break forefoot for middle forefoot positions had the smallest clearance at 67.5% of the swing phase.

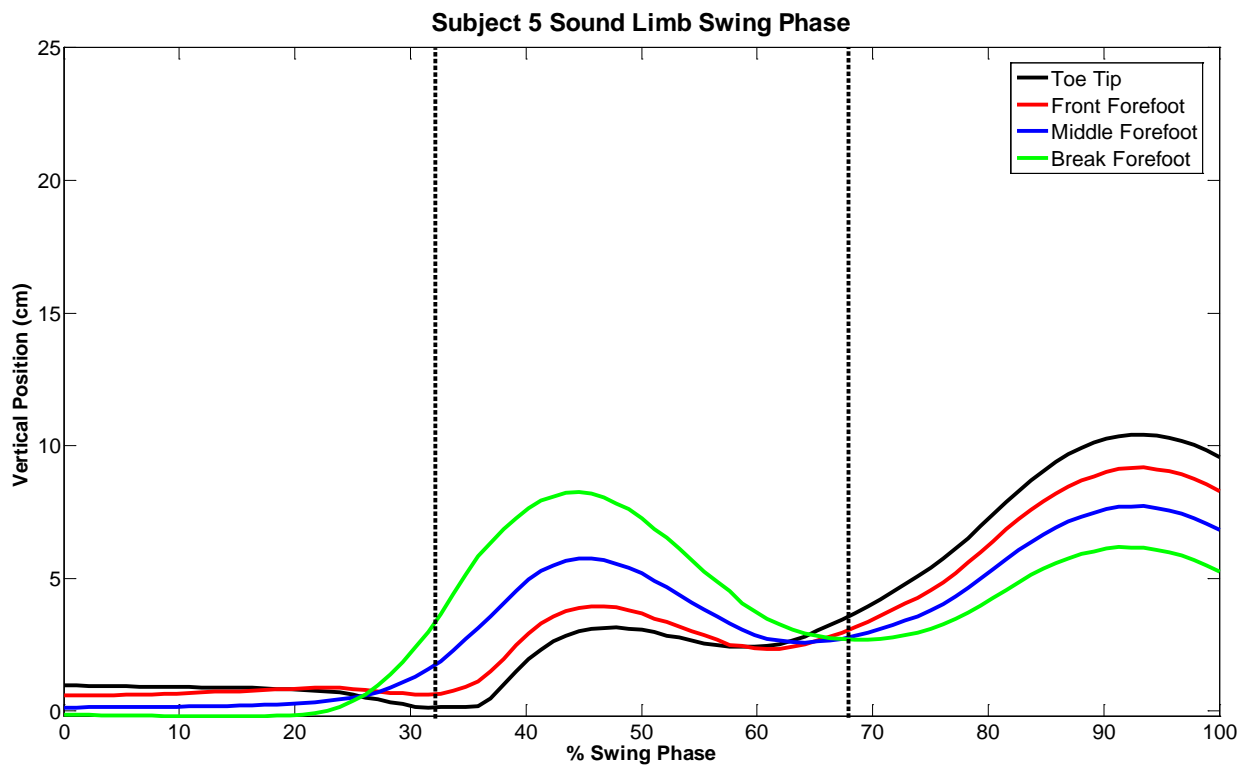


Figure 32. Sound limb forefoot marker trajectories for subject 5 during one swing phase.

Table 15. All forefoot clearance values for the sound limb of subject 5 during swing. Highlighted values correspond to the overall smallest clearance value for each location in the swing phase (32.5%, 67.5%, and the identified MFC point).

Sound Limb Minimum Foot Clearance Values (cm)					
Swing Phase	Location in Swing Phase	Toe Tip	Front Forefoot	Middle Forefoot	Break Forefoot
1	32.5%	0.14	0.64	1.88	3.65
	MFC	2.43 (59%)	2.34 (62%)	2.58 (65%)	2.69 (70%)
	67.5%	3.46	2.95	2.72	2.71
2	32.5%	0.27	0.62	1.40	2.62
	MFC	2.75 (63%)	2.60 (65%)	2.62 (70%)	2.40 (74%)
	67.5%	3.07	2.70	2.63	2.80
3	32.5%	0.41	0.80	1.83	3.35
	MFC	3.29 (64%)	3.21 (65%)	3.28 (68%)	3.25 (71%)
	67.5%	3.93	3.48	3.30	3.36
4	32.5%	0.73	1.73	3.85	6.67
	MFC	2.52 (58%)	2.43 (62%)	2.50 (65%)	2.42 (67%)
	67.5%	4.03	3.43	2.89	2.49
5	32.5%	0.21	0.90	2.51	4.71
	MFC	2.28 (62%)	2.79 (63%)	2.24 (65%)	2.27 (68%)
	67.5%	3.37	2.79	2.43	2.27
6	32.5%	0.33	1.05	2.78	5.15
	MFC	1.99 (62%)	1.96 (64%)	2.09 (68%)	2.00 (73%)
	67.5%	2.66	2.27	2.11	2.17
7	32.5%	0.42	1.20	2.97	5.38
	MFC	1.99 (61%)	1.86 (63%)	1.93 (65%)	1.97 (67%)
	67.5%	3.52	2.83	2.35	2.02
8	32.5%	0.28	0.94	2.28	4.16
	MFC	1.88 (62%)	1.80 (63%)	1.93 (65%)	2.05 (68%)
	67.5%	3.15	2.63	2.25	2.05
9	32.5%	0.39	1.23	3.13	5.69
	MFC	2.43 (64%)	2.30 (65%)	2.41 (67%)	2.45 (71%)
	67.5%	2.98	2.57	2.43	2.53

The prosthetic foot motion of subject 5 did not yield any identifiable MFC points during swing (Figure 33). However, at 32.5% of the swing phase the average clearance was 3.73 cm \pm 0.53 cm. The front forefoot position had the smallest overall clearance of the forefoot markers at this transition point most often (Table 16). At 67.5% of swing, the break forefoot position always had the smallest clearance resulting in an average of 10.44 cm \pm 1.94 cm across all swing phases. The clearance values for the prosthetic limb at the transition points were higher than those of the sound limb. Table 17 provides an overall comparison of the prosthetic and sound limb MFC results.

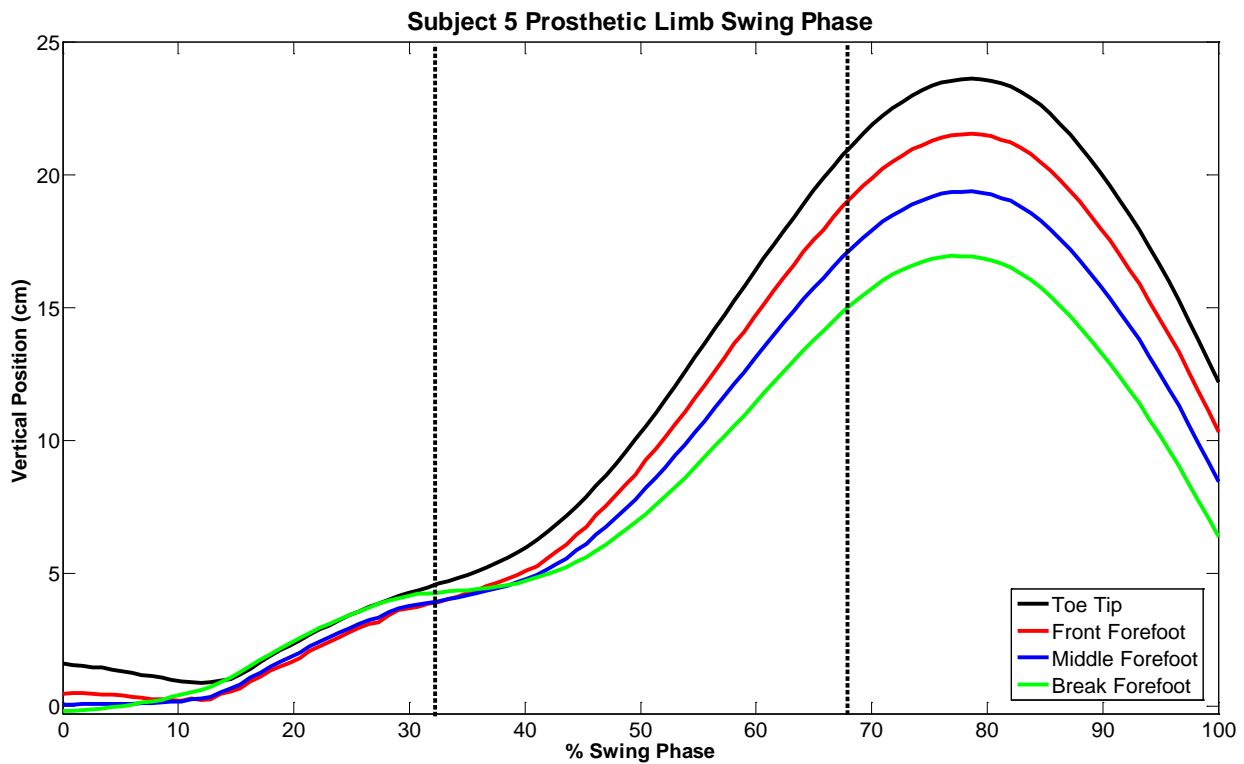


Figure 33. Prosthetic limb forefoot marker trajectories for subject 5 during one swing phase.

Table 16. All resulting clearance values for the prosthetic limb of subject 5 during swing. Highlighted values correspond to the overall smallest clearance value for each location in the swing phase (32.5% and 67.5%). MFC could not be determined for the prosthetic limb during swing due to no local minimum point in the trajectory data.

Prosthetic Limb Minimum Foot Clearance Values (cm)					
Swing Phase	Location in Swing Phase	Toe Tip	Front Forefoot	Middle Forefoot	Break Forefoot
1	32.5%	4.61	3.92	3.94	4.27
	MFC	N/A	N/A	N/A	N/A
	67.5%	20.77	18.84	16.94	14.85
2	32.5%	5.80	4.92	4.64	4.60
	MFC	N/A	N/A	N/A	N/A
	67.5%	17.13	15.30	13.65	11.88
3	32.5%	5.70	4.77	4.50	4.46
	MFC	N/A	N/A	N/A	N/A
	67.5%	16.04	14.29	12.69	10.98
4	32.5%	3.62	3.02	3.10	3.49
	MFC	N/A	N/A	N/A	N/A
	67.5%	15.29	13.57	11.98	10.30
5	32.5%	4.48	3.74	3.72	4.00
	MFC	N/A	N/A	N/A	N/A
	67.5%	13.86	12.14	10.67	9.14
6	32.5%	4.20	3.54	3.64	4.05
	MFC	N/A	N/A	N/A	N/A
	67.5%	13.77	12.11	10.59	8.98
7	32.5%	4.30	3.63	3.63	3.92
	MFC	N/A	N/A	N/A	N/A
	67.5%	13.64	11.90	10.41	8.84
8	32.5%	4.17	3.47	3.51	3.86
	MFC	N/A	N/A	N/A	N/A
	67.5%	14.73	12.91	11.34	9.66
9	32.5%	3.98	3.22	3.34	3.78
	MFC	N/A	N/A	N/A	N/A
	67.5%	14.09	12.41	10.90	9.31

Table 17. Subject 5 clearance values during the swing phase. For each swing phase the smallest value among all forefoot markers is reported at MFC, 32.5% and 67.5% of the swing phase, along with the associated marker position. Highlighted values are the MFC events identified by a clear local minimum point during the swing phase.

Prosthetic Limb and Sound Limb Minimum Foot Clearance Values (cm)						
Swing Phase	Prosthetic Limb MFC	Location in Swing Phase	Forefoot Position	Sound Limb MFC	Location in Swing Phase	Forefoot Position
1	3.92	32.5%	Front	0.14	32.5%	Toe Tip
	N/A	MFC	N/A	2.34	62%	Front
	14.85	67.5%	Break	2.71	67.5%	Break
2	4.60	32.5%	Break	0.27	32.5%	Toe Tip
	N/A	MFC	N/A	2.40	74%	Break
	11.88	67.5%	Break	2.63	67.5%	Middle
3	4.46	32.5%	Break	0.41	32.5%	Toe Tip
	N/A	MFC	N/A	3.21	65%	Front
	10.98	67.5%	Break	3.30	67.5%	Middle
4	3.02	32.5%	Front	0.73	32.5%	Toe Tip
	N/A	MFC	N/A	2.42	67%	Break
	10.30	67.5%	Break	2.49	67.5%	Break
5	3.72	32.5%	Middle	0.21	32.5%	Toe Tip
	N/A	MFC	N/A	2.24	65%	Middle
	9.14	67.5%	Break	2.27	67.5%	Break
6	3.54	32.5%	Front	0.33	32.5%	Toe Tip
	N/A	MFC	N/A	1.96	64%	Front
	8.98	67.5%	Break	2.11	67.5%	Middle
7	3.63	32.5%	Front & Middle	0.42	32.5%	Toe Tip
	N/A	MFC	N/A	1.86	63%	Front
	8.84	67.5%	Break	2.02	67.5%	Break
8	3.47	32.5%	Front	0.28	32.5%	Toe Tip
	N/A	MFC	N/A	1.80	63%	Front
	9.66	67.5%	Break	2.05	67.5%	Break
9	3.22	32.5%	Front	0.39	32.5%	Toe Tip
	N/A	MFC	N/A	2.30	65%	Front
	9.31	67.5%	Break	2.43	67.5%	Middle

Subject 6 prosthetic and sound limb foot motion during the swing phase is shown in Figure 34. Heel rise of the prosthetic foot was slightly higher than the sound foot.

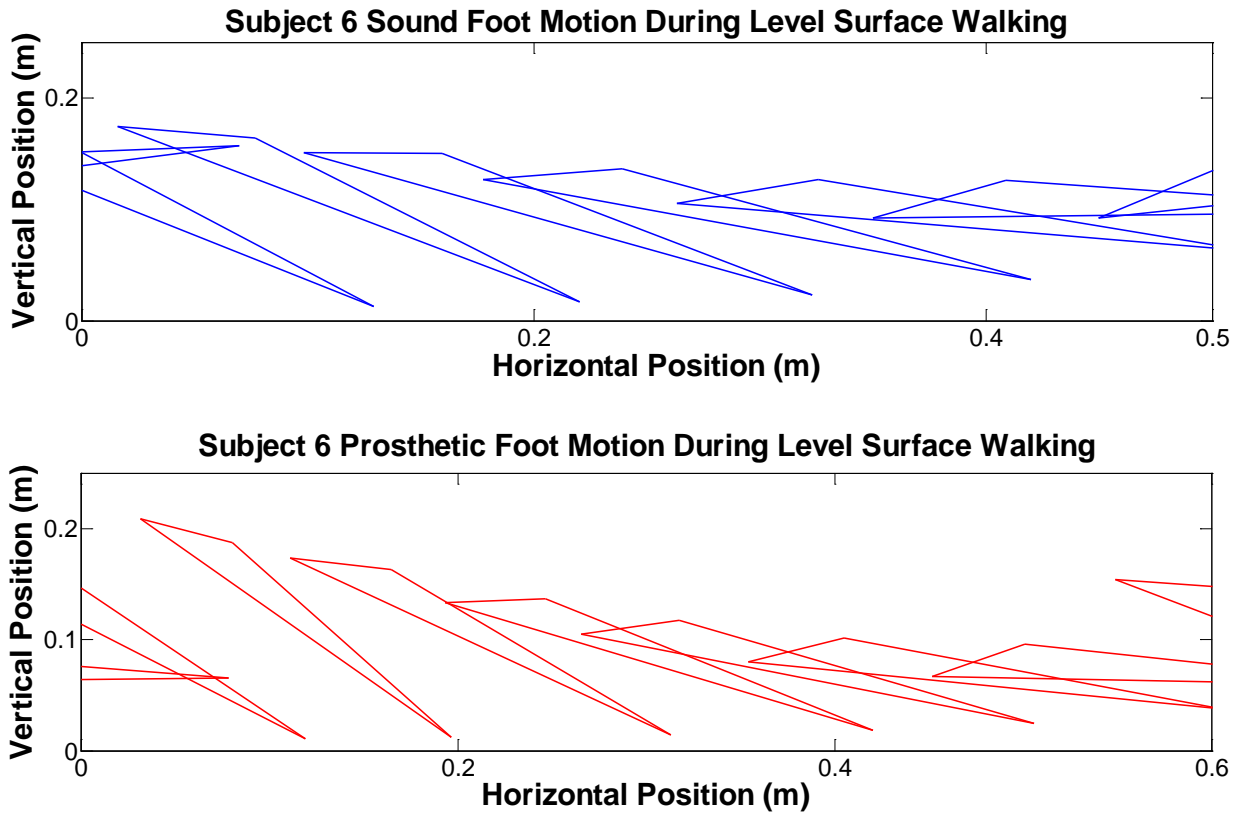


Figure 34. Comparison of the sound foot and prosthetic foot motion for subject 6 during one swing phase. This figure display is set to approximately one swing phase for each foot.

Subject 6 had a distinguished MFC point for all forefoot markers on the sound foot except the toe tip (Figure 35 and Table 18). These MFC values ranged from 0.46 cm to 1.87 cm and occurred between 51-88% of the swing phase. Since a clear MFC value could not be identified for the toe tip during swing, values reported at the transition points between the three sub-phases of swing provide an understanding of the foot clearance. At 32.5% of the swing phase the sound limb average clearance was $1.05 \text{ cm} \pm 0.28 \text{ cm}$, determined from the overall smallest clearance value in each swing phase. Most often the forefoot position had the overall smallest clearance at this transition point. At 67.5% of the swing phase, the average overall smallest clearance among the forefoot markers was $1.13 \text{ cm} \pm 0.38 \text{ cm}$, usually occurring at the break forefoot position.

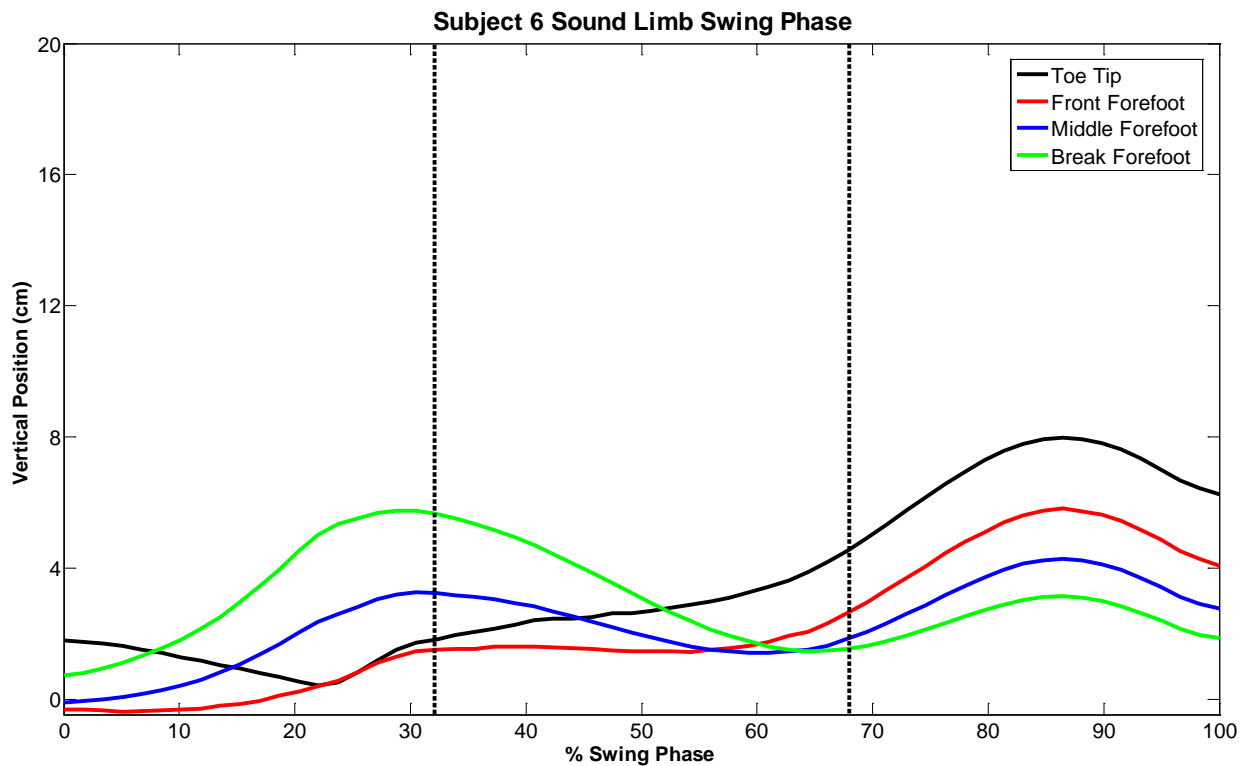


Figure 35. Sound limb forefoot marker trajectories for subject 6 during one swing phase.

Table 18. All forefoot clearance values for the sound limb of subject 6 during swing. Highlighted values correspond to the overall smallest clearance value for each location in the swing phase (32.5% and 67.5%). MFC results are not available for the toe tip position because no identifiable local minimum point for this trajectory was present during swing.

Sound Limb Minimum Foot Clearance Values (cm)					
Swing Phase	Location in Swing Phase	Toe Tip	Front Forefoot	Middle Forefoot	Break Forefoot
1	32.5%	1.81	1.50	3.24	5.67
	MFC	N/A	1.44 (56%)	1.41 (63%)	1.46 (66%)
	67.5%	4.52	2.63	1.84	1.54
2	32.5%	1.50	1.20	2.91	5.32
	MFC	N/A	0.82 (55%)	0.89 (62%)	1.03 (69%)
	67.5%	3.50	1.71	1.11	1.03
3	32.5%	1.55	1.27	3.12	5.64
	MFC	N/A	1.28 (54%)	1.33 (65%)	1.39 (72%)
	67.5%	3.50	1.82	1.38	1.48
4	32.5%	1.57	1.18	2.80	5.09
	MFC	N/A	0.81 (58%)	0.76 (67%)	0.82 (71%)
	67.5%	2.96	1.28	0.80	0.86
5	32.5%	1.41	1.09	2.82	5.24
	MFC	N/A	0.85 (57%)	0.83 (66%)	0.91 (69%)
	67.5%	3.31	1.50	0.94	0.91
6	32.5%	1.19	0.83	2.51	4.87
	MFC	N/A	0.46 (51%)	0.65 (62%)	0.85 (69%)
	67.5%	3.46	1.65	1.02	0.89
7	32.5%	1.33	0.98	2.73	5.16
	MFC	N/A	0.90 (54%)	0.84 (61%)	0.86 (67%)
	67.5%	3.75	1.86	1.13	0.89
8	32.5%	0.98	0.88	2.77	5.35
	MFC	N/A	1.11 (59%)	0.86 (67%)	0.84 (69%)
	67.5%	3.21	1.46	0.88	0.84
9	32.5%	0.53	0.60	2.76	5.60
	MFC	N/A	1.87 (74%)	1.42 (81%)	1.17 (88%)
	67.5%	3.45	1.90	1.88	2.45

Subject 6 had fewer MFC points identified during swing of the prosthetic limb in comparison to the sound limb. Only the toe tip, middle forefoot and break forefoot positions yielded trajectories having a clear local minimum (Figure 36). Of these MFC values, the smallest clearance was 0.78 cm at the middle forefoot position, and the largest clearance was 2.24 cm at the break forefoot position (Table 19). A pattern among these MFC values showed the toe tip MFC occurred between 10-13% of the swing phase, the middle forefoot MFC occurred between 28-36% of swing, and the break forefoot MFC occurred between 34-43% of swing. Figure 36 supports this pattern, as the forefoot markers undergo changes in vertical displacement earlier within the swing phase compared to other subjects. At 32.5% of the swing phase the prosthetic limb clearance was similar to the sound limb, with a value of $1.06 \text{ cm} \pm 0.33 \text{ cm}$. At 67.5% of the swing phase the average smallest clearance was $8.36 \text{ cm} \pm 1.35 \text{ cm}$ for the prosthetic limb. Table 20 provides a comparison of the minimum foot clearance values between the prosthetic and sound limb.

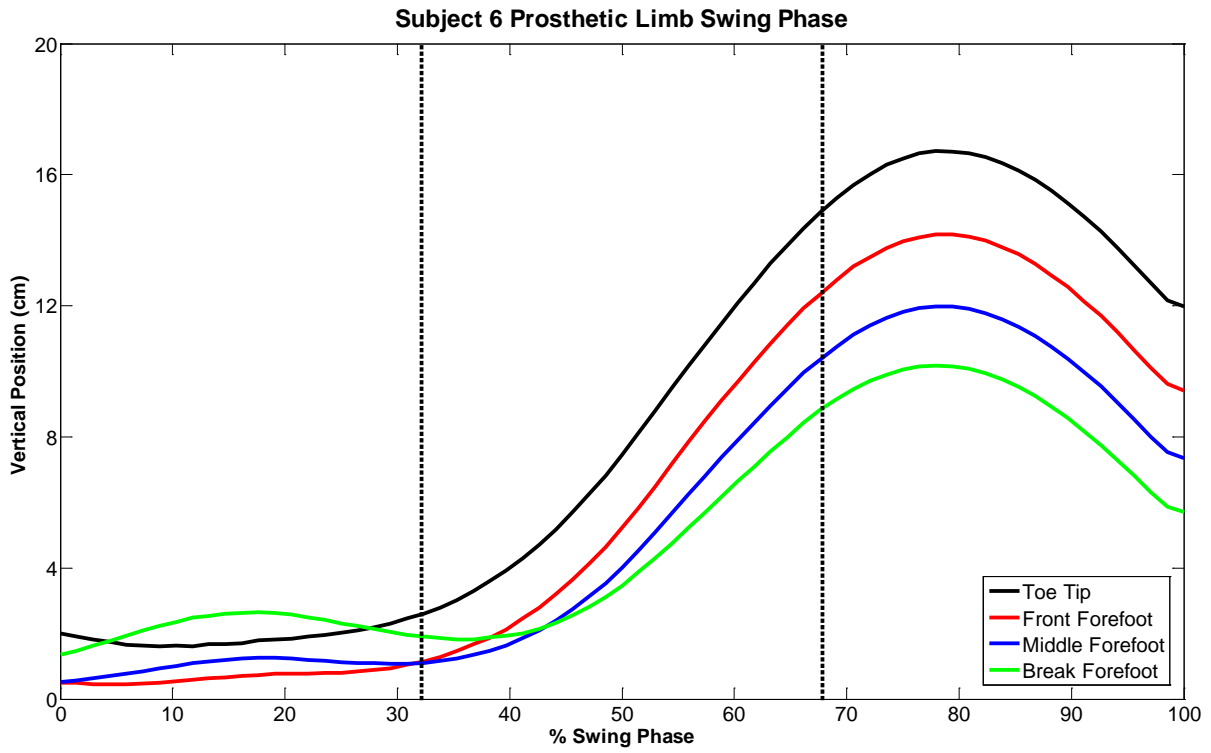


Figure 36. Prosthetic limb forefoot marker trajectories for subject 6 during one swing phase.

Table 19. All resulting clearance values for the prosthetic limb of subject 6 during swing. Highlighted values correspond to the overall smallest clearance value for each location in the swing phase (32.5% and 67.5%). MFC results that were not able to be identified are indicated with N/A.

Prosthetic Limb Minimum Foot Clearance Values (cm)					
Swing Phase	Location in Swing Phase	Toe Tip	Front Forefoot	Middle Forefoot	Break Forefoot
1	32.5%	2.60	1.14	1.10	1.90
	MFC	1.60 (10%)	N/A	N/A	1.81 (37%)
	67.5%	14.85	12.35	10.36	8.82
2	32.5%	2.06	0.70	0.84	1.83
	MFC	1.38 (13%)	N/A	N/A	1.59 (39%)
	67.5%	14.80	12.34	10.31	8.73
3	32.5%	2.79	1.26	1.09	1.73
	MFC	N/A	N/A	0.99 (28%)	1.73 (34%)
	67.5%	14.94	12.45	10.43	8.85
4	32.5%	3.35	1.74	1.58	2.24
	MFC	1.49 (10%)	N/A	N/A	2.24 (34%)
	67.5%	15.65	13.05	10.96	9.33
5	32.5%	3.13	1.65	1.47	2.13
	MFC	1.44 (10%)	N/A	N/A	2.13 (34%)
	67.5%	15.26	12.77	10.77	9.23
6	32.5%	2.32	0.92	0.94	1.80
	MFC	1.26 (11%)	N/A	0.91 (31%)	1.73 (38%)
	67.5%	16.32	13.85	11.75	10.07
7	32.5%	2.03	0.70	0.81	1.78
	MFC	1.51 (12%)	N/A	0.78 (35%)	1.35 (43%)
	67.5%	12.01	9.59	7.65	6.19
8	32.5%	2.54	1.22	1.31	2.25
	MFC	1.50 (13%)	N/A	1.29 (36%)	1.94 (43%)
	67.5%	12.06	9.65	7.75	6.34
9	32.5%	2.11	0.73	0.85	1.82
	MFC	1.26 (10%)	N/A	0.85 (34%)	1.61 (39%)
	67.5%	13.55	11.07	9.13	7.66

Table 20. Subject 6 MFC values during the swing phase. For each swing phase the smallest value among all forefoot markers is reported at 32.5% and 67.5% of the swing phase, along with the associated marker position. A MFC event could not be identified by a clear local minimum point during the swing phase for all forefoot markers, thus MFC is reported as N/A.

Prosthetic Limb and Sound Limb Minimum Foot Clearance Values (cm)						
Swing Phase	Prosthetic Limb MFC	Location in Swing Phase	Forefoot Position	Sound Limb MFC	Location in Swing Phase	Forefoot Position
1	1.10	32.5%	Middle	1.50	32.5%	Front
	N/A	MFC	N/A	N/A	MFC	N/A
	8.82	67.5%	Break	1.54	67.5%	Break
2	0.70	32.5%	Front	1.20	32.5%	Front
	N/A	MFC	N/A	N/A	MFC	N/A
	8.73	67.5%	Break	1.03	67.5%	Break
3	1.09	32.5%	Middle	1.27	32.5%	Front
	N/A	MFC	N/A	N/A	MFC	N/A
	8.85	67.5%	Break	1.38	67.5%	Middle
4	1.58	32.5%	Middle	1.18	32.5%	Front
	N/A	MFC	N/A	N/A	MFC	N/A
	9.33	67.5%	Break	0.80	67.5%	Middle
5	1.47	32.5%	Middle	1.09	32.5%	Front
	N/A	MFC	N/A	N/A	MFC	N/A
	9.23	67.5%	Break	0.91	67.5%	Break
6	0.92	32.5%	Front	0.83	32.5%	Front
	N/A	MFC	N/A	N/A	MFC	N/A
	10.07	67.5%	Break	0.89	67.5%	Break
7	0.70	32.5%	Front	0.98	32.5%	Front
	N/A	MFC	N/A	N/A	MFC	N/A
	6.19	67.5%	Break	0.89	67.5%	Break
8	1.22	32.5%	Front	0.88	32.5%	Front
	N/A	MFC	N/A	N/A	MFC	N/A
	6.34	67.5%	Break	0.84	67.5%	Break
9	0.73	32.5%	Front	0.53	32.5%	Toe Tip
	N/A	MFC	N/A	N/A	MFC	N/A
	7.66	67.5%	Break	1.88	67.5%	Middle

3.3.2 Stair Ascent

The horizontal, vertical, and resultant minimum clearance values for the forefoot during stair ascent reveal multiple marker positions along the sole of the shoe can have the smallest clearance. The resulting minimum foot clearance for each subject and each variable is provided in Table 21. Results for subjects 1 through 4 only have the toe tip marker available for comparison due to the limited marker set used during the pilot study (Subject 2 toe tip marker had visibility issues during data collection). Appendix C shows all forefoot position results and inferior heel results for stair ascent in order to understand foot placement for each subject.

Table 21. Average minimum resultant, horizontal, and vertical clearances (standard deviation) for the forefoot positions of the sound and prosthetic feet during stair ascent. The forefoot position with the smallest average clearance is presented. Horizontal clearance values are negative because the foot has not passed over the step edge.

Stair Ascent Minimum Foot Clearance Measures and Associated Forefoot Position						
Subject	Resultant Clearance (cm)		Horizontal Clearance (cm)		Vertical Clearance (cm)	
	<i>Sound Limb</i>	<i>Prosthetic Limb</i>	<i>Sound Limb</i>	<i>Prosthetic Limb</i>	<i>Sound Limb</i>	<i>Prosthetic Limb</i>
1	6.46 (2.14) Toe Tip	5.92 (1.31) Toe Tip	-9.34 (7.08) Toe Tip	-9.32 (5.30) Toe Tip	8.51 (0.68) Toe Tip	7.07 (0.38) Toe Tip
2	N/A	3.99 (1.43) Toe Tip	N/A	-5.52 (2.66) Toe Tip	N/A	5.12 (0.65) Toe Tip
3	5.06 (2.15) Toe Tip	4.77 (0.27) Toe Tip	-8.90 (8.57) Toe Tip	-9.68 (1.96) Toe Tip	6.60 (1.93) Toe Tip	4.83 (0.30) Toe Tip
4	4.31 (0.96) Toe Tip	6.28 (0.59) Toe Tip	-6.47 (4.02) Toe Tip	-12.70 (5.64) Toe Tip	5.38 (0.87) Toe Tip	6.34 (0.54) Toe Tip
5	2.55 (0.89) Toe Tip	4.35 (1.42) Break Forefoot	-3.94 (1.87) Toe Tip	-11.30 (3.76) Toe Tip	4.39 (1.43) Toe Tip	4.41 (1.30) Break Forefoot
6	3.00 (0.62) Front Forefoot	0.71 (0.29) Toe Tip	-4.71 (1.30) Toe Tip	-0.75 (0.31) Toe Tip	3.63 (0.70) Front Forefoot	3.54 (2.03) Front Forefoot

For the pilot study subjects, subjects 3 and 4 clearly had a larger horizontal clearance with the prosthetic limb while subject 1 had a horizontal clearance nearly identical between sides. The resultant clearance difference between the sound and prosthetic feet for subjects 1 and 3 was within 1 cm, with the sound limb having a larger clearance. Similarly, the vertical clearance was slightly larger with the sound foot for these two subjects. Subject 4 had larger resultant and vertical minimum clearances with the prosthetic foot.

A more thorough comparison was made for subjects 5 and 6 due to the custom forefoot marker set. Subject 5 had a larger and more variable horizontal clearance with the prosthetic foot compared to the sound foot. Since this subject approached each step with a relatively flat foot angle, the break forefoot marker on the prosthetic foot had the smallest clearance with respect to step edge for both the resultant and vertical clearances. For the sound limb, the toe tip had the smallest resultant and vertical clearances. Despite the differences in location along the forefoot for each foot, the resulting values show the resultant and vertical clearances were larger with the prosthetic limb compared to the sound limb. The forefoot trajectories during ascent for subject 5 are shown in Figures 37-38. As these figures show, the prosthetic foot approached the step at a flatter angle than the sound foot, resulting in the break forefoot position and the toe tip position, respectively, posing the biggest risk of tripping on the step edge.

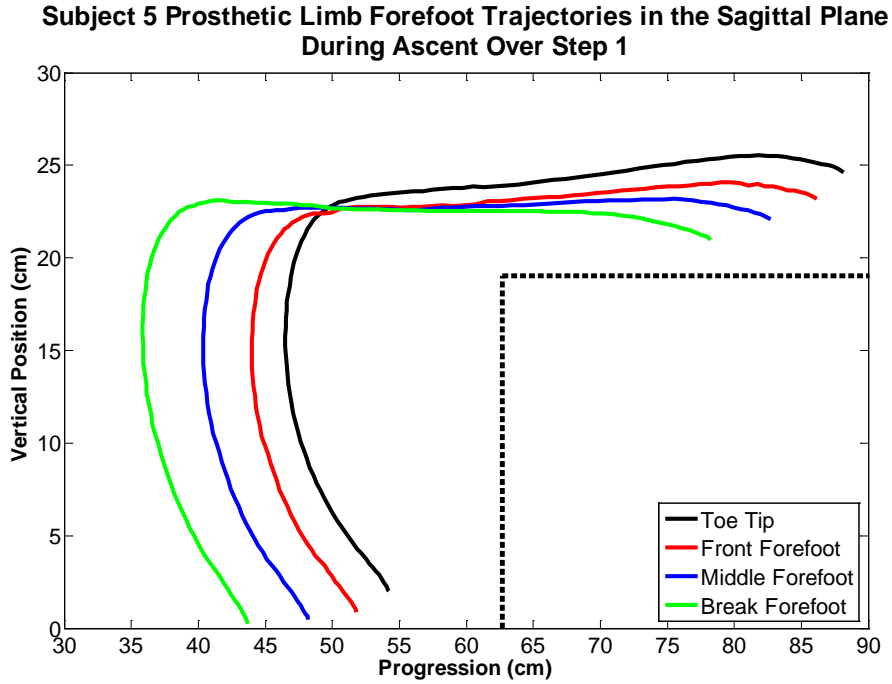


Figure 37. Subject 5 forefoot marker trajectories for the prosthetic limb during stair ascent.

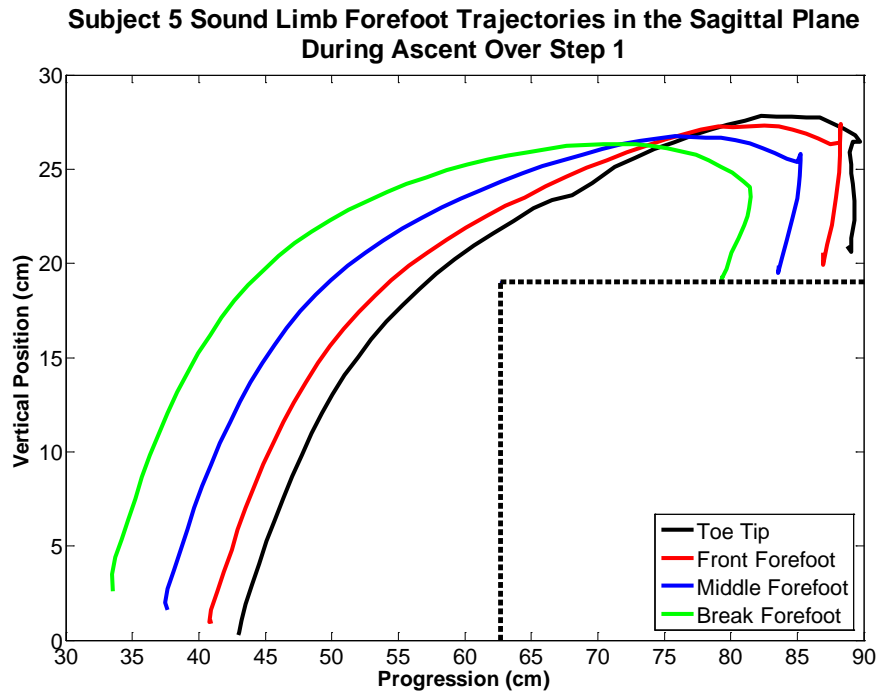


Figure 38. Subject 5 forefoot marker trajectories for the sound limb during stair ascent.

Subject 6 utilized a “sliding” technique with the prosthetic foot, where the toe tip was slid up the step riser (Figures 39-40). This resulted in the prosthetic foot toe tip having the smallest resultant clearance of any forefoot marker, with a value of 0.71 cm. In comparison, the sound foot resultant clearance occurred at the front forefoot position at an average of 3.00 cm from the step edge. The minimum vertical clearance was similar between feet, with the sound limb side having a value 0.09 cm larger than the prosthetic limb side. Both feet had the front forefoot position yield the minimum vertical clearance. For both feet, subject 6’s biggest risk of tripping on the step edge was with respect to the toe tip or front forefoot positions on the sole.

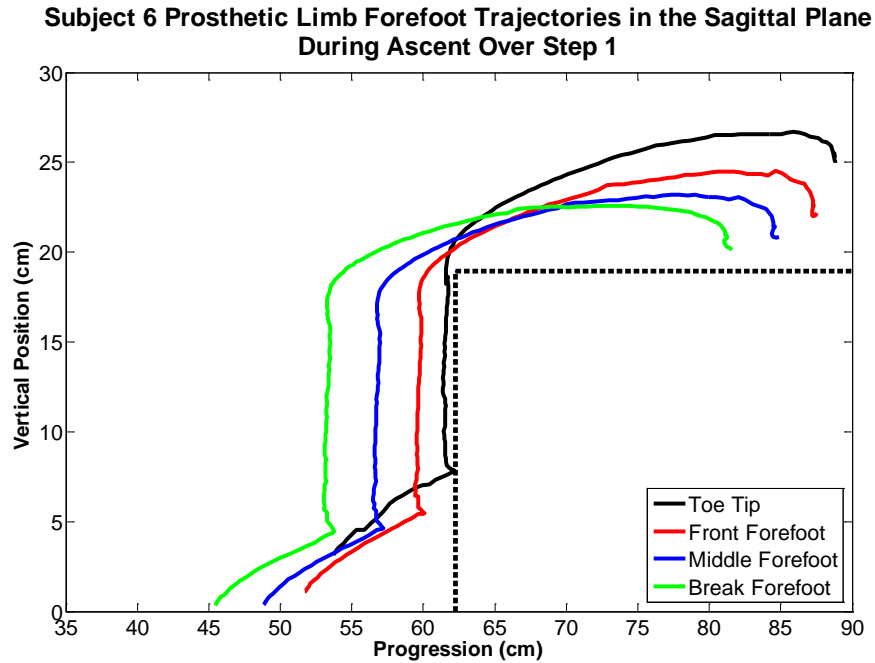


Figure 39. Subject 6 forefoot marker trajectories for the prosthetic limb during stair ascent. A sliding technique was used to progress the foot up the step, where the toe tip slid up the riser.

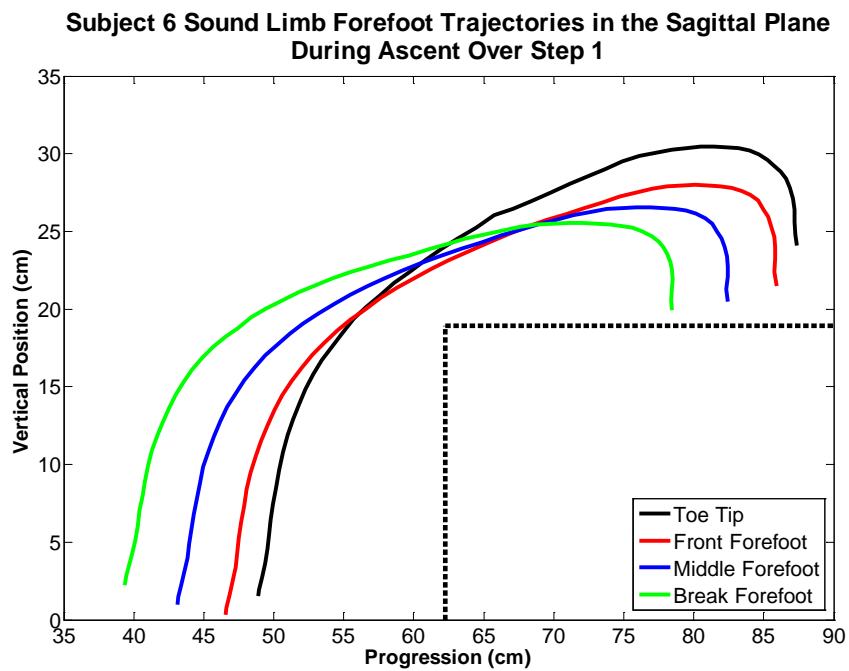


Figure 40. Subject 6 forefoot marker trajectories for the sound limb during stair ascent.

3.3.3 Stair Descent

The inferior heel position was used to determine the minimum clearance distances during stair descent; therefore, the minimum clearance results presented in Table 22 only include subjects 5 and 6. Numerical results for subjects 1 through 4 cannot be provided due to the modified marker set used during the pilot study that did not include an inferior heel marker. The superior heel marker was not used as a substitute because this position on the heel is not likely to cause a trip during stair descent. Results for the forefoot markers during stair descent for each subject are provided in Appendix C to aid in understanding foot movement and placement on a step during descent.

Table 22. Average inferior heel clearance (standard deviation) for the sound and prosthetic feet during stair descent.

Stair Descent Minimum Foot Clearance Measures for the Inferior Heel Position						
Subject	Resultant Clearance (cm)		Horizontal Clearance (cm)		Vertical Clearance (cm)	
	<i>Sound Limb</i>	<i>Prosthetic Limb</i>	<i>Sound Limb</i>	<i>Prosthetic Limb</i>	<i>Sound Limb</i>	<i>Prosthetic Limb</i>
5	3.73 (0.78)	3.85 (0.67)	5.94 (1.37)	11.35 (2.32)	5.31 (2.08)	4.09 (0.83)
6	5.12 (0.61)	4.12 (0.96)	7.52 (1.02)	12.03 (3.38)	5.93 (0.77)	4.19 (0.97)

3.3.4 Responses to Stumbling

A description of the outcome for each stumble perturbation trial is provided in Table 23. A stumble perturbation for the prosthetic limb was successfully induced near midswing for three of the six subjects. Of these, subjects 2 and 4 demonstrated an elevating strategy while subject 5

used a lowering strategy. Subjects 2 and 4 had similar recovery durations, 0.58 seconds and 0.56 seconds, respectively. Subject 5 had a recovery time of 1.47 seconds, and after the subject stepped over the obstacle with the prosthetic limb a fall occurred that required harness and cane support for regaining balance. The recovery strategy and recovery duration for subjects 3 and 6 are also reported in Table 17; further information regarding the stumbling response for these two subjects is presented in Appendix D. Since the obstacle piece became dislodged from the stumbling device upon foot-obstacle contact for subject 3, the recovery strategy is reported as “N/A” but the recovery duration is still evaluated.

Table 23. Outcome for all stumble perturbation trials and the associated recovery strategy and recovery duration.

Subject	Knee Type	Trial Outcome	Recovery Strategy	Recovery Duration (sec)
1	NMPK	Missed obstacle	N/A	N/A
2	MPK	Prosthetic limb obstructed	Elevating	0.58
3	MPK	Dislodged obstacle, stepped on with sound limb	N/A	0.23
4	MPK	Prosthetic limb obstructed	Elevating	0.56
5	NMPK	Prosthetic limb obstructed	Lowering	1.47
6	MPK	Sound limb obstructed	Elevating	0.63

The stumble recovery measures and corresponding level surface walking results for subjects 2, 4, and 5 are presented in Tables 24-26 and Figures 41-49. Similar results for subjects 3 and 6 are presented in Appendix D. Unperturbed level surface walking trials for all subjects,

except subject 1, yielded a range of trunk deviation in the sagittal plane between 11.86 degrees and 39.14 degrees with respect to vertical. In the frontal plane, the trunk angle ranged from 9.68 degrees to the left of vertical to 11.48 degrees to the right of vertical. The angular velocity during unperturbed level surface walking ranged from 12.44 deg/s to 21.47 deg/s.

Table 24. Average maximum and minimum trunk angles and average angular velocity while walking unperturbed over a level surface. Negative frontal plane trunk angles signify trunk tilt to the left of vertical.

Subject	Sagittal Plane (deg)		Frontal Plane (deg)		Angular Velocity (deg/s)
	Average Max	Average Min	Average Max	Average Min	Average
2	28.33	20.46	2.75	-1.86	12.44
4	29.11	23.46	11.48	4.48	15.06
5	31.13	18.30	3.14	-9.68	21.21

Table 25. Trunk angles in the sagittal and frontal planes at foot-obstacle contact, and the maximum and minimum trunk angles occurring during the stumble recovery duration. Negative frontal plane trunk angles signify trunk tilt to the left of vertical.

Subject	Sagittal Plane (deg)			Frontal Plane (deg)		
	At Contact	Recovery Max	Recovery Min	At Contact	Recovery Max	Recovery Min
2	30.68	35.51	28.79	-1.31	1.09	-1.67
4	28.40	32.18	24.84	-0.11	4.27	-0.11
5	23.51	58.17	21.82	-5.30	11.31	-5.60

Table 26. Trunk angular velocity at foot-obstacle contact and the maximum and minimum trunk angular velocity occurring during the stumble recovery duration.

Subject	Angular Velocity (deg/s)		
	At Contact	Recovery Max	Recovery Min
2	11.50	38.50	3.88
4	7.38	40.52	0.70
5	18.10	175.10	4.63

Subject 2 used a cane in each hand while walking to help support body weight and increase stability during stance. Obstruction of the prosthetic foot during swing produced relatively small deviations in the trunk angle in the sagittal and frontal planes when comparing the maximum and minimum angles during the recovery duration to the angles at initial foot-obstacle contact. During recovery, trunk flexion in the sagittal plane increased approximately 5 degrees following contact with the obstacle. Both the maximum and minimum trunk flexion angles in the sagittal plane were greater than the average baseline walking maximum trunk flexion by 7.18 degrees and 0.46 degrees, respectively (Figure 41). The frontal plane trunk angle had a slight tilt to the left as the prosthetic limb (right limb) was elevated over the obstacle, with a shift back toward the right side occurring so gait could continue (Figure 42). Angular velocity at the instant of contact with the obstacle was within 1 deg/s of the average level surface walking angular velocity (Figure 43). During recovery, the angular velocity decreased immediately following contact with the obstacle to 3.88 deg/s before rapidly increasing to 38.50 deg/s. The angular velocity decreased again just prior to heel-strike of the first recovered step.

Subject 2 Sagittal Plane Trunk Angle

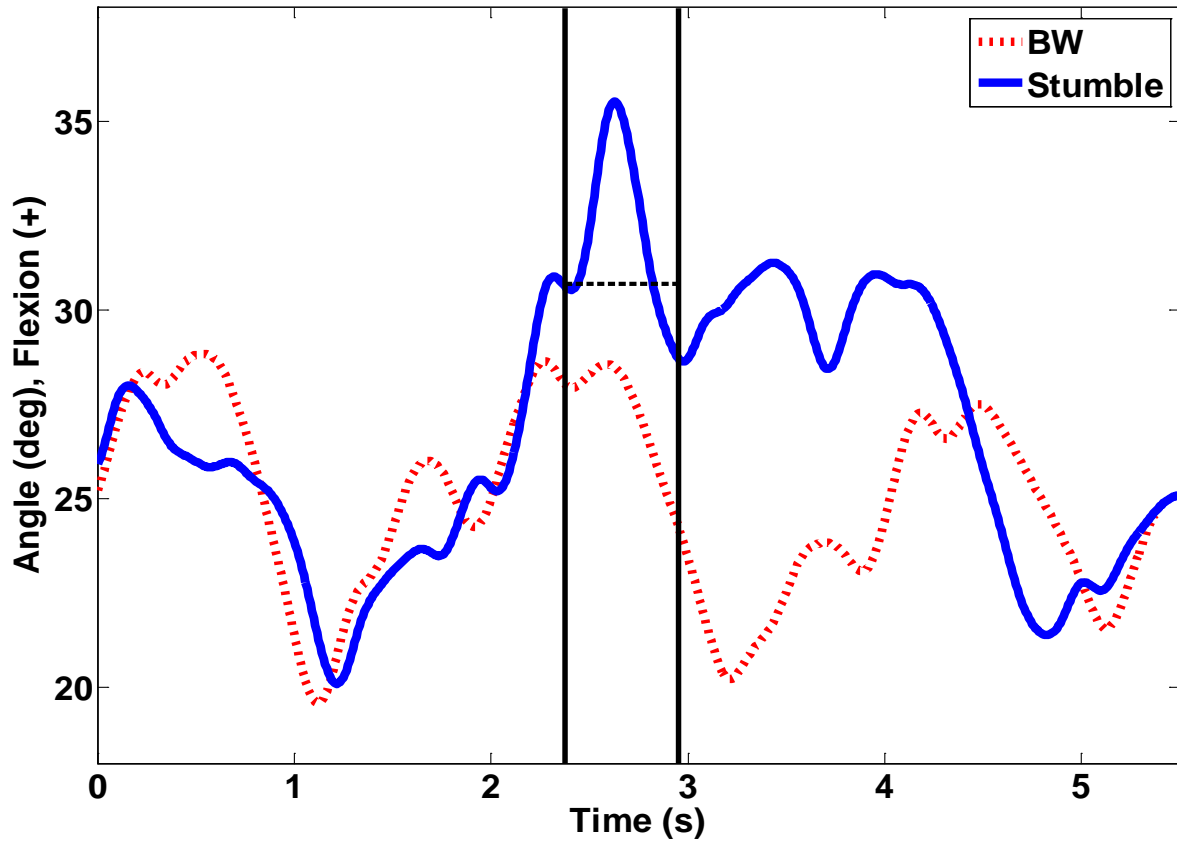


Figure 41. Sagittal plane trunk angle during the stumble perturbation trial and during a baseline walking trial for subject 2. Initial contact with the obstacle and heel-strike of the prosthetic limb recovery step are identified by vertical lines. The sagittal plane trunk angle at initial contact is represented throughout the recovery phase by a dashed line.

Subject 2 Frontal Plane Trunk Angle

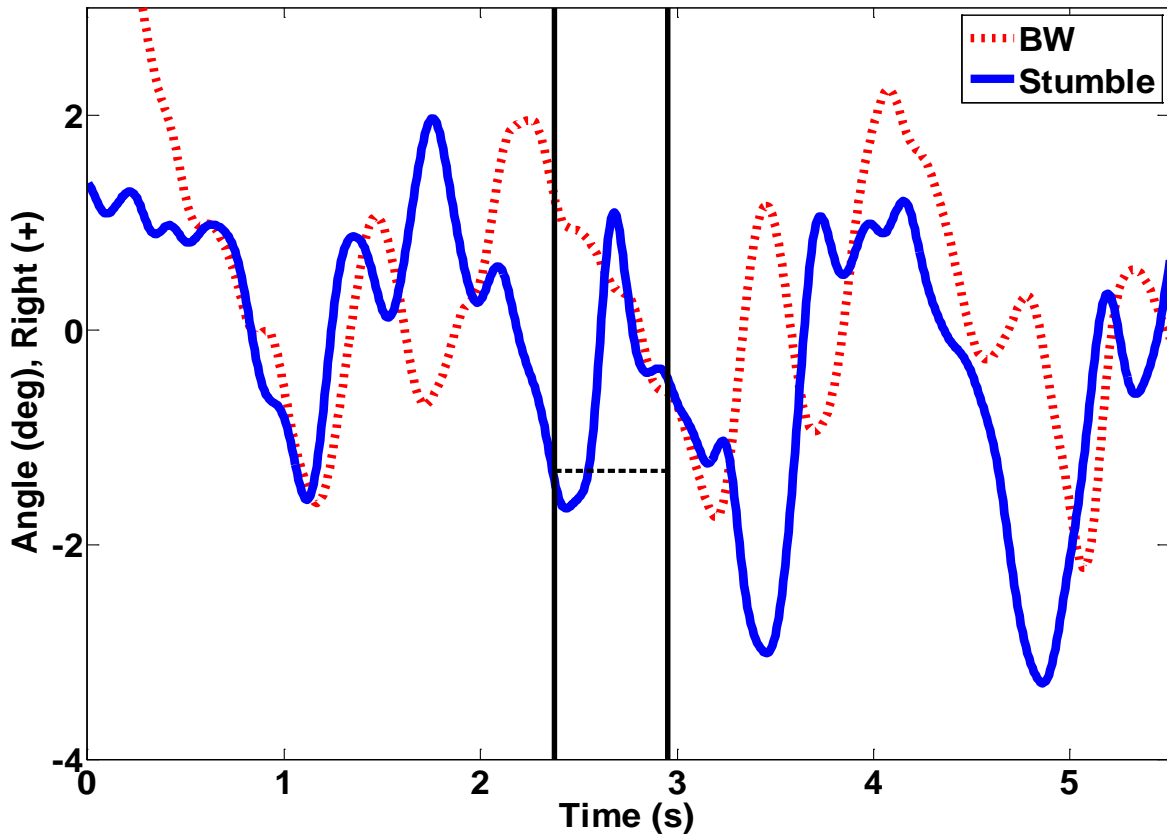


Figure 42. Frontal plane trunk angle during the stumble perturbation trial and during a baseline walking trial for subject 2. Initial foot-obstacle contact and heel-strike of the prosthetic limb recovery step are identified by vertical lines. The trunk angle at initial contact is represented throughout the recovery duration by a dashed line.

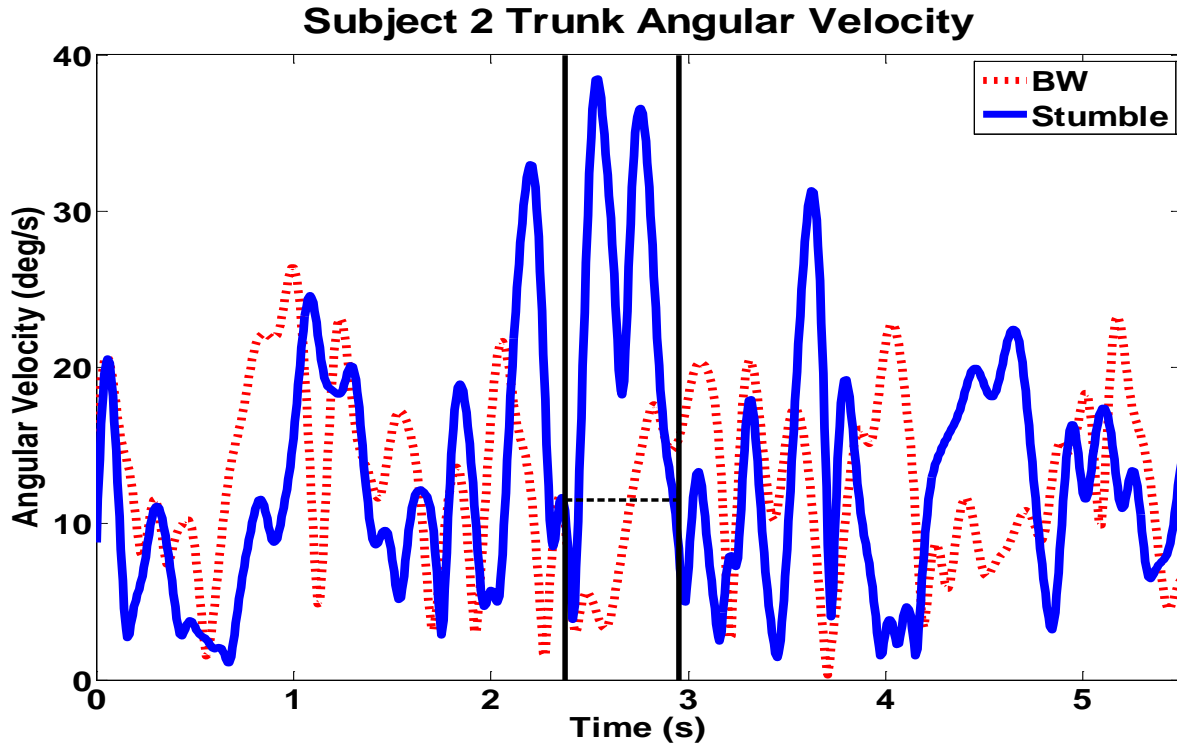


Figure 43. Trunk angular velocity during the stumble perturbation trial and during a baseline walking trial for subject 2. Initial foot-obstacle contact and heel-strike of the prosthetic limb recovery step are identified by vertical lines. The angular velocity at initial contact is represented throughout the recovery duration by a dashed line.

The recovery response for subject 4 was minimal, as the sound limb provided stabilization and the plantar flexors assisted in elevating the body and flexed prosthetic limb over the obstacle. Immediately following contact with the obstacle an increase of approximately 4 degrees in trunk angle was seen in both the sagittal and frontal planes (Figures 44-45). There was a 3.07 degree increase in sagittal plane maximum flexion during the stumble recovery duration compared to the level surface walking maximum average. The frontal plane angle during the recovery was trunk tilt to the right side. These angular changes resulted in a 33.14 deg/s trunk angular velocity increase during the recovery (Figure 46). A minimum angular velocity of 0.70 deg/s was reached approximately halfway through the recovery period, corresponding to the point at which the body center of mass was at its highest point over the obstacle.

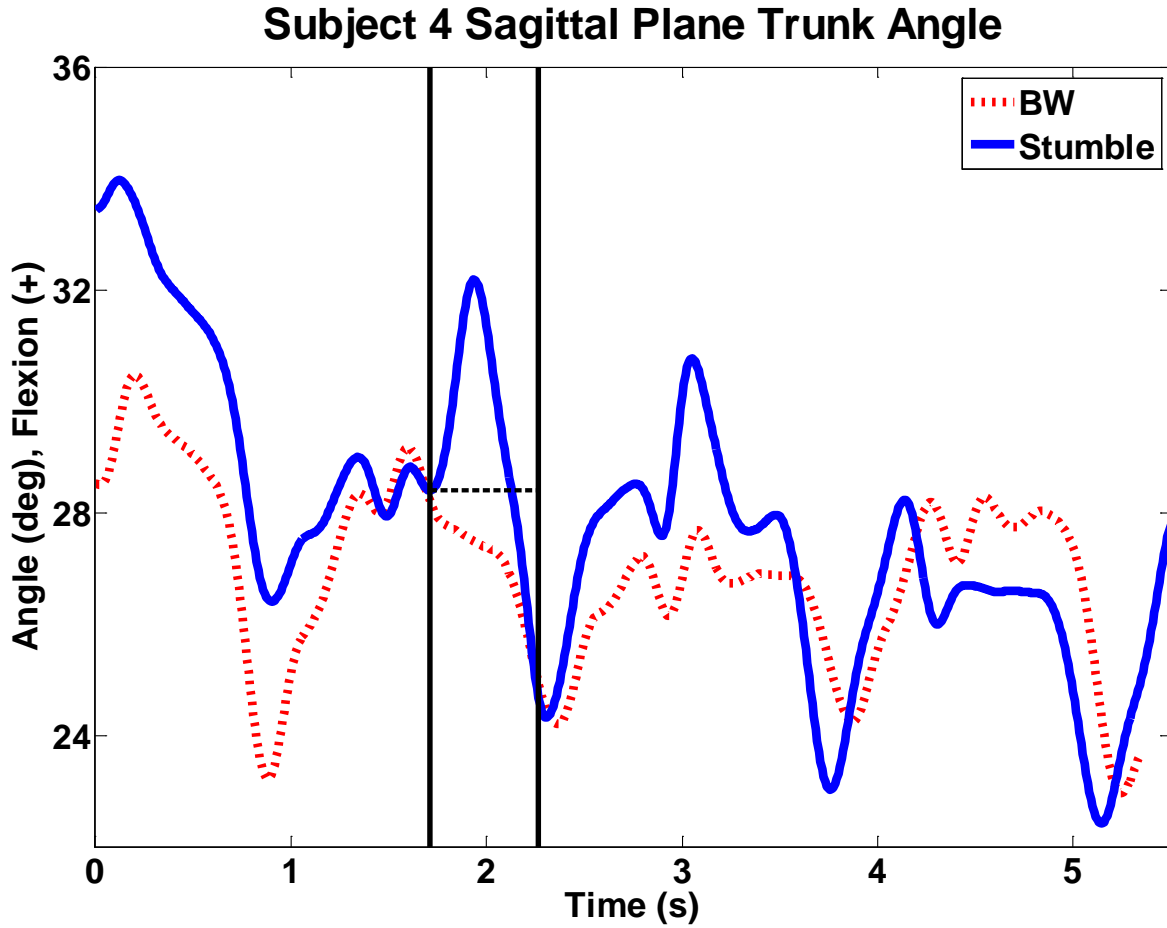


Figure 44. Sagittal plane trunk angle during the stumble perturbation trial and during a baseline walking trial for subject 4. Initial contact with the obstacle and heel-strike of the first recovered step are identified by vertical lines. The sagittal plane trunk angle at initial contact is represented throughout the recovery phase by a dashed line.

Subject 4 Frontal Plane Trunk Angle

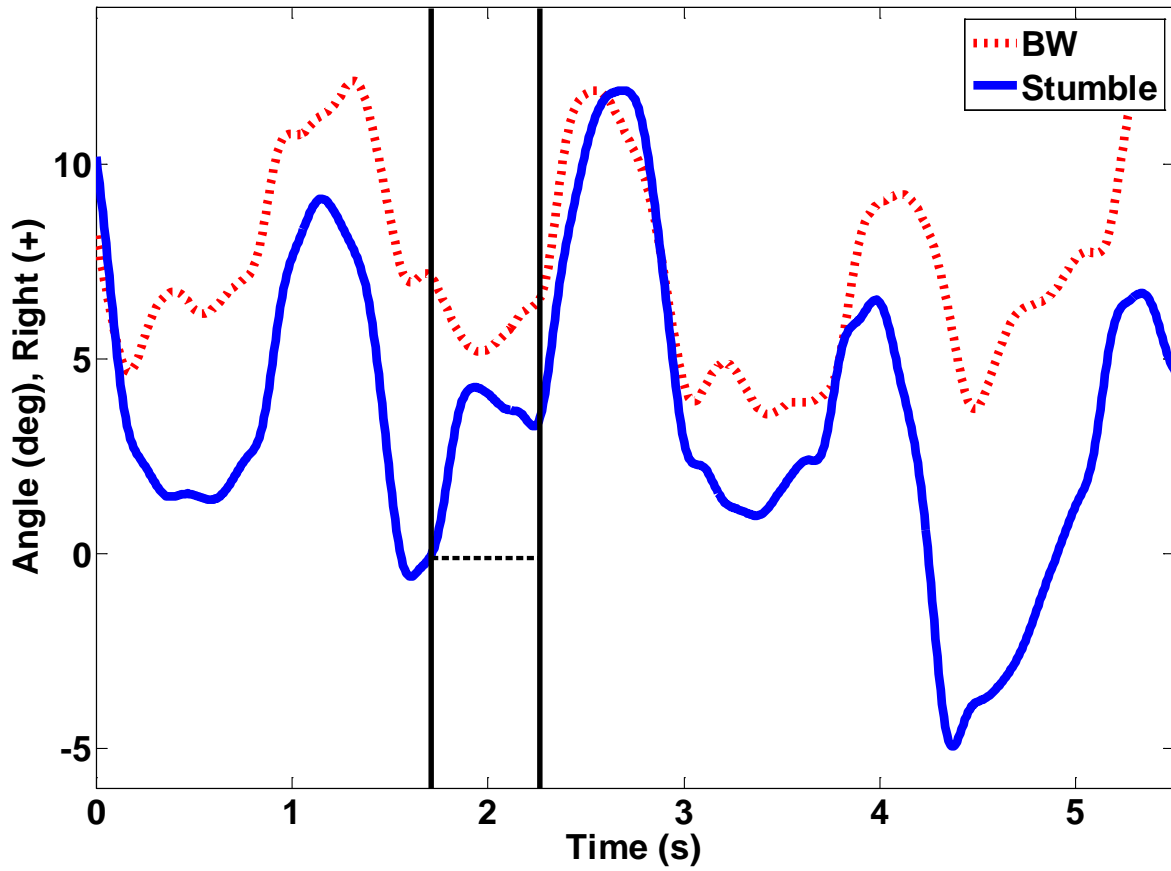


Figure 45. Frontal plane trunk angle during the stumble perturbation trial for subject 4. Initial foot-obstacle contact and heel-strike of the prosthetic limb recovery step are identified by vertical lines. The trunk angle at initial contact is represented throughout the recovery duration by a dashed line.

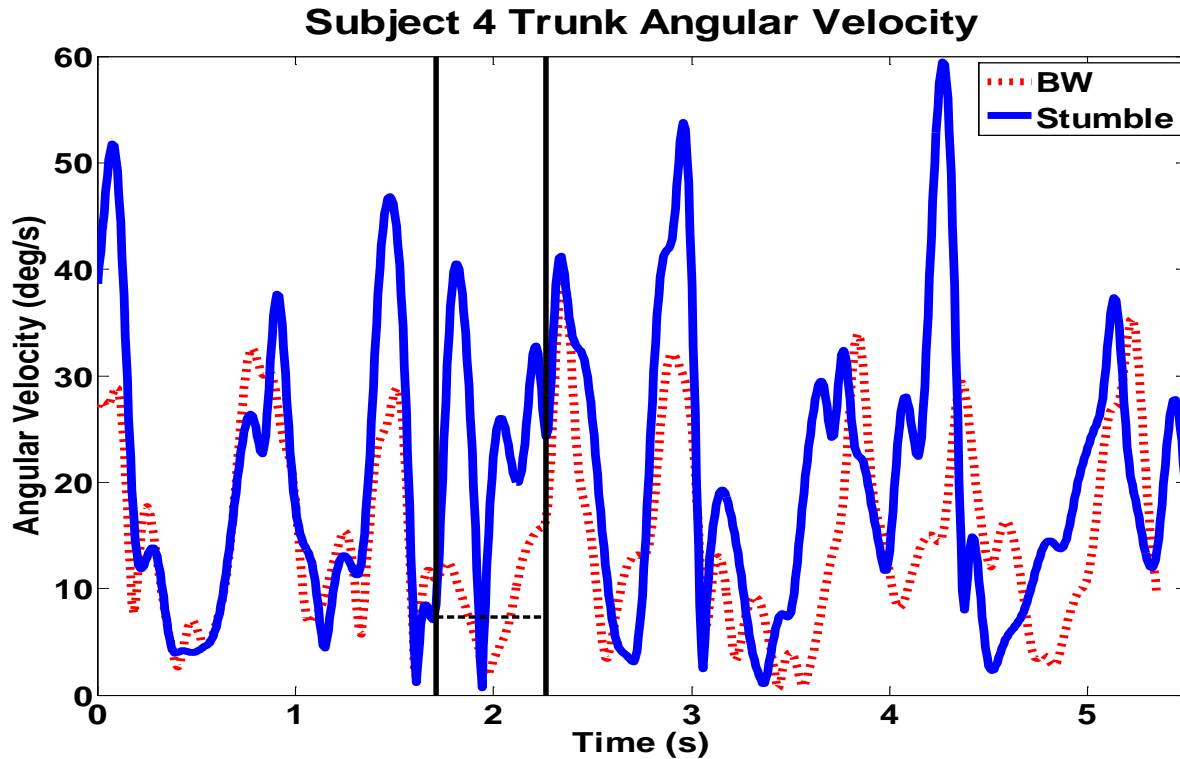


Figure 46. Trunk angular velocity during the stumble perturbation trial for subject 4. Initial foot-obstacle contact and heel-strike of the prosthetic limb recovery step are identified by vertical lines. The angular velocity at initial contact is represented throughout the recovery duration by a dashed line.

The stumble recovery response for subject 5 reached a maximum trunk flexion angle of 58.17 degrees in the sagittal plane as the obstructed prosthetic limb was lowered and the sound limb took a small supporting step forward (Figure 47). The step with the sound limb helped to reduce the trunk's forward momentum. Initially, contact with the obstacle led to a brief and small decrease in trunk flexion in response to obstacle contact. The frontal plane trunk angle response showed two periods of increased trunk tilt to the right: one upon lowering of the obstructed foot and one prior to the prosthetic limb recovery step heel-strike (Figure 48). At both of these times, the frontal plane trunk angle increased to approximately 11 degrees right of vertical. The trunk angular velocity reached a maximum 175.10 deg/s during the stumble

recovery, coinciding with the small step forward with the sound limb (Figure 49). Upon heel-strike of the sound limb the trunk angle in the sagittal plane had reached its maximum. Following the recovery duration, subject 5 experienced another sharp increase in trunk deviation and trunk angular velocity. A loss of balance occurred after the subject stepped over the obstacle with the prosthetic limb in full extension and made heel contact. The loss of balance did result in an unknown amount of harness support to keep the subject from falling forward uncontrollably.

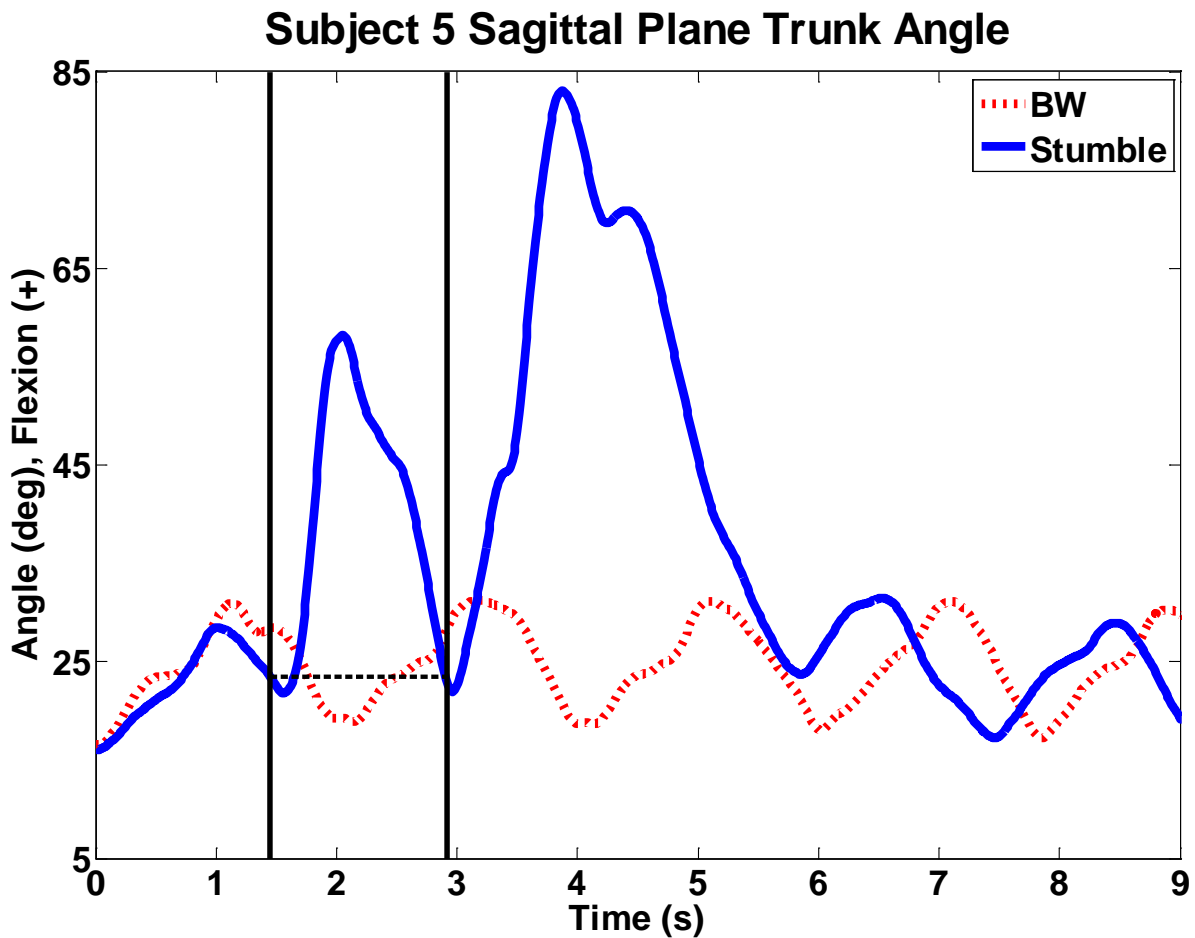


Figure 47. Sagittal plane trunk angle during the stumble perturbation trial and during a baseline walking trial for subject 5. Initial contact with the obstacle and heel-strike of the prosthetic limb recovery step are identified by vertical lines. The sagittal plane trunk angle at initial contact is represented throughout the recovery duration by a dashed line.

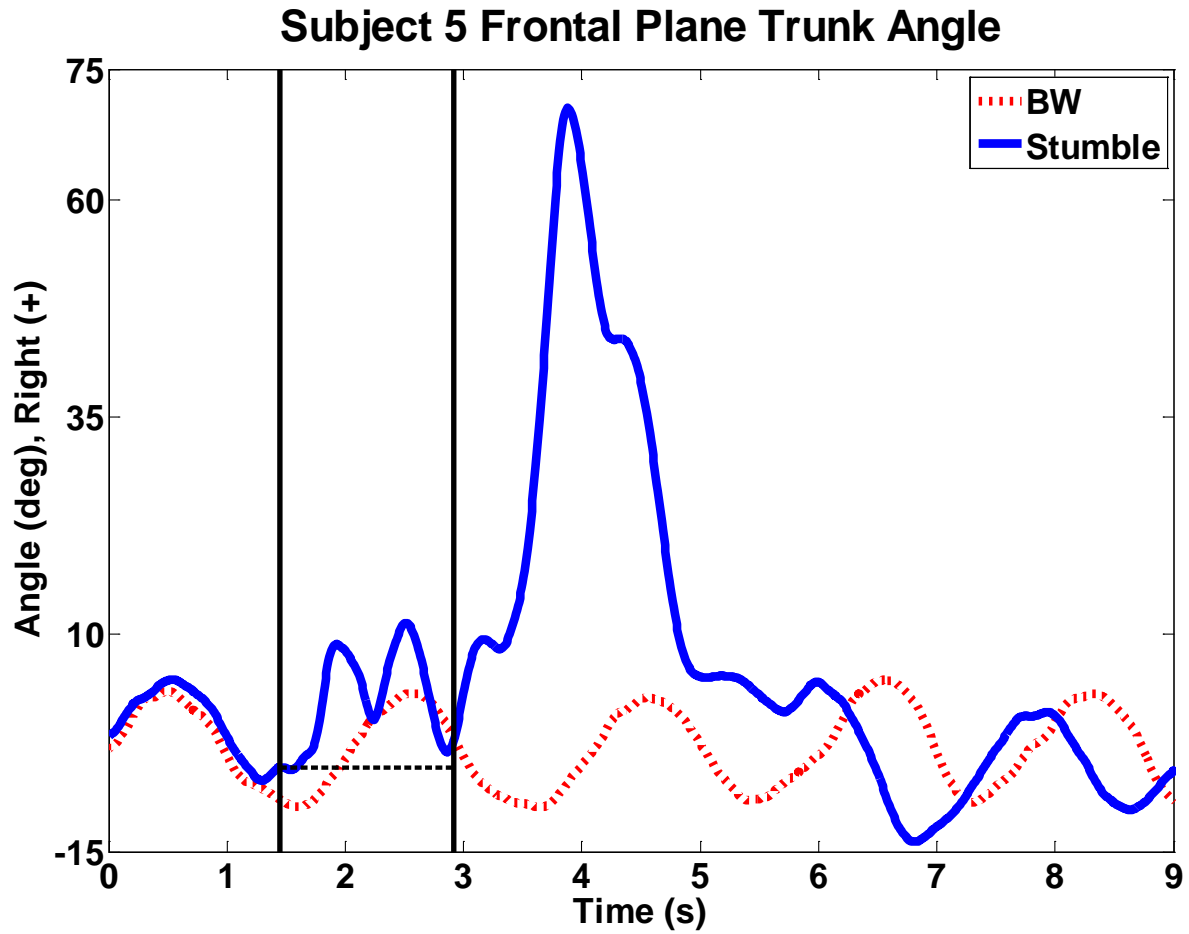


Figure 48. Frontal plane trunk angle during the stumble perturbation trial and during a baseline walking trial for subject 5. Initial contact with the obstacle and heel-strike of the prosthetic limb recovery step are identified by vertical lines. The frontal plane trunk angle at initial contact is represented throughout the recovery duration by a dashed line.

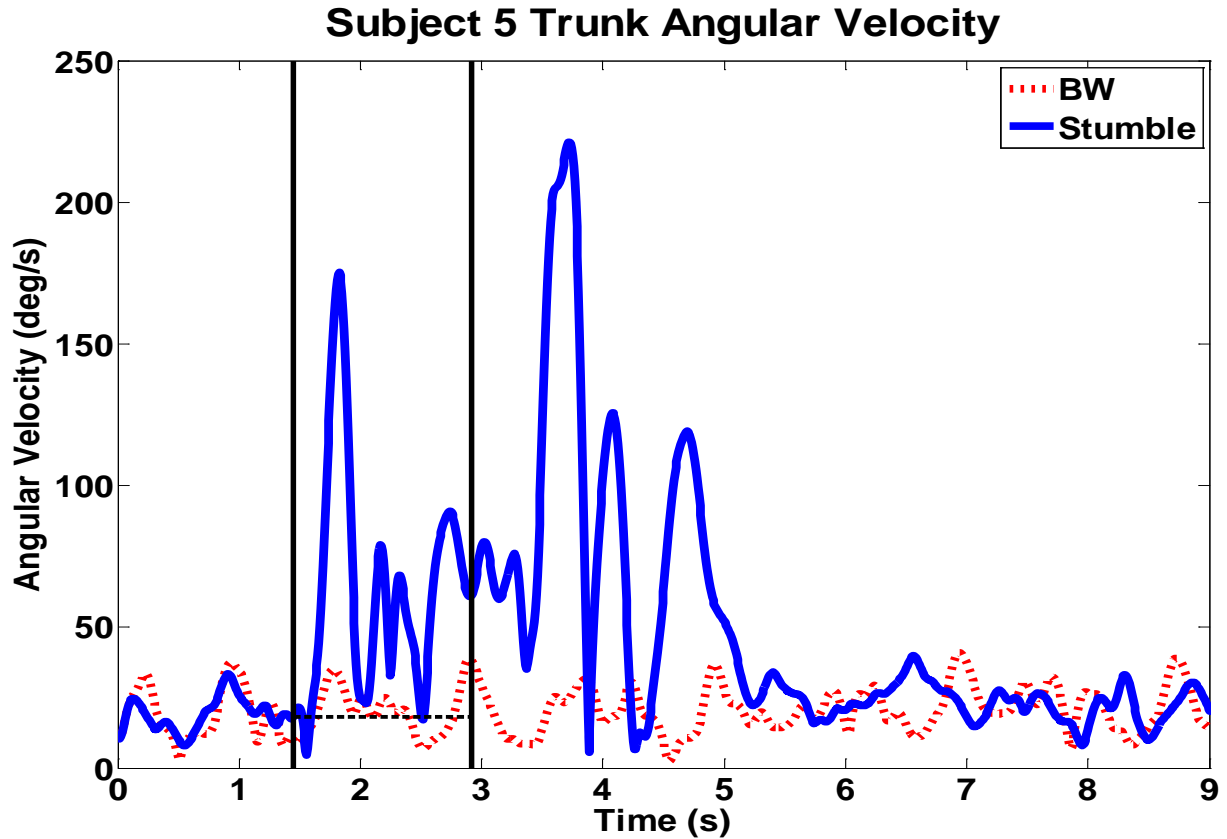


Figure 49. Trunk angular velocity during the stumble perturbation trial and during a baseline walking trial for subject 5. Initial contact with the obstacle and heel-strike of the prosthetic limb recovery step are identified by vertical lines. The angular velocity at initial contact is represented throughout the recovery duration by a dashed line.

3.4 DISCUSSION

3.4.1 Minimum Foot Clearance during Level Surface Walking

Four of six subjects had smaller minimum foot clearance during swing with the prosthetic limb in comparison to the sound limb (subjects 2, 3, 4, and 5). Among all subjects and the swing phases where MFC was clearly identified, the largest MFC value for the prosthetic limb was 7.95 cm at the toe tip position and the largest MFC value for the sound limb was 4.84 cm at the toe tip

position. The prosthetic limb MFC was generally more variable than the sound limb MFC. Five of the subjects had the sound limb MFC occur during midswing and four subjects had the prosthetic limb MFC occur during initial swing.

Comparing just the prosthetic limb and sound limb swing phases for all subjects revealed variability within the foot progression angle such that different points along the sole of the shoe could lead to a trip incident. Therefore, the toe tip marker should not be the only forefoot position considered when assessing MFC while walking over a level surface. The methodology developed in this thesis allows for clear identification of four points along the sole of the shoe such that differences in shoe geometry between subjects will not skew the results. For example, a tennis shoe with a raised toe tip height will theoretically shift the position for the smallest MFC value more posterior on the shoe sole, whereas a shoe with a flat sole will have a greater chance for MFC to occur at the toe tip position. Furthermore, this method allowed for various prosthetic foot kinematic patterns to be analyzed, as a lack of ankle dorsiflexion and knee flexion will impact the motion of the foot.

Additionally, this methodology provided a means to assess foot clearance during the swing phase when a clear local minimum point identifying the MFC position was not present in a forefoot marker trajectory. The risk of tripping by catching a point along the sole of the forefoot on the ground is highest during the initial swing and midswing sub-phases, while the potential for catching the heel is highest during terminal swing. Looking at the transition points between the three sub-phases of swing allowed a degree of comparison to be made between the prosthetic and sound limb when MFC could not be identified. Based on the findings presented in this thesis, the prosthetic limb clearance at 67.5% of the swing phase was typically higher than the sound limb by a few centimeters. This infers that the lack of proprioception in the prosthetic

limb ankle and knee joints impacts the gait biomechanics of the prosthetic limb. The prosthetic limb achieves knee extension earlier during the swing phase than the sound limb does (see Appendix B). Since amputees want to make sure their prosthetic knee is set in extension before they place weight on it, this adaptation allows them to ensure the knee is properly set prior to heel-strike. For example, subject 1 presented in this thesis visually had a more pronounced swing-through of the prosthetic shank during terminal swing than other subjects did. To produce knee extension for heel-strike, the prosthetic shank appeared to move through the swing phase with a higher velocity than those subjects using a MPK joint. Since subject 1 had a NMPK joint and needed to physically keep the knee in extension during stance, there was a greater need to ensure the knee reached extension prior to heel-strike. However, additional results are needed for subjects using a NMPK joint to clarify the relationship between the lack of proprioception and its impact on terminal swing foot clearance and knee extension.

The spatial-temporal results during level surface walking for the subjects presented in this thesis (see Appendix B) also support the MFC results. Subjects 2, 5, and 6 had the most temporal variability in when MFC occurred during the swing phase. These three subjects had the slowest gait speeds of all subjects (under 0.57 m/s) and the most asymmetric step length between the sound and prosthetic limb in comparison to all subjects. Despite these subjects having a longer step length with the prosthetic limb, their MFC values occurred during initial swing. These results may indicate a desire to quickly move the prosthetic limb through swing, resulting in MFC during initial swing, and also the need to take a longer step in order to ensure full knee extension is achieved before heel-strike. Subject 2 had the most asymmetric stride duration between the limbs despite the use of a cane in each hand; stride duration variability has been associated with an increase in age and correlated with poor balance in older adults.

The degree of knee flexion during the swing phase also indicated an impact on MFC during level surface walking (see Appendix B). The prosthetic knee angle for subjects 2 and 3 was less than the angle seen in the sound limb, and these two subjects had lower MFC values with the prosthetic limb in comparison to the sound limb. For subject 1 the prosthetic knee angle was greater than the sound knee angle and the resulting MFC values were higher for the prosthetic limb. The remaining subjects either had conflicting results for MFC with respect to knee angle or comparisons could not be made due to the inability to identify MFC. Further analysis is needed to determine the overall degree to which knee angle during swing impacts MFC in unilateral transfemoral amputees. Since these individuals adopt various gait patterns, results may show multiple trends between knee angle and MFC as was seen for the subjects presented in this thesis.

Based on the Americans with Disabilities Act, a trip hazard is identified by any vertical change in level over 0.635 cm (equivalent to 0.25 inch) [87]. For vertical height changes between 0.635 cm and 1.27 cm (0.50 inch), a beveled slope is required at the transition; however, door thresholds are allowed a 1.27 cm maximum height. Based on these guidelines for public facilities, the risk of tripping is high if an individual's minimum foot clearance is unable to safely clear 1.27 cm.

Among the subjects analyzed in this thesis, subjects 3, 5, and 6 are at the greatest risk of tripping during the swing phase of the prosthetic limb. The remaining subjects have prosthetic limb MFC values above 1.27 cm, and most subjects had a sound limb clearance greater than the prosthetic limb. However, all subjects are at risk of tripping during initial swing while the foot is still low to the ground. In addition, able-bodied older adults have a MFC likely to result in a trip based on the maximum vertical height change of 1.27 cm (previous research has found MFC for

older adults to be $1.11 \text{ cm} \pm 0.53 \text{ cm}$ [19]). Older adults who have a fear of falling or history of falling have an increased MFC ($2.02 \text{ cm} \pm 0.51 \text{ cm}$ [20]), but while their risk of tripping over a door threshold is decreased, a larger vertical change in surface level could result a trip.

3.4.2 Stair Ambulation Minimum Foot Clearance

During stair ascent, the prosthetic limb horizontal foot clearance was larger than the resultant foot clearance for all subjects. The methods employed for stair ascent varied by individual, but all subjects did ascend the steps with a single-step progression and moved their sound limb up to the next step first. This method allowed the subjects to use their sound limb for support as the prosthetic limb was progressed up the step. All subjects kept their prosthetic knee joint in extension during ascent, but subjects 1, 3, 4, and 5 clearly displayed circumduction to progress the prosthetic limb over the step edge. These subjects also displayed a larger prosthetic foot horizontal clearance for the toe tip than the other subjects, likely a result from circumduction of the prosthetic limb.

Subjects 1, 3, and 6 had smaller vertical clearance and resultant clearance values for the prosthetic foot than the sound foot. These results indicate that a lack proprioception in the prosthetic limb can lead to decreased foot clearance during stair ascent. Subject 6 utilized a sliding technique with the prosthetic foot to ascend the steps, which could be seen as a method to help obtain some proprioceptive feedback during ascent. However, if the vertical clearance after the step edge is reached is not large enough for the break forefoot position to clear the edge then there is still an increased risk of tripping on the prosthetic limb side during ascent.

Since the inferior heel marker was not available for analysis of the pilot study subjects during stair descent, comparisons were only made for subjects 5 and 6. The results for stair

descent show trends of a larger inferior heel horizontal clearance with the prosthetic foot and a smaller inferior heel vertical clearance with the prosthetic foot. These results indicate the lack of ankle plantar flexion in the prosthetic limb affects the descent motion. Since the prosthetic ankle cannot plantar flex to push off the step, the vertical clearance is low to the step tread. A larger horizontal clearance is necessary to ensure clearance over the step edge is obtained before vertical descent begins.

All subjects, except subject 2, descended the stairs by moving the prosthetic limb down to the next step first. Subject 4 was the only subject to attempt a step-over-step descent method; however, a brief disruption in balance resulted in single-step progression during descent. Progression of the prosthetic limb down the step first allows the prosthetic knee to be kept in extension, since the sound limb is capable of flexing at the ankle and knee joints to obtain clearance over the step. Sound limb proprioception also aids in ensuring successful clearance of the sound foot over the step edge. Subjects 3, 5, and 6 utilized a sliding technique with the prosthetic limb during vertical descent of the foot (Figure 50) in order gain some sense of proprioception.

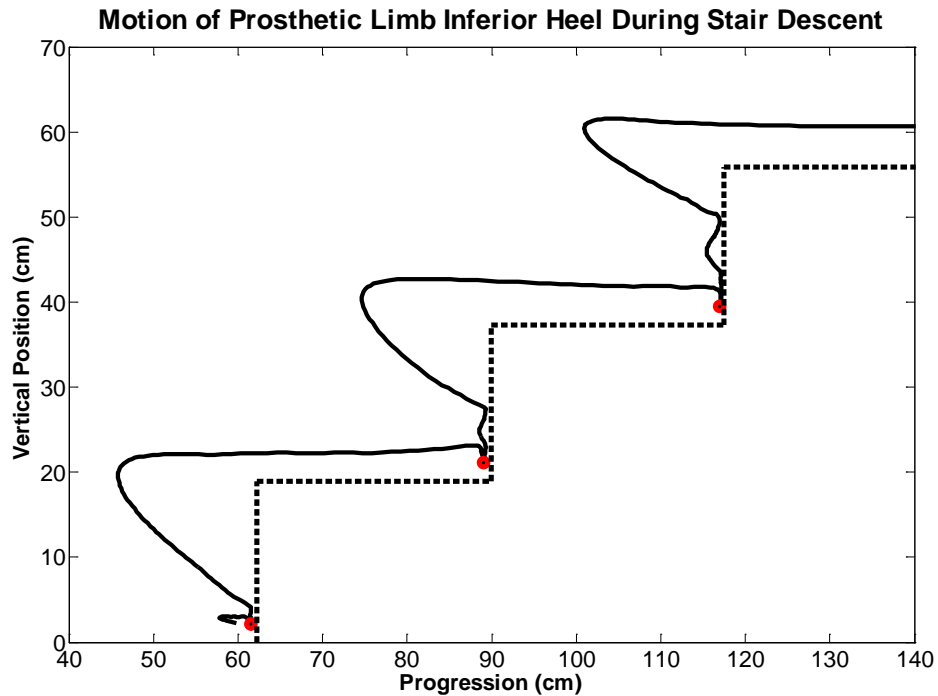


Figure 50. Example of the sliding technique used by subjects 3, 5, and 6 during stair descent with the prosthetic limb. The heel of the shoe was slid down the step riser to reach the step tread.

3.4.3 Responses to Stumbling

Results from the stumbling perturbation trials indicate the ability to control trunk motion during the recovery period is affected by the resulting motion of the prosthetic knee joint. The subjects who utilized an elevating strategy had smaller trunk deviation in the sagittal and frontal planes, reduced angular velocity, and smaller recovery duration because the knee joint flexed such that additional hip flexion and body elevation were sufficient to allow clearance of the prosthetic foot over the obstacle. The subject who utilized a lowering strategy in response to the stumbling perturbation maintained the prosthetic knee in full extension when progressing the prosthetic foot over the obstacle, which led to substantial trunk motion during recovery and an uncontrollable fall following the prosthetic limb recovery step.

Due to the lack of subjects having undergone the stumble perturbation at this time, it is unclear whether the elevating strategy is preferred by older adult unilateral transfemoral amputees. Able-bodied older adults tend to use the lowering strategy to recover following a stumble, as was seen in subject 5, but the lack of proprioception in the ankle and knee joints and the type of prosthetic knee joint used may lead to an elevating strategy, as was seen in subjects 2 and 4. However, since subjects 2 and 4 were younger than subject 5, physical ability to maintain control of the body's momentum may have led to the successful utilization this recovery method. Subject 5 also kept the NMPK joint in extension during swing, and the flexion resistance set within the knee was high enough that passive flexion of the knee joint would likely have not occurred upon foot-obstacle contact.

The stumbling recovery measures presented in this thesis allow for initial comparisons to be made to previous research regarding induced trips among able-bodied older adults. Previous research has found that a faster response time following the foot-obstacle contact will promote a better recovery response and reduce the risk of falling. In this thesis, this was seen in the two subjects who utilized an elevating strategy, as they had a sufficient response time following obstacle contact for successful recovery to occur. Further, previous research has found average trunk flexion in the sagittal plane at recovery step heel-strike to be approximately 35 degrees for older adults who did not have a history of falling and who were able to successfully recover following the perturbation. Across the three subjects who experienced a stumbling perturbation in this thesis, the average trunk flexion was $25.33 \text{ deg} \pm 3.10 \text{ deg}$ in the sagittal plane at recovery step heel-strike. This smaller degree of trunk flexion in comparison to able-bodied older adults may be due to amputee gait adaptations and the need to obtain some degree of knee extension prior to heel-strike in order to prevent knee collapse.

4.0 GEOMETRIC MODELING OF THE PROSTHETIC LIMB

4.1 METHODS

4.1.1 Experimental Measurements

A geometric model of the prosthetic limb foot, shank, and thigh segments was developed using measurements of the prosthetic limb for subject 5. The measurements needed to create the geometric model were obtained using a standard tape measure and a small anthropometer. Measurements were taken during laboratory visit 3 when the study prosthetist disassembled the prosthetic limb into the three respective segments. The foot segment contained the prosthetic foot inside of the subject's shoe, the shank segment consisted of the prosthetic knee with the pylon and pylon adapter attached, and the thigh segment consisted of the residual limb and socket with any distal socket adapters attached. Table 27 lists the measurements taken for each segment with a short description of each measurement. These measurements were used to create the geometric model of the prosthetic limb, described in detail in Section 4.1.2. In addition to taking these measurements, the foot, shank, and socket were weighed on a force plate to determine their mass and placed on a reaction board to determine their center of mass (COM) location. These direct measurements for mass and COM were used to verify the accuracy of the geometric model in calculating the inertial properties of the prosthetic limb.

Table 27. Measurements of the foot, shank, and thigh segments needed for the geometric model of the prosthetic limb.

Foot Segment	
Mass	Mass of the entire foot segment.
Medial-Lateral Distance	Distance between the medial and lateral edges of the shoe, measured every 3 cm along the length of the shoe, starting at the heel (0 cm) with last measurement at the toe tip.
Superior-Inferior Distance	Distance between the inferior edge of the shoe sole and the superior edge of the shoe, measured every 3 cm along the length of the shoe, starting at the heel (0 cm) with last measurement at the toe tip.
Shank Segment	
Mass	Mass of the entire shank segment.
Knee Length	Length of the knee joint measured from the proximal to distal edges of the housing.
Knee Medial-Lateral Distance	Distance between the medial and lateral edges of the housing, measured at the proximal edge and at the distal edge of the knee joint.
Knee Anterior-Posterior Distance	Distance between the anterior and posterior edges of the housing, measured at the proximal edge and distal edge of the knee joint.
Pylon Length	Length of the pylon measured from the proximal to distal points of the pylon.
Pylon Material	The type of material the pylon is made of (e.g. aluminum, titanium, carbon fiber).
Pylon Adapter Length	The length of the adapter attached to the distal end of the pylon.
Pylon Adapter Outer Diameter	If applicable, measure the outer diameter of the adapter attached to the distal end of the pylon.
Adapter Material	The type of material the adapter is made of (e.g. aluminum, titanium, stainless steel), or record the brand/model number if engraved on the adapter.
Thigh Segment	
Socket Material	The type of material the socket is made of (e.g. Vivak/CoPoly, carbon fiber).
Socket Thickness	Thickness of the socket measured on the lateral side near the proximal end of the socket.
Socket Thigh Flap Length	Length of the thigh flap section measured on the lateral side of the socket.
Socket Medial-Lateral Distance	Distance between the medial and lateral edges of the socket, measured every 3 cm along the length of the socket starting at the distal point of the thigh flap and ending at the point where the socket begins to curve to its distal point.

Table 27 (continued).

Socket Anterior-Posterior Distance	Distance between the anterior and posterior edges of the socket, measured every 3 cm along the length of the socket starting at the distal point of the thigh flap and ending at the point where the socket begins to curve to its distal point.
Socket Distal Section Length	Length of the distal section of the socket, taken as a straight measurement; starting at the point of the last anterior-posterior distance measurement and ending at the distal point of the socket.
Adapter(s) Length	Length of the adapter(s) attached to the distal end of the socket.
Adapter(s) Outer Diameter	Measurement of the outer diameter of the adapter(s) attached to the distal end of the socket. If adapter is square in shape, measure the medial-lateral and the anterior-posterior distances.
Adapter(s) Material	Record the type of material the adapter(s) is made of (e.g. aluminum, titanium, stainless steel) or record the brand/model if engraved on the adapter(s).

4.1.2 Geometric Modeling of the Prosthetic Limb

The foot segment was modeled using a series of stadium solids along the length of the shoe as shown in Figure 51. Based on the distance between each measurement along the length of the foot, the height of each stadium solid was 3 cm except for the most distal stadium solid, which depended on the distance between the two distal measurements. At each measurement position along the length of the foot the medial-lateral and anterior-posterior distances were used to calculate the volume, center of mass location, and moment of inertia of each stadium solid. Calculation of these inertial properties is performed following the mathematical model presented by Yeadon [66]; specific equations are presented in Appendix E. The foot segment was assumed to be homogeneous with uniform density throughout the segment. However, since the density of

the segment could not be determined using known material specifications, density was calculated using the measured mass of the foot segment and the calculated volume of the foot segment.

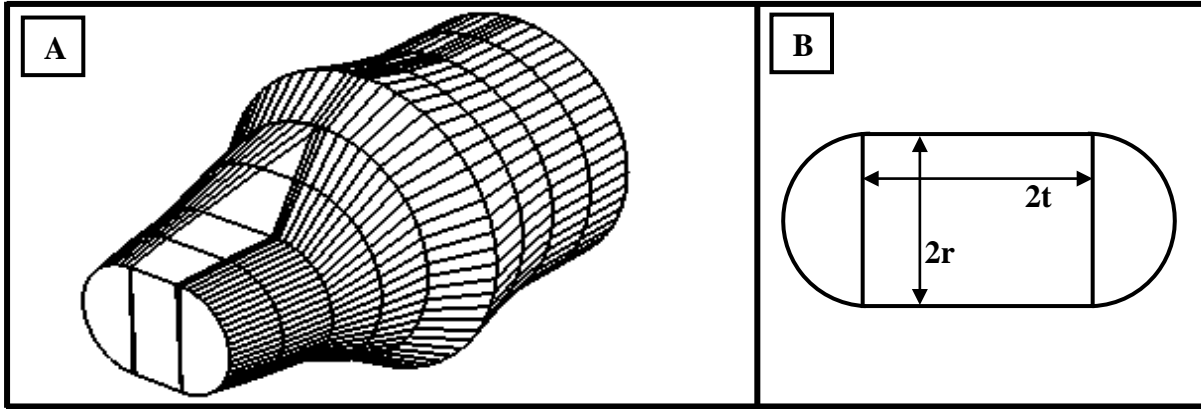


Figure 51. (A) Three-dimensional model of the foot segment using a series of stadium solids. (B) Cross-section of a stadium solid, defined as a rectangle with length $2t$ and width $2r$, adjoined by a semi-circle at each edge of the rectangle. The $2r$ distance is the measured superior-inferior distance. The measured medial-lateral distance is adjusted to yield the $2t$ distance.

For the shank segment, the knee joint was modeled as a rectangular prism and the pylon and pylon adapter were modeled as hollow circular cylinders as shown in Figure 52. A simplification for the knee joint geometry was made due to the complexity of the actual prosthesis. Additionally, the knee joint was assumed to be homogeneous with uniform density throughout the rectangular prism. The pylon and pylon adapter geometry is near identical to the actual shape. Calculation of the inertial properties for these individual pieces of the shank segment were performed following the equations given in the *Handbook of Equations for Mass and Area Properties of Various Geometrical Shapes* [113]; the specific equations are given in Appendix E. The density of the pylon adapter was 4510 kg/m^3 for commercially pure ASTM Grade 1 titanium and the density of the pylon was 2700 kg/m^3 for aluminum used in orthopaedic

applications. The density of the knee joint was found using the calculated knee joint volume and measured mass of the shank segment, adjusted for the mass of the pylon and pylon adapter.

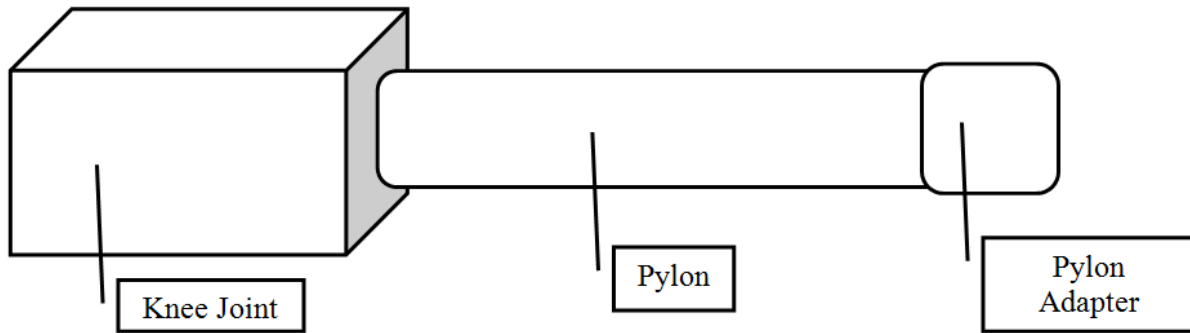


Figure 52. Geometric model of the shank segment, modeled as a rectangular prism and two hollow cylinders.

The thigh segment consisted of the residual limb and the socket, including any adapters at the distal end of the socket. The residual limb and socket were modeled as the same series of geometric shapes (Figure 53). The residual limb was assumed to fill the entire inner volume of the socket. The residual limb geometry was determined by adjusting for socket thickness, which was assumed to be constant throughout the socket. The thigh segment geometry contained a right-angled wedge shape at the proximal portion of the socket to model the thigh flap section of the segment. This was followed by a series of elliptical cylinders, with the number of cylinders dependent upon the number of medial-lateral and anterior-posterior measurements taken along the length of the socket. The distal portion of the socket was modeled as an elliptical paraboloid. Adapters at the distal end of the socket were modeled as rectangular prisms and/or hollow circular cylinders as necessary. The inertial properties for these individual sections of the thigh segment were found using the equations given in the *Handbook of Equations for Mass and Area*

Properties of Various Geometrical Shapes [113]; the specific equations are provided in Appendix E. The socket material was plastic and assumed to be Co-Polyester (trade name VIVAK®) having a density of 2700 kg/m^3 . A residual limb density of 1100 kg/m^3 was used based on previous literature for body segment density [73]. The residual limb density was assumed to be uniform throughout the segment.

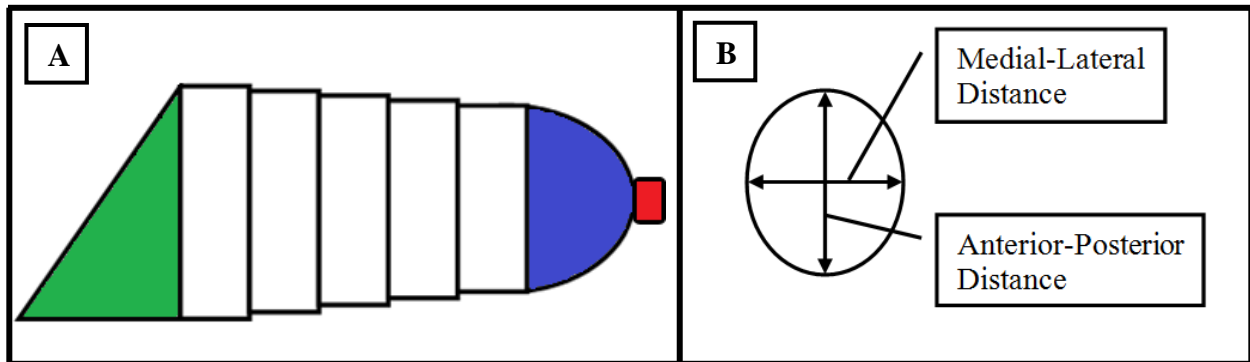


Figure 53. (A) Geometric model of the thigh segment. Both the socket and residual limb are modeled as a series of geometric shapes: proximal right-angled wedge (green), intermediate elliptical cylinders (white), distal elliptical paraboloid (blue), and socket adapter (red). (B) Cross-section of an elliptical cylinder.

4.2 RESULTS

The geometric model results for mass, center of mass location from the proximal point, and mass moment of inertia about the proximal point for the foot, shank, and thigh segments of the prosthetic limb are reported in Table 28. For comparison, the direct measurements recorded during laboratory visit 3 for the foot and shank segment mass and COM location are included in Table 28. Comparison between the socket inertial properties found using the geometric model

and the direct measurements collected during visit 3 are provided in Table 29. The mass of the foot and shank segments found using the geometric model are the same as the direct measurements because the measured mass values were used to calculate density for these segments. The mass difference between the geometric model estimate for the socket and the direct measurement of the socket was 0.235 kg.

Table 28. The prosthetic limb segment inertial properties found using the geometric modeling approach along with the direct measurements taken during laboratory visit 3.

Inertial Property	Foot Segment (Model)	Foot Segment (Measured)	Shank Segment (Model)	Shank Segment (Measured)	Thigh Segment (Model)
Mass (kg)	1.556	1.556	1.183	1.183	4.860
COM location from proximal (m)	0.130	0.130	0.116	0.145	0.201
Moment of Inertia from proximal (kg/m ²)	0.0283	N/A	0.0200	N/A	0.1716

Table 29. Socket inertial properties for the geometric modeling approach and the direct measurements taken during laboratory visit 3.

Socket Only Inertial Properties			
Inertial Property	Socket Geometric Model	Socket Direct Measurement	Percent Difference
Mass (kg)	1.542	1.307	16.50
COM location from proximal (m)	0.201	0.265	27.47
Moment of Inertia from proximal (kg/m ²)	0.0785	N/A	N/A

The geometric model for the foot segment identified a COM location the same as the direct measurement. The shank COM location found using the geometric model underestimated the direct measurement by 0.029 m from the proximal point, yielding a 22.22 percent difference between the results. The socket COM location was also underestimated using the geometric model in comparison to the direct measurement, resulting in a 27.47 percent difference. The moment of inertia results using the geometric model found the shank segment has the smallest moment of inertia while the thigh segment has the largest, which was the expected result based on each segment's mass value.

4.3 DISCUSSION

A geometric modeling approach for the prosthetic limb was able to successfully produce inertial properties for each limb segment given simplifying assumptions and the direct measurement of the foot and shank segment masses. The shank segment had the smallest mass of the three segments because the prosthetic knee joint used in this analysis was a polycentric NMPK joint that does not contain a hydraulic or pneumatic cylinder. The foot segment mass was heavier than the shank segment because the shoe modeled in this analysis was a work boot.

For all segments, the density for each individual geometric shape was assumed to be uniform throughout. In order for this to hold, the simplifying assumption of segment homogeneity was applied for the foot segment and prosthetic knee joint due to the assortment of materials within these geometries. For example, the prosthetic foot contains the inner mechanical mechanism surrounded by a dense foam cover for aesthetic purpose, and then the prosthetic foot is placed inside of the shoe. All of these materials have different densities,

therefore, the measured foot segment mass must be used along with its calculated volume in order to determine a uniform density value for the foot segment. The same reasoning was applied for the prosthetic knee joint. As a result, both the foot segment and shank segment mass calculated by the geometric model was identical to the measured mass.

The mass of the thigh segment can only be verified based on comparison between the geometric model estimate for mass of the socket and its direct measurement. The geometric model overestimates the mass of the socket by 16.50 percent, which could be attributed to the use of a right-angled wedge shape to model the proximal portion of the segment. This geometric shape has a rectangular base and straight sides, thus an elliptical or circular shaped geometry would more closely resemble the true thigh flap appearance.

The geometric model chosen for the shank segment resulted in the center of mass location being more proximal than the direct measurement. This result is expected due to the geometric model calculation for center of mass relying solely on the length measurements for the segment's individual pieces, whereas the direct measurement for center of mass took into consideration the physical mass distribution within the shank. The prosthetic knee joint was modeled as a solid object even though it was not, thus leading to a heavier proximal portion in the shank segment. Further analysis using the geometric modeling approach is needed in order to determine if a more appropriate geometric shape for the prosthetic knee joint can be found. For example, a rectangular prism is not identical to the geometry of the prosthetic knee joint; however, due to the complexity of the prosthetic knee joint design, this simplifying geometry assumption was made. It may possible to model the prosthetic knee joint more in-depth by using the method of stadium solids, similar to that of foot segment, in order to capture the slight tapering nature of the prosthesis along its length.

The thigh segment inertial properties are directly affected by the assumption that the residual limb volume is the same as the inner volume of the socket. Residual limb shrinkage is possible over time, which would result in the geometric model of the residual limb overestimating its true mass. Due to the need for the socket to provide a secure fit for an individual, it is assumed this difference would not be large enough to significantly alter the inertial property results for the thigh segment.

Comparison of the geometric model results to previous research where the inertial properties of the prosthetic limb were determined cannot be made due to the lack of these studies reporting the measured values. Only the work of Goldberg reported the measured results for the prosthetic limb segments in children [75]. However, comparing the geometric model outcomes for the foot, shank, and thigh segments to the measurements for these children, as well as to published work for able-bodied individuals, the calculated outcomes for mass and mass moment of inertia are within the correct order of magnitude [114].

Overall, the developed geometric model of the prosthetic limb is a convenient method for determining the inertial properties of the limb segments when equipment for direct measurement of the mass, COM location and moment of inertia are not available. This geometric model should be used with future subjects participating in the full research study in order to obtain sufficient results for addressing the current void in the literature regarding inertial properties of the prosthetic limb segments for adult unilateral transfemoral amputees.

5.0 CONCLUSIONS

The methodology developed in this thesis for the investigation of minimum foot clearance during level surface walking and during stair ascent and descent is important for future biomechanical analysis of unilateral transfemoral amputee gait. During level surface walking, the ability to analyze multiple points along the bottom of the shoe sole allowed MFC to be identified regardless of shoe geometry differences or variations in amputee gait, such as the foot-floor angle during the swing phase. The use of multiple points along the shoe sole also allowed for a better spatial understanding of where on the foot the risk of floor contact during gait was the greatest. Additionally, the developed marker set and associated analysis technique allowed for MFC to be identified temporally within the swing phase, or if no MFC point was identified based on variations in gait style, then the swing phase clearance of the prosthetic and sound feet were compared using distinct transition points in the gait cycle between initial swing and midswing, and midswing and terminal swing. During stair ambulation, the developed methodology for MFC using a custom shoe marker set allowed for a comprehensive analysis of foot clearance and foot placement strategies among unilateral transfemoral amputees, regardless of shoe geometry or gait style. Spatial analysis of the foot with respect to the step edge was possible using five clearance measures. Together these measures provided insight into where along the shoe sole the risk catching the foot on the step edge may be the greatest.

Assessing the recovery period following an induced trip is important for understanding unilateral transfemoral amputee fall risk and how falls can be prevented. The severity of the stumble perturbation outcome in terms of trunk kinematics and recovery duration may be related to the type of recovery strategy utilized. Through further stumbling analysis in older adults with unilateral transfemoral amputation, information regarding successful recovery responses can be provided to physical rehabilitation programs for translation into practice methods. For example, individual physical rehabilitation programs for older adult amputees should take into consideration not only a patient's physical ability and use of any assistive device, but also the type of prosthetic knee joint that is being used. Review of the elevating and lowering strategies should also be conducted in order to determine which method would be appropriate for the patient should a stumble occur while walking. Educating patients during the physical rehabilitation period about recovery from stumbles or trips is a preventative measure that may help reduce the number of fall events in older adult unilateral transfemoral amputees.

The minimum foot clearance and stumble perturbation outcome measures developed in this thesis address a current void in unilateral transfemoral amputee research. Among previous unilateral transfemoral amputee gait research, neither of these areas has been specifically examined for the older adult population. While MFC and the recovery method used following a stumble with respect to prosthetic knee joint type have been briefly examined for young and middle-aged adult subjects, the outcomes from these studies cannot be directly translated to the older adult amputee population due to age differences, as has been shown in the able-bodied population. Furthermore, prior work has yet to assess trunk kinematics during stumble recovery for older adult unilateral transfemoral amputees, despite this outcome measure being widely examined in the able-bodied older adult population. Moving forward, research with unilateral

transfemoral amputees should focus on the older adult population, so knowledge regarding amputee gait will be enhanced and comparisons to able-bodied older adults can be made. With proper understanding of unilateral transfemoral amputee gait in older adults, efforts can then be focused on reducing the fall risk in this population.

The geometric model of the prosthetic limb developed in this thesis was able to successfully determine the inertial properties of the foot, shank, and thigh segments. Despite the simplifying geometry and assumptions used in this modeling approach, the resulting measurements were comparable to direct measurements taken for the foot, shank, and socket segments. Additional geometric modeling of the prosthetic limb will likely yield trends in the density of the foot segment and prosthetic knee joint, which will eliminate the need for measured mass in the geometric model calculations. Specifically, for subjects who utilize a prosthetic knee joint that has already been analyzed, the density will already be known so direct measurement of the mass of the shank segment will be unnecessary. This eliminates the need for the prosthetic limb to be taken apart, and the inertial properties can be determined based only on dimensional measurements. Furthermore, a geometric modeling approach reduces the equipment, personnel, and time needed to determine the inertial properties of the prosthetic limb in a gait laboratory setting.

While previous studies have used a direct measurement approach for determining the inertial properties of the prosthetic limb segments, the inertial property values found for these adult subjects has not been reported. Standard anthropometric literature for able-bodied adults provides an easy method for determining segment inertial properties, but this resource is absent for adult unilateral transfemoral amputees. Proper identification of the lower limb segment inertial properties is important for accurate lower limb joint moment analysis. Using the

geometric modeling approach to determine prosthetic limb inertial properties will provide a simple and accurate way to obtain these values for joint moment calculations. Through joint moment analysis, a better understanding of when knee collapse is likely to occur during the gait cycle is possible. As a result, physical rehabilitation programs may be able to help older adult unilateral transfemoral amputees understand their risk for knee collapse more fully, thus leading to fewer falls over time.

The major limitation in this thesis was the subject population analyzed. Due to timing constraints only six subjects had completed the biomechanics laboratory session. Four of the subjects were part of a pilot study that had a modified protocol and marker set, so results for these subjects were limited in terms of stair descent and stumbling perturbation trials. Age was also a limiting factor in this research. Unfortunately this analysis cannot be considered one focusing solely on older adults since three of the subjects were below the age of 65. Furthermore, there were not enough subjects to make comparisons regarding the effect prosthetic knee joint type had on unilateral transfemoral amputee gait, but four of the six subjects were using the MPK joint. In terms of the protocol, the consistency of the stumbling perturbation device was another limitation. A stumbling perturbation was only successfully induced for three subjects, two of which occurred while foam obstacles were being used to apply the stumble. Therefore, the stumbling outcomes for these subjects may be different than what would have been seen if wood obstacles were used.

Future work in the area of unilateral transfemoral amputee gait analysis should address current voids in the literature: minimum foot clearance during normal walking and during stair ambulation, trunk kinematics following a stumbling perturbation and the recovery strategy used by older adult amputees, and reporting of inertial properties for the prosthetic limb segments. In

general, attention needs to be placed on the older adult population as the fall risk for these individuals is not fully understood like it is for their able-bodied counterparts. Further, consistency in methodology for unilateral transfemoral amputee gait analysis across studies would be beneficial, as various techniques have been used for assessing functional ambulatory ability. For example, stair and ramp ambulation have been evaluated for unilateral transfemoral amputees using various clinical assessments, which can make it challenging to compare outcomes across studies or with biomechanics-based results.

Lastly, the methodology developed in this thesis will be used for analysis of subjects participating in the full research study. The long term goal of this research study is to effectively identify functional differences and similarities between MPK joints and NMPK joint when used by older adult unilateral transfemoral amputees as they perform various ambulatory tasks. While comparisons between the two different knee joint types was beyond the scope of this thesis, results from the full research study will allow for a better understanding of their overall functionality and help ascertain the impact knee joint type may have on the fall risk within the older adult unilateral transfemoral amputee population.

APPENDIX A

AMPUTEE MOBILITY PREDICTOR ASSESSMENT

The amputee mobility predictor (AMP) assessment is a short physical performance test that is used to determine functional ability and associated classification level. Subjects were evaluated with the AMP assessment during visit 1 to verify their K-level allowed inclusion in the study. The AMP assessment was done a second time during visit 4 to determine if the subject's K-level changed while using the opposing knee type. The following table shows each item of the AMP assessment with a short description and the item's scoring options [42]. Safety precautions were taken during the evaluation and no item was performed if either the evaluator or subject was uncertain of a safe outcome.

Table 30. Amputee Mobility Predictor evaluation form used during visits 1 and 4 [42].

Item Number and Task	Scoring Procedure	Score
1. Sitting balance: sit forward in a chair with arms folded across chest for 60 seconds.	Cannot sit upright independently for 60 sec. or requires support from observer (0) Can sit upright independently for 60s (1)	
2. Sitting reach: reach forward and grasp the ruler. (Tester holds ruler 12in beyond extended arm(s) of subject, positioned midline to the subject's sternum.)	Does not attempt the task (0) Cannot grasp or requires arm support of chair or device (1) Reaches forward and successfully grasps the ruler (2)	

Table 30 (continued).

<p>3. Chair to chair transfer: 2 chairs at 90°. Start in armless chair. Subject may choose side for 2nd chair to be on. Use of hands is permitted.</p>	<p>Cannot transfer independently or requires physical assistance to complete (0) Performs independently, but appears unsteady (1) Performs independently, appears to be steady and safe (2)</p>	
<p>4. Arises from a chair: ask subject to fold arms across chest and stand up from a sitting upright, forward position. If unable, use arms or assistive device.</p>	<p>Unable, without help (physical assistance) (0) Able, uses arms/assist device to help (1) Able, without using arms (2)</p>	
<p>5. Attempts to arise from a chair: if attempt in No. 4 was not successfully completed without arms then ignore No. 4 and complete No. 5: Allow another attempt without penalty. If subject has difficulty and requires additional attempts or physical assistance, grade according to No. 5.</p>	<p>Unable, without help (physical assistance) (0) Able to complete, requires > 1 attempt (1) Able to rise in a single attempt (2)</p>	
<p>6. Immediate standing balance: (first 5 seconds of standing) First attempt is without assistive device. If support is required, allow after first attempt. Begin timing immediately after the amputee reaches upright standing posture. Steady posture with normal foot movement to adjust is permitted without penalty.</p>	<p>Unsteady posture (stagger, quick move of foot to maintain balance or excessive sway) (0) Steady, using walking aid or other support (1) Steady, without walker or other support (2)</p>	
<p>7. Standing balance: Time for 30 seconds.</p>	<p>Unsteady (0) Steady but uses walking aid or other support (1) Standing without support (2)</p>	
<p>8. Single-limb standing balance: (stopwatch ready) Time the duration of single-limb standing on both the sound and prosthetic limb up to 30 seconds. Grade the quality, not the time.</p> <p>Sound side: _____ seconds</p> <p>Prosthetic side: _____ seconds</p>	<p><u>Sound limb side</u> Unsteady (0) Steady but uses walking aid or other support for 30s (1) Single-limb standing without support for 30s (2)</p> <p><u>Prosthetic limb side</u> Unsteady (0) Steady but uses walking aid or other support for 30s (1) Single-limb standing without support for 30s (2)</p>	

Table 30 (continued).

<p>9. Standing reach: Stand with feet 2-4in apart. Reaches forward and grasp the ruler. (Tester holds ruler 12in beyond extended arm(s) of subject, positioned on midline to the subject's sternum.)</p>	<p>Does not attempt (0) Cannot grasp or requires arm support on assistive device (1) Reaches forward and successfully grasps item with no support (2)</p>	
<p>10. Nudge test: (same setup as No. 7) Feet as close together as possible, examiner pushes firmly on subject's sternum with palm of hand 3 times (toes should rise).</p>	<p>Begins to fall (0) Stagger, grabs, catches self, or uses assistive device (1) Steady, free of assistive device (2)</p>	
<p>11. Eyes closed: (same setup as No. 7; stopwatch ready) Stand with feet 2-4in apart, time for 30 seconds. If support is required, grade as unsteady.</p>	<p>Unsteady or uses assistive device (0) Steady without any use of assistive device (1)</p>	
<p>12. Picking up objects off the floor: Pick up a pencil off the floor; placed midline, 12in in front of foot. Do not move feet.</p>	<p>Unable to pick up object and return to standing (0) Performs with some help (table, chair, walking aid, etc.) (1) Performs independently (without help from object or person) (2)</p>	
<p>13. Sitting down: Ask subject to fold arms across chest and sit down. If unable, use arms or assistive device.</p>	<p>Unsafe (misjudged distance, falls into chair) (0) Uses arms, assistive device, or not a smooth motion (1) Safe, smooth motion (2)</p>	
<p>14. Initiation of gait: Immediately after told to "go".</p>	<p>Any hesitancy or multiple attempts to start (0) No hesitancy (1)</p>	
<p>15. Step length and height: Walk a measured distance of 12ft twice (up and back). Four scores are required: 2 scores (a & b) for each leg. "Marked deviation" is defined as extreme substitute movements to permit clearing the floor.</p>	<p>a. Swing foot Does not advance a minimum of 12in (0) Advances a minimum of 12in (1)</p>	<p>Prosthesis _____ Sound _____</p>
	<p>b. Foot clearance Foot does not completely clear floor without deviation (foot shuffling, sliding, circumduction) (0) Foot completely clears floor without marked deviation (1)</p>	<p>Prosthesis _____ Sound _____</p>
<p>16. Step continuity: Score while subject is performing No. 15.</p>	<p>Stopping or discontinuity between steps (stop & go gait) (0) Steps appear continuous (1)</p>	

Table 30 (continued).

<p>17. Turning: 180° turn when subject is returning to chair during No. 15.</p>	<p>Unable to turn, requires intervention to prevent falling (0) More than 3 steps but completes task without intervention (1) No more than 3 continuous steps with or without assistive aid (2)</p>	
<p>18. Variable cadence: Walk a distance of 12ft fast, as safely as possible 4 times. (Speeds may vary from slow to fast and fast to slow, varying cadence.)</p>	<p>Unable to vary cadence in a controlled manner (0) Asymmetrical increase in cadence controlled manner (1) Symmetrical increase in speed in a controlled manner (2)</p>	
<p>19. Stepping over obstacle: Place a movable box of 4in in height in the walking path.</p>	<p>Cannot step over the box (0) Catches foot, interrupts stride (1) Steps over without interrupting stride (2)</p>	
<p>20. Stairs: (must have at least 2 steps) Try to go up and down these stairs without holding on to the railing. Don't hesitate to permit subject to hold on to the railing. Safety first, if examiner feels that any risk is involved omit and score as 0.</p>	<p><u>Ascending</u> Unsteady, cannot do (0) One step at a time, or must hold on to railing or device (1) Steps over step, does not hold onto the railing or device (2)</p>	
	<p><u>Descending</u> Unsteady, cannot do (0) One step at a time, or must hold on to railing or device (1) Steps over step, does not hold onto the railing or device (2)</p>	
<p>21. Assistive device selection: Add points for the use of an assistive device if used for 2 or more items in No. 14 to 20. If testing without prosthesis use of appropriate assistive device is mandatory.</p>	<p>Bed bound (0) Wheelchair (1) Walker (2) Crutches (axillary or forearm) (3) Cane (straight or quad) (4) None (5)</p>	
TOTAL SCORE		____ / 47

APPENDIX B

SUPPORTING OUTCOME MEASURES FOR LEVEL SURFACE WALKING

B.1 ANALYSIS METHODS

Motion capture data was collected at 120 Hz and all marker trajectories for the level surface walking trials were exported to MATLAB (The MathWorks, Inc.) for post-processing. For the spatial-temporal outcome measures the marker data was filtered with a fourth order Butterworth filter, with a sampling frequency of 120 Hz and a cutoff frequency of 6 Hz. All heel-strike and initial forefoot motion events were identified and verified visually using the superior heel and toe marker trajectories, respectively [102].

Gait speed was defined as the average pelvic center of mass velocity along the direction of progression [115]. The pelvic center of mass was determined from the anterior and posterior superior iliac spine markers. The first derivative of this center of mass position during gait was used to calculate the average gait speed over the length of the trial.

Cadence was calculated as the number of steps taken per minute during the trial [48]. Stride duration, which is the time to complete one gait cycle, was defined using two consecutive heel-strikes for the each foot. Single-limb stance duration was defined as the time between heel-strike and initial forefoot motion events for each foot during the stance phase of gait. Double-

limb support duration was defined as the period of time when both feet were in contact with the floor during gait. Step length was defined as the anterior-posterior distance between two consecutive heel-strike events. Step width was defined as the medial-lateral distance between two consecutive heel-strikes events. For all spatial-temporal results, the average and standard deviation for each subject was obtained from three level surface walking trials.

The results for stride duration, single-limb support duration, double-limb support duration, step length, and step width were analyzed using a symmetry index to determine the degree of symmetry between the prosthetic and sound limbs [73, 116-117]. The symmetry index (SI) equation is given below, where PL is the prosthetic limb gait parameter value and SL is the sound limb gait parameter value:

$$SI = \frac{PL - SL}{0.5(PL + SL)} \times 100\%$$

A symmetry index value of zero corresponds to perfect symmetry between the prosthetic and sound limb. A positive symmetry index means the prosthetic limb gait parameter is greater than the sound limb side, and a negative symmetry index represents the sound limb value being greater than the prosthetic limb.

Knee joint angle was defined as the relative angle between the longitudinal axis of the thigh and shank segments. The thigh segment was the vector between the hip joint center and the lateral knee. The hip joint center was found as the center point between the anterior-superior iliac spine marker and the posterior-superior iliac spine marker on each limb side. The shank segment was the vector between the lateral knee and lateral ankle. A knee angle of zero degrees corresponds to full extension of the knee joint; a positive knee angle corresponds to knee flexion and a negative knee angle corresponds to knee hyper-extension.

B.2 SPATIAL-TEMPORAL RESULTS

Gait speed ranged from 0.28 m/s to 1.09 m/s for the six subjects analyzed in this thesis, yielding an overall average gait speed of 0.67 m/s.

Table 31. Average gait speed (standard deviation) across three level surface walking trials.

Subject	Gait Speed (m/s)
1	1.02 (0.03)
2	0.57 (0.05)
3	1.09 (0.02)
4	0.85 (0.04)
5	0.47 (0.03)
6	0.28 (0.02)

Cadence ranged from 60.92 steps/min to 114.45 steps/min for the six subjects included in this thesis. The overall average cadence for this subject population was 87.80 steps/min.

Table 32. Average cadence (standard deviation) across three level surface walking trials.

Subject	Cadence (steps/min)
1	105.31 (0.84)
2	77.72 (7.65)
3	114.45 (4.02)
4	97.02 (2.71)
5	71.36 (1.20)
6	60.92 (2.21)

All subjects had relatively symmetric stride duration between the prosthetic and sound limb (Table 33). Subject 6 had near perfect symmetry between the limbs, while subject 2 had the largest asymmetry with the sound limb having a greater stride time. Four of the six subjects had longer stride duration with the prosthetic limb.

Table 33. Average stride duration (standard deviation) for 9 strides taken with each limb while walking on a level surface, and the resulting symmetry indices (positive index denotes prosthetic limb value is larger than sound limb).

Stride Duration			
Subject	Sound Limb (s)	Prosthetic Limb (s)	Symmetry Index (%)
1	1.33 (0.04)	1.33 (0.03)	0.22 (2.01)
2	1.84 (0.13)	1.82 (0.12)	-1.63 (5.93)
3	1.20 (0.03)	1.20 (0.03)	-0.27 (3.34)
4	1.42 (0.03)	1.43 (0.04)	0.31 (3.25)
5	1.95 (0.07)	1.95 (0.06)	0.21 (3.90)
6	2.27 (0.08)	2.27 (0.12)	0.01 (2.84)

All subjects had a longer single-limb stance duration when they were standing on their sound limb (Table 34). The symmetry index results show subject 6 had the most symmetric single-limb stance time between the sound and prosthetic limb.

Table 34. Average single-limb stance duration (standard deviation) for 12 stance phases with each limb while walking on a level surface, and the symmetry index results (negative index value denotes sound limb duration is greater than prosthetic limb duration).

Single-Limb Stance Duration			
Subject	Sound Limb (s)	Prosthetic Limb (s)	Symmetry Index (%)
1	0.85 (0.04)	0.66 (0.02)	-25.97 (4.46)
2	1.27 (0.12)	1.10 (0.11)	-14.21 (6.01)
3	0.71 (0.03)	0.52 (0.03)	-31.83 (5.70)
4	0.89 (0.04)	0.72 (0.01)	-21.75 (3.67)
5	1.19 (0.07)	1.04 (0.06)	-13.92 (5.33)
6	1.83 (0.09)	1.70 (0.10)	-6.55 (4.97)

Double-limb support duration results show half of the subjects (subjects 1, 2, and 5) had a shorter double-limb support duration when the prosthetic limb was leading, while the other half of subjects had a shorter double-limb support duration when the sound limb was leading (Table 35). Subject 5 had the largest asymmetry between the double-limb support duration times for the prosthetic and sound limbs. Subjects 4 and 6 had relatively symmetric double-limb support durations when either the prosthetic or sound limb was the leading foot at heel-strike, with the prosthetic limb duration slightly longer.

Table 35. Average double-limb support duration (standard deviation) for 12 steps taken with each limb while walking on a level surface. Sound limb double-limb support periods occur when the sound limb is the leading foot, and prosthetic limb double-limb support occurs when the prosthetic limb is the leading foot. A negative symmetry index represents the sound limb value is greater than the prosthetic limb.

Double-Limb Support Duration			
Subject	Sound Limb (ms)	Prosthetic Limb (ms)	Symmetry Index (%)
1	94.44 (10.86)	87.96 (15.09)	-9.69 (17.02)
2	349.07 (78.67)	190.74 (40.06)	-58.20 (13.46)
3	34.26 (12.11)	52.78 (12.26)	45.58 (47.97)
4	91.67 (11.18)	94.17 (11.82)	1.69 (14.84)
5	256.82 (43.91)	55.00 (16.29)	-125.03 (16.05)
6	619.44 (63.00)	624.07 (60.59)	1.62 (17.46)

Five of the six subjects displayed a longer step length with the prosthetic limb (Table 36). Subjects 1 and 4 had the most symmetric step length between the prosthetic and sound limb (these subjects were the same person, using a NMPK joint and MPK joint, respectively).

Table 36. Average step length (standard deviation) for 12 steps taken with each limb while walking on a level surface, and the resulting symmetry indices (positive index denotes prosthetic limb value is larger than sound limb).

Step Length			
Subject	Sound Limb (cm)	Prosthetic Limb (cm)	Symmetry Index (%)
1	62.41 (1.56)	63.81 (2.48)	2.17 (5.30)
2	45.41 (1.95)	56.99 (2.87)	22.14 (6.97)
3	58.92 (1.81)	62.25 (3.75)	5.45 (5.18)
4	58.57 (1.77)	56.58 (4.12)	-3.67 (7.86)
5	36.66 (2.04)	51.23 (2.65)	33.12 (7.00)
6	28.69 (3.71)	33.56 (1.29)	17.31 (14.82)

All subjects, except subject 4, had a larger step width when taking a step forward with the prosthetic limb (Table 37). Subject 3 had the highest asymmetric step width between the prosthetic and sound limb.

Table 37. Average step length (standard deviation) for 12 steps taken with each limb while walking on a level surface, and the resulting symmetry index (positive index denotes prosthetic limb value is larger than sound limb).

Step Width			
Subject	Sound Limb (cm)	Prosthetic Limb (cm)	Symmetry Index (%)
1	21.99 (2.13)	22.78 (1.98)	3.59 (10.51)
2	10.53 (1.13)	10.99 (1.68)	6.44 (24.02)
3	20.92 (1.78)	24.17 (2.69)	14.92 (16.40)
4	20.71 (2.33)	20.16 (1.41)	-2.34 (17.28)
5	21.42 (1.03)	21.89 (2.96)	1.40 (14.86)
6	24.37 (1.39)	24.17 (1.58)	5.01 (3.00)

B.3 KNEE JOINT ANGLE RESULTS

Subject 1 knee joint angle plots show the prosthetic limb transitions to the swing phase at approximately 50% of the gait cycle and the sound limb at approximately 60% of the gait cycle (Figure 54). The prosthetic limb also has smaller deviation in knee joint angle during swing phase. Both knee joints retain slight flexion during the stance phase, with the sound limb showing an increase to 20.07 degrees of flexion during the shock absorption period at the beginning of the gait cycle. The prosthetic limb mean maximum knee angle during swing was 70.48 degrees while the sound limb mean maximum angle was 62.89 degrees.

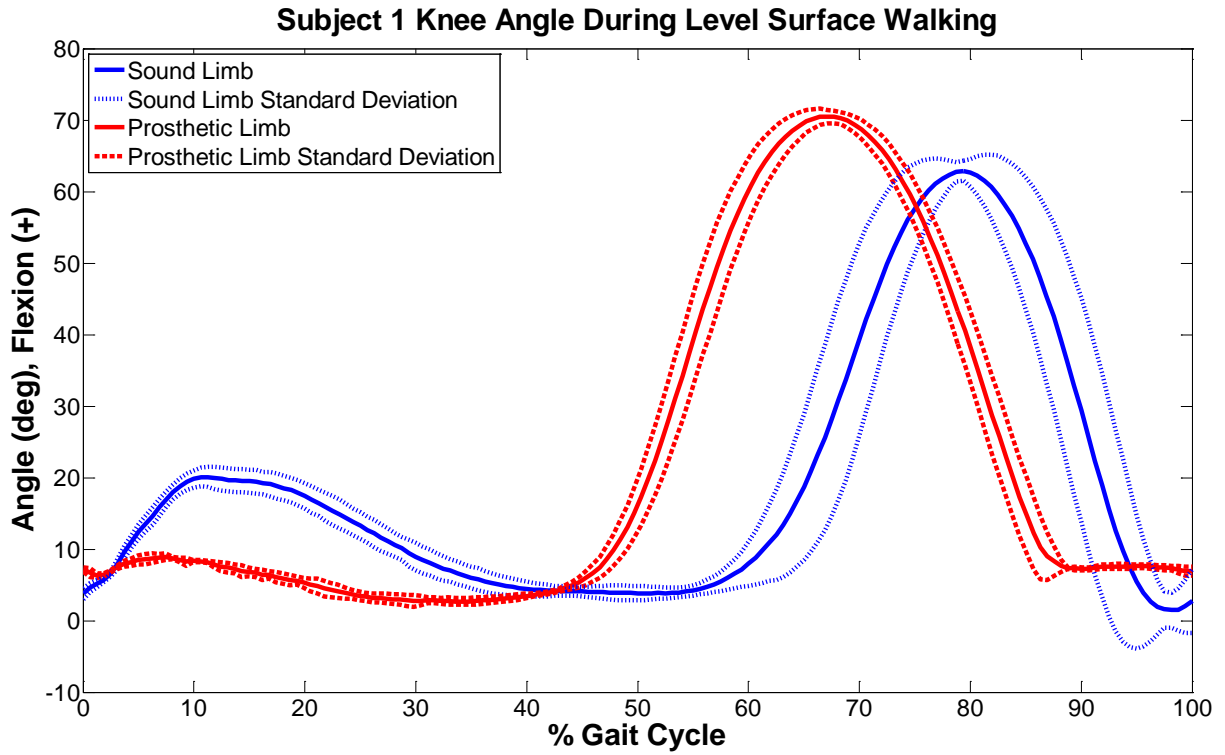


Figure 54. Subject 1 knee joint angles for the sound and prosthetic limb during level surface walking. Solid lines represent the mean knee angle across gait cycles; dashed lines show the standard deviation. Heel-strike occurs at zero and 100% of the gait cycle.

Subject 2 maintained the prosthetic knee in hyper-extension during the stance phase of the gait cycle (Figure 55). The prosthetic limb entered the swing phase at approximately 55% of the gait cycle and reached a mean maximum knee angle of 48.53 degrees. The sound limb knee joint flexed to 11.84 degrees on average during shock absorption at the beginning of the gait cycle. This was followed by a slow increase in flexion until the swing phase began at approximately 65% of the gait cycle, reaching an average maximum knee angle of 69.39 degrees. This gradual increase in flexion was likely impacted by the subject walking with a cane in each hand which provided stability during gait.

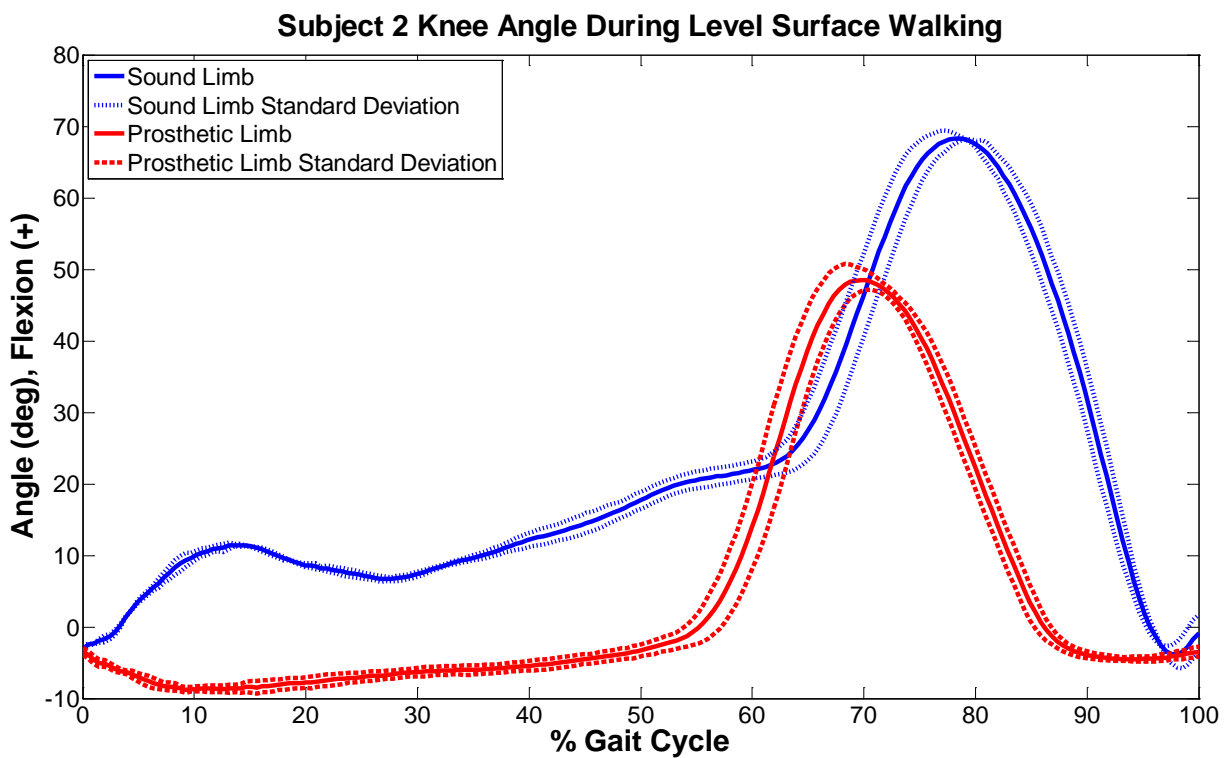


Figure 55. Subject 2 knee joint angles for the sound and prosthetic limbs during level surface walking. Solid lines represent the mean knee angle across gait cycles; dashed lines show the standard deviation. Heel-strike occurs at zero and 100% of the gait cycle.

Subject 3 had very little deviation in the prosthetic knee angle across gait cycles. The prosthetic knee joint maintained less than five degrees of hyper-extension throughout the stance phase (Figure 56). The swing phase for the prosthetic limb was initiated at approximately 50% of the gait cycle and the mean maximum knee flexion during swing was 52.40 degrees. The sound limb knee joint had an average of 13.38 degrees of knee flexion during shock absorption, and then the knee was shifted into extension during the remainder of the stance phase. There was larger deviation in the sound limb swing phase, which began around 45% of the gait cycle. A mean maximum knee flexion angle of 60.26 degrees was seen for the sound limb during swing. This subject did walk with a cane in the sound limb side hand.

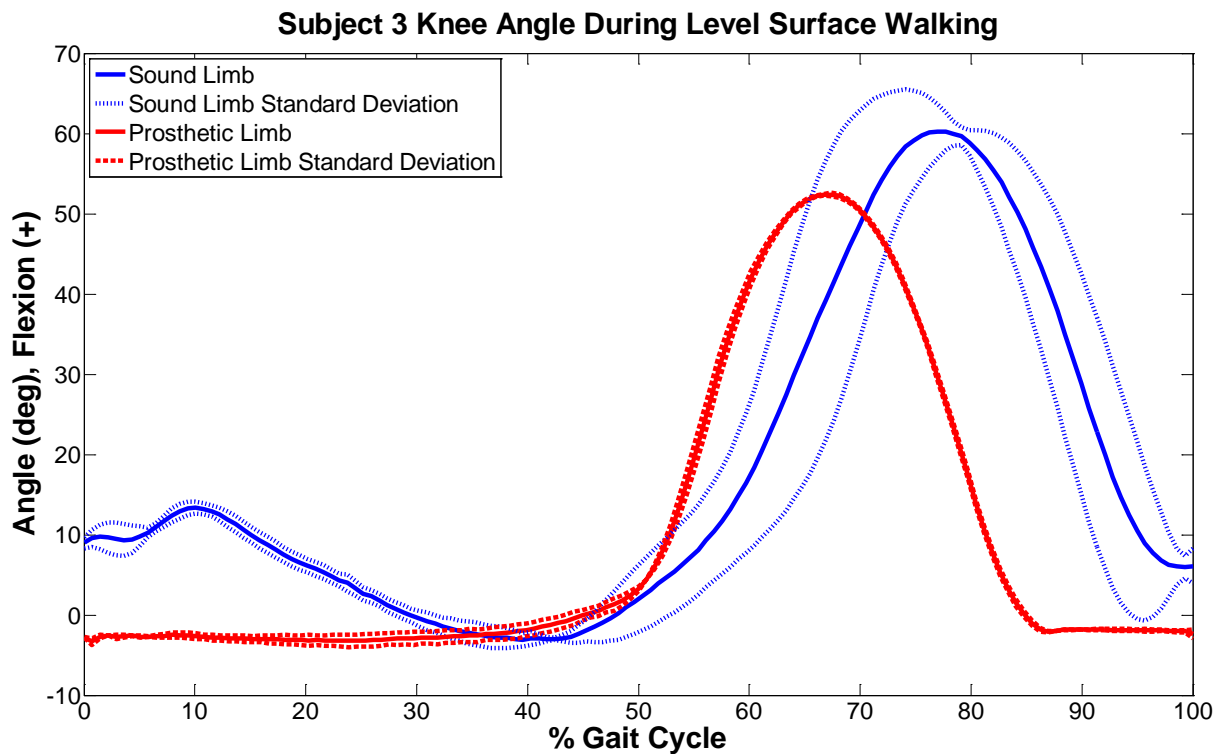


Figure 56. Subject 3 knee joint angles for the sound and prosthetic limbs during level surface walking. Solid lines represent the mean knee angle across gait cycles; dashed lines show the standard deviation. Heel-strike occurs at zero and 100% of the gait cycle.

Subject 4 knee joint angle plots show the prosthetic knee was slightly hyper-extended during the stance phase until approximately 50% of the gait cycle when the swing phase began (Figure 57). The mean maximum prosthetic knee flexion during the swing phase was 49.28 degrees. The sound limb knee joint had an average of 19.28 degrees of flexion during the shock absorption period of the stance phase, and the knee joint remained slightly flexed during the stance phase until the swing phase began around 60% of the gait cycle. The sound limb mean maximum knee flexion was 62.57 degrees.

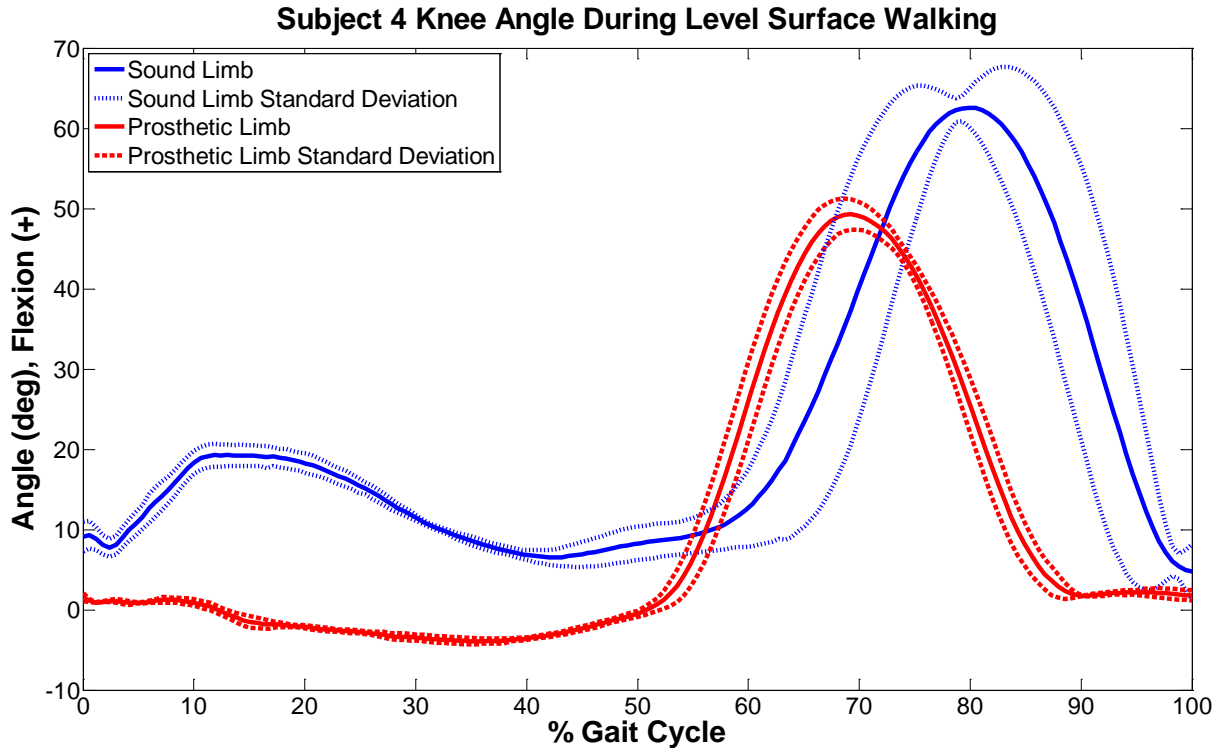


Figure 57. Subject 4 knee joint angles for the sound and prosthetic limbs during level surface walking. Solid lines represent the mean knee angle across gait cycles; dashed lines show the standard deviation. Heel-strike occurs at zero and 100% of the gait cycle.

Subject 5 kept the prosthetic knee in less than five degrees of hyper-extension throughout the stance phase of the gait cycle (Figure 58). During the swing phase the mean maximum average knee flexion was 1.24 degrees, occurring at 88% of the gait cycle. The sound limb had more deviation during the stance phase than the swing phase. The sound knee was flexed at heel-strike continued flexing for shock absorption, yielding a mean of 19.49 degrees. Then, the sound knee joint angle showed movement toward full extension near 50% of the gait cycle before entering into the swing phase around 60% of the gait cycle. The sound knee flexed to a mean maximum angle of 67.33 degrees during the swing phase. The subject used a cane held in the sound limb side hand while walking.

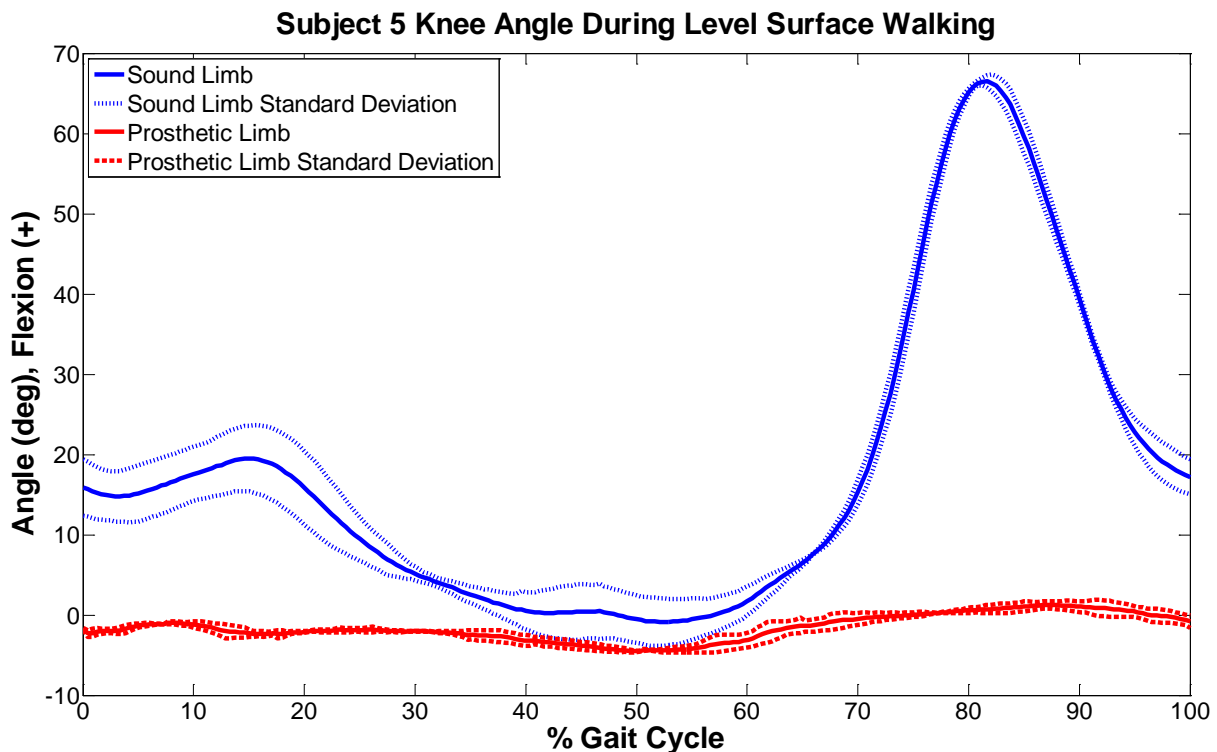


Figure 58. Subject 5 knee joint angles for the sound and prosthetic limbs during level surface walking. Solid lines represent the mean knee angle across gait cycles; dashed lines show the standard deviation. Heel-strike occurs at zero and 100% of the gait cycle.

Subject 6 had more knee flexion in the prosthetic limb than the sound limb during the entire gait cycle (Figure 59). The prosthetic limb knee angle plot shows an average knee flexion of 15.44 degrees during shock absorption at the beginning of the stance phase, and then a gradual increase in knee flexion until the mean maximum knee flexion angle of 51.91 degrees occurred at 86% of the gait cycle. The sound limb entered the stance phase with a small amount of hyperextension and then gradually increased knee flexion until the swing phase began around 70% of the gait cycle. The sound limb mean maximum knee angle during swing was 42.63 degrees, and more deviation was seen during the sound limb swing phase than during the prosthetic knee swing phase.

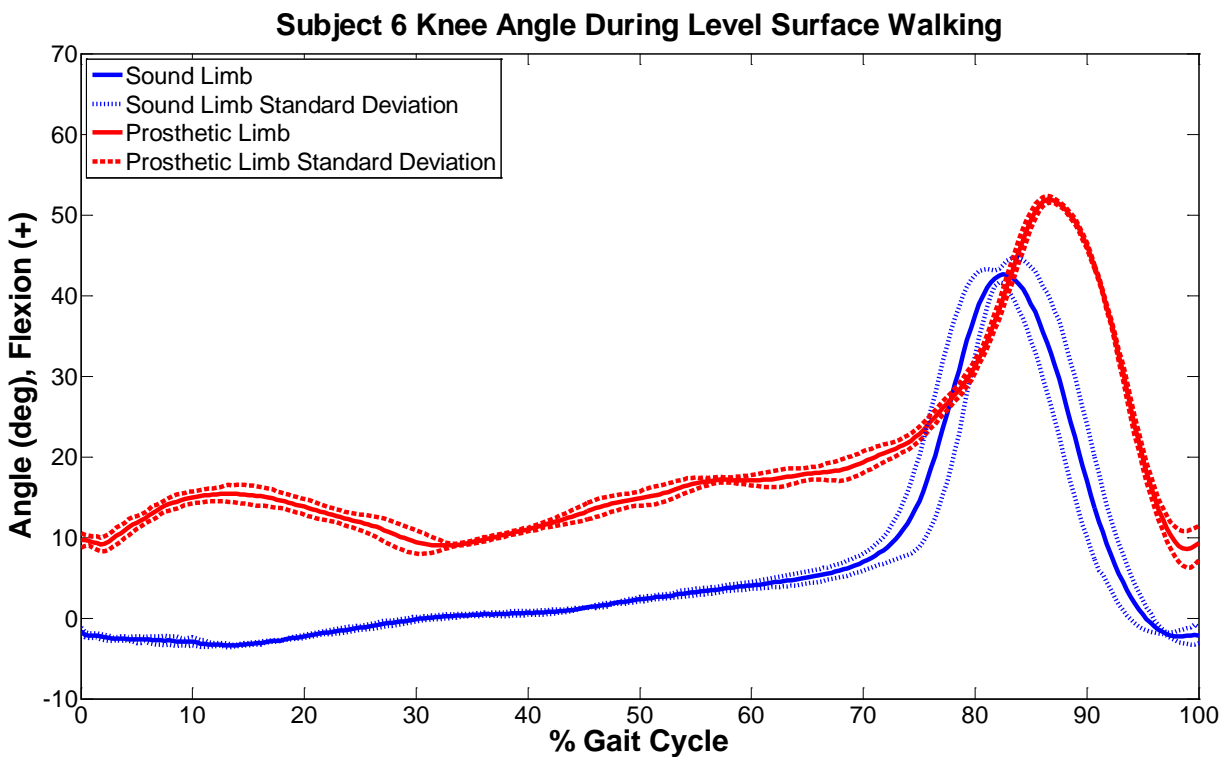


Figure 59. Subject 6 knee joint angles for the sound and prosthetic limbs during level surface walking. Solid lines represent the mean knee angle across gait cycles; dashed lines show the standard deviation. Heel-strike occurs at zero and 100% of the gait cycle.

APPENDIX C

FOOT CLEARANCE RESULTS FOR STAIR AMBULATION

C.1 STAIR ASCENT

The average distances for all foot clearance measures, for the both the prosthetic and sound limb during stair ascent, are given in Table 38. The values highlighted in gray are the overall minimum clearance values for the forefoot for each measure. Only the toe tip marker was available to analyze clearance for subjects 1 through 4. Subject 2 had marker visibility issues for the sound limb. The resultant clearance for the inferior heel marker was not calculated because the inferior heel does not pose a very high risk for inducing a trip during stair ascent.

Table 38. Mean (standard deviation) minimum foot clearance distances during stair ascent for all subjects. The gray highlighted values signify the overall minimum clearance for the forefoot. The resultant clearance was not analyzed for the inferior heel marker; a dash indicates N/A.

Stair Ascent Minimum Foot Clearance Measures							
Subject	Position	Resultant Clearance (cm)		Horizontal Clearance (cm)		Vertical Clearance (cm)	
		Sound Limb	Prosthetic Limb	Sound Limb	Prosthetic Limb	Sound Limb	Prosthetic Limb
1	Toe tip	6.46 (2.14)	5.92 (1.31)	-9.34 (7.08)	-9.32 (5.30)	8.51 (0.68)	7.07 (0.38)
2	Toe tip	-	3.99 (1.43)	-	-5.52 (2.66)	-	5.12 (0.65)
3	Toe tip	5.06 (2.15)	4.77 (0.27)	-8.90 (8.57)	-9.68 (1.96)	6.60 (1.93)	4.83 (0.30)
4	Toe tip	4.31 (0.96)	6.28 (0.59)	-6.47 (4.02)	-12.70 (5.64)	5.38 (0.87)	6.34 (0.54)
5	Toe tip	2.55 (0.89)	5.32 (0.78)	-3.94 (1.87)	-11.30 (3.76)	4.39 (1.43)	5.92 (1.15)
	Front Forefoot	4.22 (1.11)	4.68 (1.19)	-6.49 (2.11)	-13.81 (3.66)	5.54 (1.52)	4.85 (1.06)
	Middle Forefoot	6.23 (1.58)	4.54 (1.28)	-10.28 (2.43)	-17.43 (3.67)	6.76 (1.72)	4.63 (1.15)
	Break	7.26 (1.87)	4.35 (1.42)	-15.11 (3.22)	-21.85 (3.67)	7.37 (1.86)	4.41 (1.30)
	Inferior Heel	-	-	-5.20 (1.15)	-4.44 (0.54)	3.52 (1.58)	6.86 (0.49)
6	Toe tip	3.29 (0.67)	0.71 (0.29)	-4.71 (1.30)	-0.75 (0.31)	4.31 (0.73)	3.85 (2.74)
	Front Forefoot	3.00 (0.62)	1.74 (0.77)	-5.96 (1.70)	-2.11 (0.74)	3.63 (0.70)	3.54 (2.03)
	Middle Forefoot	3.69 (0.59)	2.93 (1.25)	-9.96 (1.41)	-4.67 (1.05)	4.15 (0.57)	3.96 (1.21)
	Break	4.21 (0.59)	3.85 (0.98)	-14.63 (1.51)	-8.13 (1.05)	4.56 (0.64)	4.49 (0.72)
	Inferior Heel	-	-	-4.14 (1.60)	-0.42 (1.96)	2.22 (0.10)	4.85 (1.01)

C.2 STAIR DESCENT

The results in Table 39 are average distances for foot clearance of the prosthetic and sound limb during stair descent. The values highlighted in gray are the overall minimum clearance values for the inferior heel for each variable, as this marker was used to assess the risk of tripping. Only the toe tip marker was available to analyze the forefoot clearance of subjects 1 through 4. Subject 2 had marker visibility issues for the sound limb. Overall, the resultant clearance for the forefoot markers was not calculated because the forefoot is not the focus for assessing trip risk

during stair descent. Subjects 3, 4, and 5 have negative vertical clearance values for the sound limb foot because the toe tip had passively tilted down over the step edge prior to initial forefoot motion as a result of the prosthetic limb progression. The same pattern was seen in the prosthetic foot for subjects 2 and 4. Subject 4 had large horizontal clearance values for the toe tip due to an attempt to descend the stairs with a step-over-step method. Subject 6 had a shoe size smaller than the step tread, which resulted in negative horizontal clearance values because the forefoot markers were behind the step edge during stance.

Table 39. Mean (standard deviation) minimum foot clearance distances during stair descent for all subjects. The gray highlighted values signify the overall minimum clearance for the forefoot. The resultant clearance was not analyzed for the forefoot markers; a dash indicates N/A.

Stair Descent Minimum Foot Clearance Measures							
		Resultant Clearance (cm)		Horizontal Clearance (cm)		Vertical Clearance (cm)	
Subject	Position	Sound Limb	Prosthetic Limb	Sound Limb	Prosthetic Limb	Sound Limb	Prosthetic Limb
1	Toe tip	-	-	3.66 (4.06)	6.50 (0.52)	1.22 (1.65)	4.73 (0.88)
2	Toe tip	-	-	-	9.69 (0.37)	-	-4.81 (0.79)
3	Toe tip	-	-	5.20 (1.27)	2.08 (0.27)	-2.44 (0.55)	1.68 (0.17)
4	Toe tip	-	-	17.54 (9.79)	29.24 (22.60)	-7.18 (0.44)	-0.48 (10.89)
5	Toe tip	-	-	9.46 (0.95)	4.93 (0.71)	-5.81 (0.81)	3.38 (0.71)
	Front Forefoot	-	-	6.98 (0.81)	2.70 (0.74)	-4.40 (0.66)	1.98 (0.82)
	Middle Forefoot	-	-	3.56 (0.80)	-0.83 (0.72)	-2.19 (0.58)	2.34 (1.05)
	Break	-	-	-0.65 (0.79)	-5.24 (0.66)	0.46 (0.33)	3.30 (0.95)
	Inferior Heel	3.73 (0.78)	3.85 (0.67)	5.94 (1.37)	11.35 (2.32)	5.31 (2.08)	4.09 (0.83)
6	Toe tip	-	-	-0.58 (2.67)	-1.67 (0.76)	1.59 (0.55)	4.53 (0.41)
	Front Forefoot	-	-	-3.13 (2.50)	-2.88 (0.76)	0.97 (0.39)	2.73 (0.46)
	Middle Forefoot	-	-	-6.37 (2.32)	-5.42 (0.70)	1.75 (0.42)	2.31 (0.65)
	Break	-	-	-9.97 (2.13)	-8.36 (0.58)	2.76 (0.36)	2.43 (0.78)
	Inferior Heel	5.12 (0.61)	4.12 (0.96)	7.52 (1.02)	12.03 (3.38)	5.93 (0.77)	4.19 (0.97)

APPENDIX D

RESPONSES TO STUMBLING

The stumble perturbation outcome measures for subjects 3 and 6 are presented in this section. Table 40 provides the average trunk angle and velocity values seen during an unperturbed walking trial over a level surface. Tables 41-42 show the resulting trunk values during the recovery period durations. During the perturbation for subject 3, the obstacle became unattached from the device, slid across the floor, and was stepped on by the sound foot. The perturbation for subject 6 obstructed the sound limb.

Table 40. Average trunk angles and angular velocity while walking unperturbed over a level surface for subjects 3 and 6.

Subject	Sagittal Plane (deg)		Frontal Plane (deg)		Angular Velocity (deg/s)
	Average Max	Average Min	Average Max	Average Min	Average
3	17.61	11.86	6.32	-0.10	21.47
6	39.14	31.11	1.04	-7.46	12.76

Table 41. Trunk angles in the sagittal and frontal planes during the stumble recovery durations for subjects 3 and 6.

Subject	Sagittal Plane (deg)			Frontal Plane (deg)		
	At Contact	Recovery Max	Recovery Min	At Contact	Recovery Max	Recovery Min
3	14.18	14.18	11.80	0.84	0.97	-0.74
6	33.96	42.10	33.96	-3.72	4.23	-3.83

Table 42. Trunk angular velocity during the stumble recovery durations.

Subject	Angular Velocity (deg/s)		
	At Contact	Recovery Max	Recovery Min
3	22.32	44.66	13.42
6	3.76	60.99	3.33

Subject 3 displayed a decrease of approximately 3 degrees in sagittal plane trunk angle during the stumble recovery duration, as the prosthetic foot was preparing for heel-strike (Figure 60). Following this heel-strike an increase in sagittal plane trunk flexion occurred when the subject stepped on the dislodged obstacle with the sound limb during the next step. During the recovery duration, as the trunk angle in the sagittal plane decreased, the trunk angle in the frontal plane also decreased, corresponding to trunk tilt toward the left of vertical (Figure 61). A maximum angular velocity maximum of 44.66 deg/s occurred at the instant of prosthetic limb heel-strike (Figure 62).

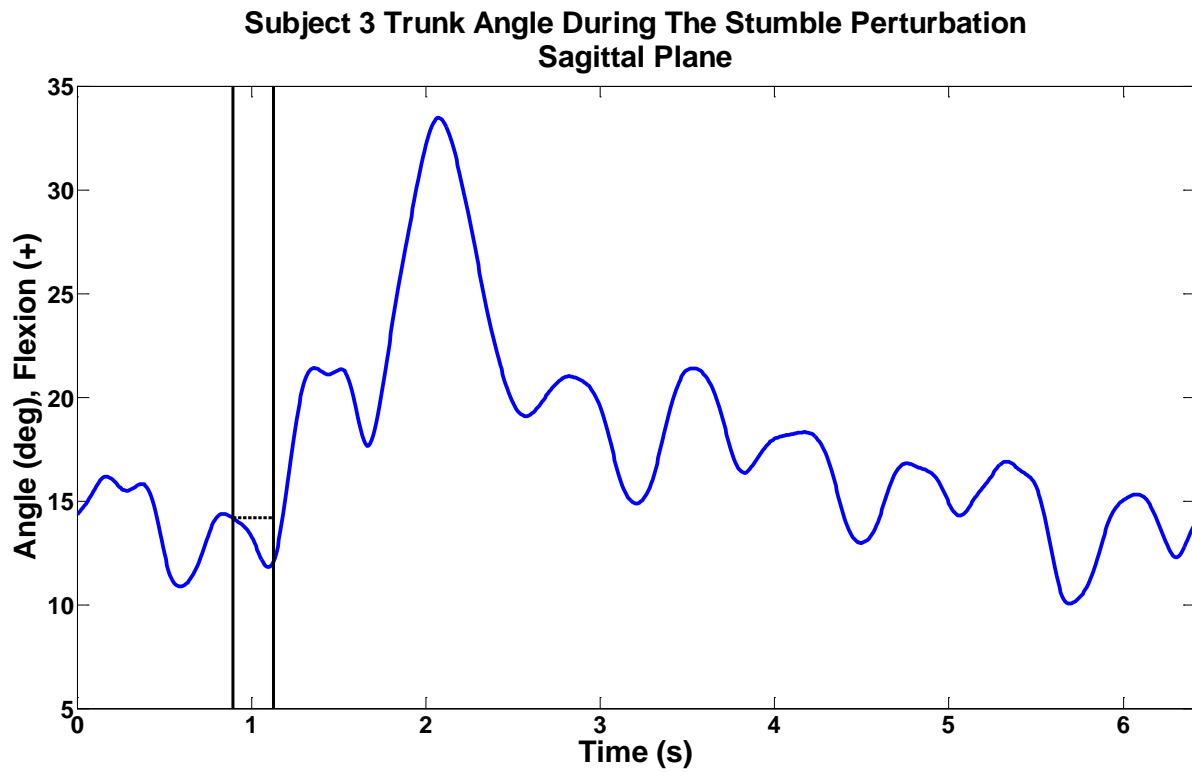


Figure 60. Sagittal plane trunk angle during the stumble perturbation trial for subject 3. Initial contact with the obstacle and heel-strike of the first recovered step are identified by vertical lines. The sagittal plane trunk angle at initial contact is represented throughout the recovery duration by a dashed line.

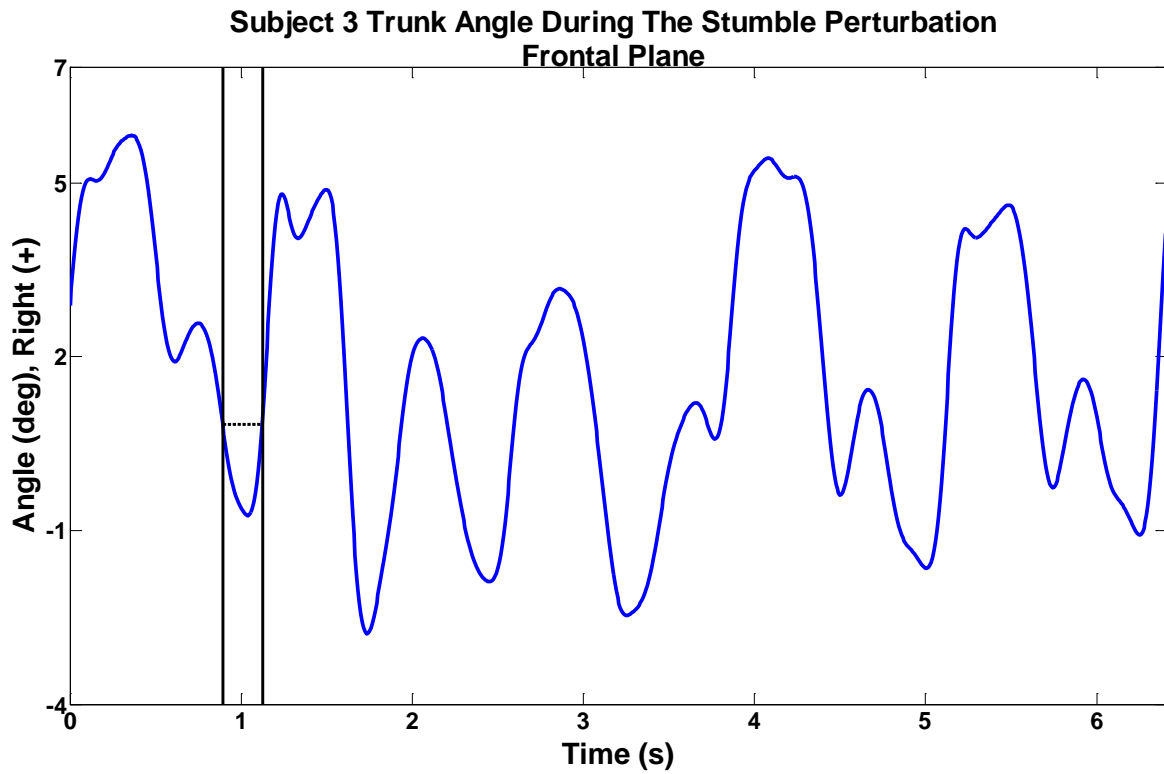


Figure 61. Frontal plane trunk angle during the stumble perturbation trial for subject 3. Initial contact with the obstacle and heel-strike of the first recovered step are identified by vertical lines. The frontal plane trunk angle at initial contact is represented throughout the recovery duration by a dashed line.

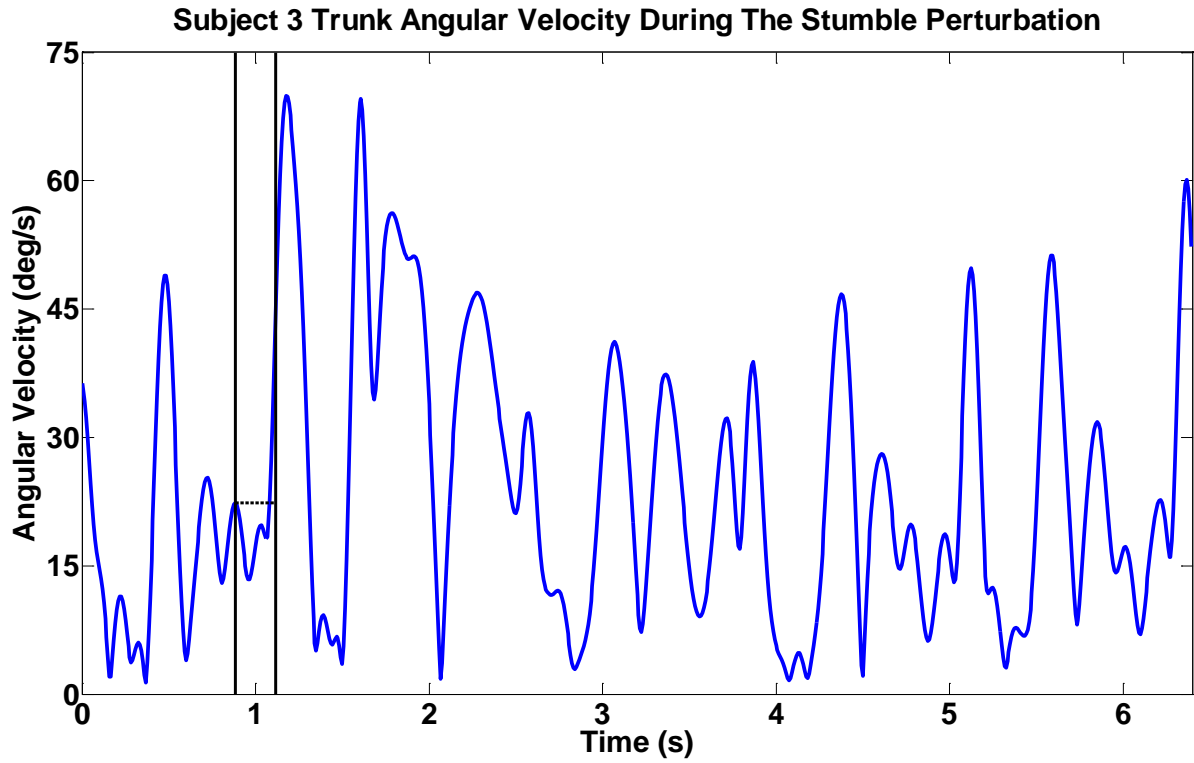


Figure 62. Trunk angular velocity during the stumble perturbation trial for subject 3. Initial contact with the obstacle and heel-strike of the first recovered step are identified by vertical lines. The angular velocity at initial contact is represented throughout the recovery duration by a dashed line.

Subject 6 had a gait speed of 0.28 m/s and walked with a walker. There was an 8.14 degree difference in the sagittal plane trunk angle between the time of initial contact with the obstacle and the maximum trunk angle during the recovery duration (Figure 63). Compared to the subject's average maximum trunk angle in the sagittal plane during normal unperturbed walking, there was only a 2.96 degree difference between the maximum values, likely contributed to the use of a walker. The trunk angle in the frontal plane saw a movement of approximately 8 degrees toward the right side (same side as the obstructed foot) following contact with the obstacle (Figure 64). The trunk angular velocity rapidly increased to 57.23 deg/s after initial contact with the obstacle, and the angular velocity reached a similar peak just prior to heel-strike of the first recovered step (Figure 65).

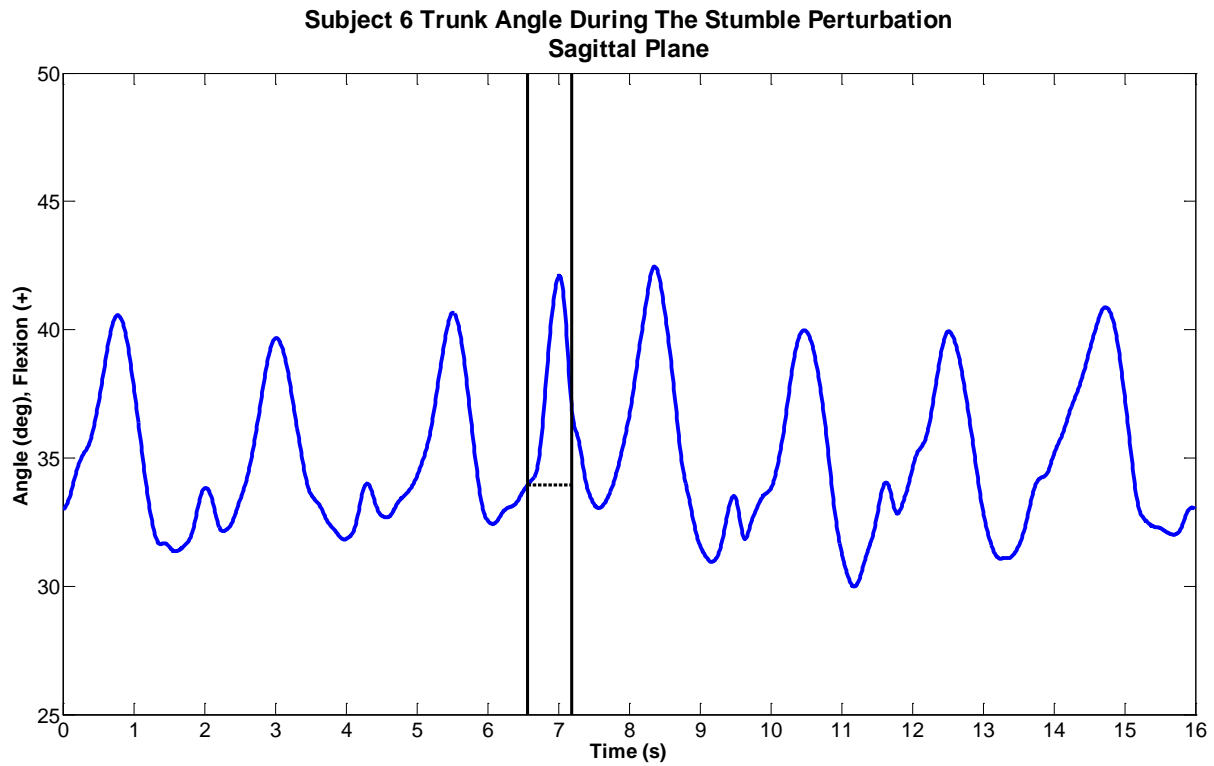


Figure 63. Sagittal plane trunk angle during the stumble perturbation trial for subject 6. Initial contact with the obstacle and heel-strike of the first recovered step are identified by vertical lines. The sagittal plane trunk angle at initial contact is represented throughout the recovery duration by a dashed line.

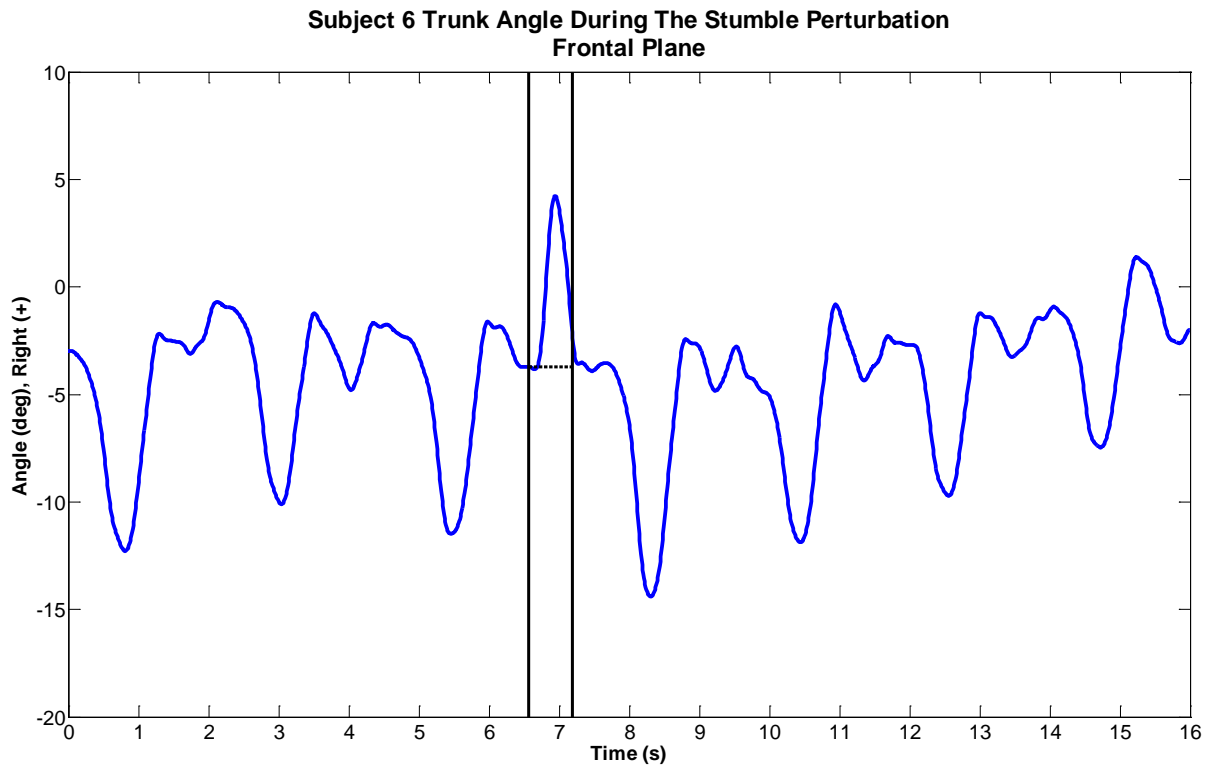


Figure 64. Frontal plane trunk angle during the stumble perturbation trial for subject 6. Initial contact with the obstacle and heel-strike of the first recovered step are identified by vertical lines. The frontal plane trunk angle at initial contact is represented throughout the recovery duration by a dashed line.

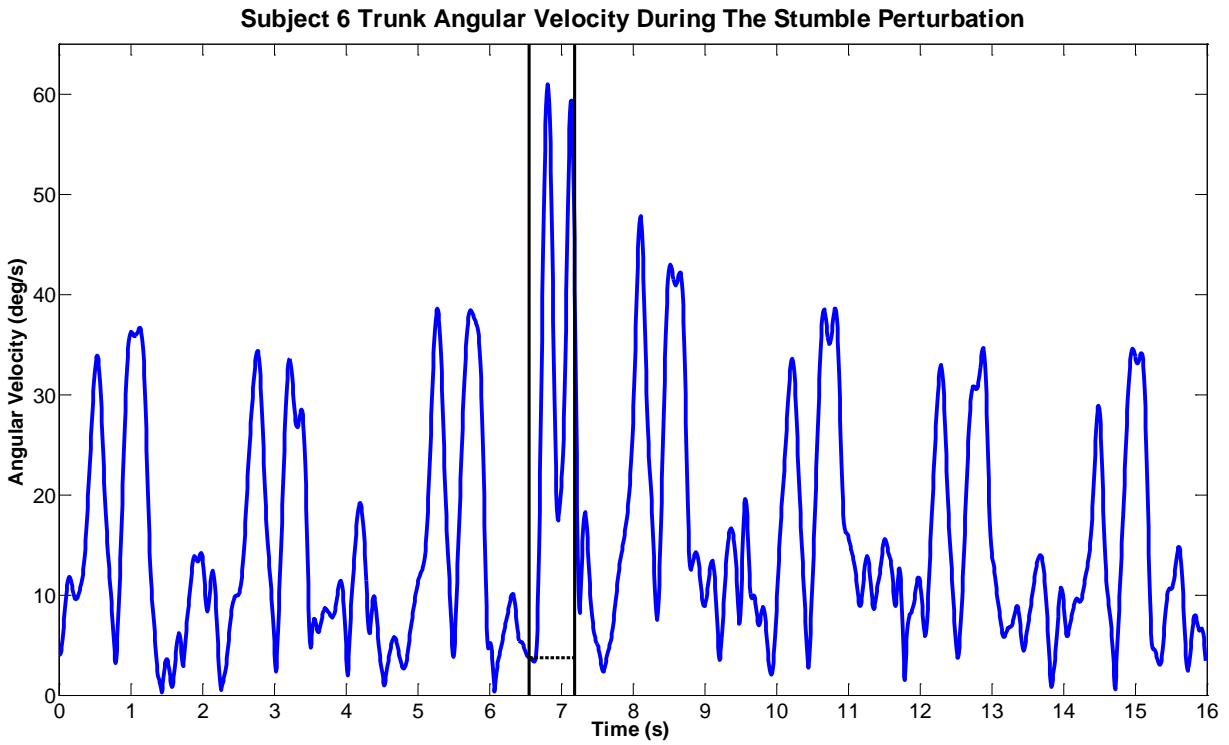


Figure 65. Trunk angular velocity during the stumble perturbation trial for subject 6. Initial contact with the obstacle and heel-strike of the first recovered step are identified by vertical lines. The angular velocity at initial contact is represented throughout the recovery duration by a dashed line.

APPENDIX E

EQUATIONS FOR THE GEOMETRIC MODEL OF THE PROSTHETIC LIMB USED TO DETERMINE SEGMENT INERTIAL PROPERTIES

E.1 FOOT SEGMENT

For each stadium solid in the foot segment, the lower bound stadium used the subscript 0 and upper bound stadium used the subscript 1. The following equations are from the mathematical model presented by Yeadon for a series of stadium solids [66].

Half the width of the rectangle of the stadium is defined by r , and half the length of the rectangle of the stadium is defined by t . Parameters r and t for a stadium at some distance, h , from the lower bounding stadium are:

$$r = r_0(1 + ah) \quad t = t_0(1 + bh)$$
$$a = \frac{r_1 - r_0}{r_0} \quad b = \frac{t_1 - t_0}{t_0}$$

For a stadium that has uniform density ρ , area $A(h)$, and thickness hdz , the stadium solid mass was given by:

$$m = \int_0^1 \rho A(h) h dz = \rho h r_0 [4t_0 F1(a, b) + \pi r_0 F1(a, a)]$$

The simplifying expressions in the mass equation were defined as:

$$F1(a, b) = 1 + \frac{a + b}{2} + \frac{ab}{3}$$

$$F1(a, a) = 1 + \frac{2a}{2} + \frac{a^2}{3}$$

Since the density of the foot segment was unknown but assumed to be constant, density was obtained using the measured mass and calculated volume of the foot segment.

$$\rho = \frac{m}{V}$$

$$V = hr_0[4t_0F1(a, b) + \pi r_0^2F1(a, a)]$$

The center of mass location from the proximal end of the foot segment (the posterior edge of the heel) was found using:

$$\bar{h} = \frac{\rho h^2[4r_0t_0F2(a, b) + \pi r_0^2F2(a, a)]}{m}$$

The simplifying expressions in the center of mass equation were defined as:

$$F2(a, b) = \frac{1}{2} + \frac{a + b}{3} + \frac{ab}{4}$$

$$F2(a, a) = \frac{1}{2} + \frac{2a}{3} + \frac{a^2}{4}$$

The mass moment of inertia about the medial-lateral axis at the proximal edge of the foot was found by determining the moment of inertia about the foot segment center of mass and then using the parallel axis theorem to move the rotational point some the distance, d , to the proximal edge.

$$I_x = I_{x_{COM}} + md^2$$

$$I_{x_{COM}} = \int_0^1 J_x \rho h dh + \int_0^1 h^2 A(h) h dh$$

$$I_{x_{COM}} = \rho h \left[\frac{4r_0 t_0^3 F4(a, b)}{3} + \frac{\pi r_0^4 F4(a, a)}{4} \right] + \rho h^3 [4r_0 t_0 F3(a, b) + \pi r_0^2 F3(a, a)]$$

The simplifying expressions in the mass moment of inertia equation were defined as:

$$F4(a, b) = 1 + \frac{a + 3b}{2} + \frac{3ab + 3b^2}{3} + \frac{3ab^2 + b^3}{4} + \frac{ab^3}{5}$$

$$F4(a, a) = 1 + \frac{4a}{2} + \frac{6a^2}{3} + \frac{3a^3 + a^3}{4} + \frac{a^4}{5}$$

$$F3(a, b) = \frac{1}{3} + \frac{a + b}{4} + \frac{ab}{5}$$

$$F3(a, a) = \frac{1}{3} + \frac{2a}{4} + \frac{a^2}{5}$$

E.2 SHANK SEGMENT

All shank segment equations were provided in the *Handbook of Equations for Mass and Area Properties of Various Geometrical Shapes* [113]. The pylon and pylon adapter were modeled as hollow circular cylinders. The standard dimensions of a pylon are 0.030 m outer diameter and

0.025 m inner diameter. Thus, the inner diameter of the pylon adapter matched the outer diameter of the pylon. To find the volume of a hollow cylinder the following equation was used:

$$V = \pi h(R^2 - r^2)$$

The density of the pylon and pylon adapter were known based on their material type, so the mass of each piece was calculated:

$$m = \rho V$$

The center of mass of a hollow cylinder was found using the equation:

$$\bar{L} = \frac{L}{2}$$

The moment of inertia for a hollow cylinder about its center of mass with a medial-lateral axis of rotation is:

$$I_{x_{COM}} = m \left[\frac{h^2}{12} + \frac{R^2 + r^2}{4} \right]$$

The knee joint was modeled as a rectangular prism. The volume equation took into account the knee length (L), the medial-lateral distance (W), and the anterior-posterior distance (H).

$$V = LHW$$

The density of the knee joint was found using the knee volume and the measured mass of the shank segment minus the calculated masses of the pylon and pylon adapter.

$$\rho = \frac{m}{V}$$

The center of mass location of the knee joint was found using the equation:

$$\bar{L} = \frac{L}{2}$$

The moment of inertia of the knee joint about its center of mass with respect to the medial-lateral axis was found by:

$$I_{xCOM} = \frac{m(L^2 + H^2)}{12}$$

The parallel axis theorem was used to determine the moment of inertia for the entire shank segment about the proximal point of the segment.

$$I_x = I_{xCOM} + md^2$$

E.3 THIGH SEGMENT

All thigh segment equations were provided in the *Handbook of Equations for Mass and Area Properties of Various Geometrical Shapes* [113]. The proximal portion of the socket and residual limb was a right-angled wedge shape. The height of the shape was represented by h , the medial-lateral distance was a , and the anterior-posterior distance was b . The volume was found by the equation:

$$V = \frac{abh}{2}$$

Using either the density of the socket material or the density of the residual limb, the mass of the thigh flap section was found for the socket and residual limb portions of the thigh:

$$m = \rho V$$

The moment of inertia for a right-angled wedge shape about its center of mass for a medial-lateral axis of rotation was found using:

$$I_{xCOM} = \frac{m(2h^2 + 3b^2)}{36}$$

A series of elliptical cylinders formed the intermediate length of the socket and residual portions of the thigh segment. The symbol a represented half of the anterior-posterior distance and the symbol b represented half of the medial-lateral distance. The volume was given by the equation:

$$V = \pi abh$$

Again, since socket and residual limb density were known, the mass of the elliptical cylinders was found:

$$m = \rho V$$

The center of mass location for an elliptical cylinder was half of its height:

$$\bar{h} = \frac{h}{2}$$

The moment of inertia at the center of mass for an elliptical cylinder about the medial-lateral axis of rotation was given by the equation:

$$I_{x_{COM}} = \frac{m}{12} (3a^2 + h^2)$$

For the distal elliptical paraboloid shape, the symbols a and b represent half of the anterior-posterior and medial-lateral distance, respectively. The volume equation was:

$$V = \frac{\pi abh}{2}$$

The center of mass for an elliptical paraboloid was given by:

$$\bar{h} = \frac{h}{3}$$

The moment of inertia about the center of mass of an elliptical paraboloid with respect to a medial-lateral axis of rotation was:

$$I_{x_{COM}} = \frac{m}{18} (3a^2 + h^2)$$

The thigh segment moment of inertia was reported at the proximal edge. To determine this value, the parallel axis theorem was applied to the entire thigh segment moment of inertia found at its center of mass, such that the moment of inertia was moved to the correct proximal location:

$$I_x = I_{x_{COM}} + md^2$$

BIBLIOGRAPHY

- [1] Lord, S.R., C. Sherrington, and H.B. Menz, *Falls in older people: risk factors and strategies for prevention*. Cambridge: Cambridge University Press, 2001.
- [2] Centers for Disease Control and Prevention, National Center for Injury Prevention and Control. *WISQARS Leading Causes of Death Reports, National and Regional, 1999-2009*. 01 June 2010 [cited 2012 June]; Available from: http://webappa.cdc.gov/sasweb/ncipc/leadcaus10_us.html.
- [3] Centers for Disease Control and Prevention, National Center for Injury Prevention and Control. *WISQARS Leading Causes of Nonfatal Injury Reports*. 18 October 2010 [cited 2012 June]; Available from: <http://webappa.cdc.gov/sasweb/ncipc/nfilead2001.html>.
- [4] Alexander, B.H., F.P. Rivara, and M.E. Wolf, *The Cost and Frequency of Hospitalization for Fall-Related Injuries in Older Adults*. *American Journal of Public Health*, 1992. **82**(7): p. 1020-23.
- [5] Centers for Disease Control and Prevention, National Center for Injury Prevention and Control. *Cost of Fall Injuries in Older Persons in the United States, 2005 – Figures 1-2*. 29 February 2012 [cited 2012 June]; Available from: <http://www.cdc.gov/homeandrecreationalsafety/Falls/data/cost-estimates-figures1-2.html>.
- [6] Centers for Disease Control and Prevention, *Public Health and Aging: Trends in Aging – United States and Worldwide*. *MMWR*, 2003. **52**(6): p. 101-06.
- [7] Kang, H.G., and J.B. Dingwell, *Separating the effects of age and walking speed on gait variability*. *Gait & Posture*, 2008. **27**: p. 572-77.
- [8] Pijnappels, M., et al., *Identification of elderly fallers by muscle strength measures*. *Eur J Appl Physiol*, 2008. **102**: p. 585-92.
- [9] Lord, S.R., D.G. Lloyd, and S.K. Li, *Sensori-motor function, gait patterns and falls in community-dwelling women*. *Age and Aging*, 1996. **25**: p. 292-99.

- [10] Hausdorff, J.M., D.A. Rios, and H.K. Edelberg, *Gait Variability and Fall Risk in Community-Living Older Adults: A 1-Year Prospective Study*. Arch Phys Med Rehabil, 2001. **82**: p. 1050-56.
- [11] Hausdorff, J.M., et al., *Increased gait unsteadiness in community-dwelling elderly fallers*. Arch Phys Med Rehabil, 1997. **78**: p. 278-83.
- [12] Grabiner, P.C., S.T. Biswas, and M.D. Grabiner, *Age-related changes in spatial and temporal gait variables*. Arch Phys Med Rehabil, 2001. **82**: p. 31-35.
- [13] van Dieën, J.H., M. Pijnappels, and M.F. Bobbert, *Age-related intrinsic limitations in preventing a trip and regaining balance after a trip*. Safety Science, 2005. **43**: p. 437-53.
- [14] Chamberlin, M.E., et al., *Does Fear of Falling Influence Spatial and Temporal Gait Parameters in Elderly Persons Beyond Changes Associated With Normal Aging?* Journal of Gerontology, 2005. **60A**(9): p. 1163-67.
- [15] Barrett, R.S., P.M. Mills, and R.K. Begg, *A systematic review of the effect of ageing and falls history on minimum foot clearance characteristics during level walking*. Gait & Posture, 2010. **32**: p. 429-35.
- [16] Koepsell, T.D., et al., *Footwear style and risk of falls in older adults*. American Geriatrics Society, 2004. **52**: p. 1495-1501.
- [17] Winter, D.A. *Biomechanics and motor control of human movement*. New York: John Wiley & Sons, 1990.
- [18] Winter, D.A., *Foot trajectory in human gait: a precise and multifactorial motor control task*. Phys Ther, 1992. **72**: p. 45-53.
- [19] Winter, D.A., et al., *Biomechanical Walking Pattern Changes in the Fit and Healthy Elderly*. Phys Ther, 1990. **70**: p. 340-47.
- [20] Khandoker, A.H., et al., *Investigating scale invariant dynamics in minimum toe clearance variability of the young and elderly during treadmill walking*. IEEE Transactions on Neural Systems and Rehabilitation Engineering, 2008. **16**(4): p. 380-89.
- [21] Centers for Disease Control and Prevention. *National diabetes fact sheet: national estimates and general information on diabetes and prediabetes in the United States, 2011*. Atlanta, GA: U.S. Department of Health and Human Services, Centers for Disease Control and Prevention, 2011.
- [22] Ziegler-Graham, K., et al., *Estimating the Prevalence of Limb Loss in the United States: 2005 to 2050*. Arch Phys Med Rehabil, 2008. **89**: p. 422-29.

- [23] Ephraim, P.L., et al., *Epidemiology of limb loss and congenital limb deficiency: a review of the literature*. Arch Phys Med Rehabil, 2003. **84**: p. 747-61.
- [24] Dillingham, T.R., L.E. Pezzin, and E.J. MacKenzie, *Limb Amputation and Limb Deficiency: Epidemiology and Recent Trends in the United States*. Southern Medical Journal, 2002. **95**(8): p. 875-83.
- [25] MacKenzie, E.J., et al., *Health-care costs associated with amputation or reconstruction of a limb-threatening injury*. J Bone Joint Surg Am, 2007. **89**: p. 1685-92.
- [26] Miller, W.C., M. Speechley, and B. Deathe, *The prevalence and risk factors of falling and fear of falling among lower extremity amputees*. Arch Phys Med Rehabil, 2001. **82**(8): p. 1031-37.
- [27] Miller, W.C., et al., *The influence of falling, fear of falling, and balance confidence on prosthetic mobility and social activity among individuals with a lower extremity amputation*. Arch Phys Med Rehabil, 2001. **82**(9): p. 1238-44.
- [28] Gauthier-Gagnon, C., M.C. Grisé, and D. Potvin, *Enabling factors related to prosthetic use by people with transtibial and transfemoral amputation*. Arch Phys Med Rehabil, 1999. **80**: p. 706-13.
- [29] Gauthier-Gagnon, C., M.C. Grise, and D. Potvin, *Predisposing factors related to prosthetic use by people with a transtibial and transfemoral amputation*. J Prosthet Orthotics, 1998. **10**(4): p. 99-109.
- [30] Hafner, B.J., and D.G. Smith, *Differences in functional and safety between Medicare Functional Classification Level-2 and -3 transfemoral amputees and influence of prosthetic knee joint control*. Journal of Rehabilitation Research & Development, 2009. **46**(3): p. 417-34.
- [31] Sapin, E., et al., *Functional gait analysis of trans-femoral amputees using two different single-axis prosthetic knees with hydraulic swing-phase control: kinematic and kinetic comparison of two prosthetic knees*. Prosthetics and Orthotics International, 2008. **32**(2): p. 201-18.
- [32] Michael, J.W., *Modern Prosthetic Knee Mechanisms*. Clinical Orthopaedics and Related Research, 1999. **361**: p. 39-47.
- [33] Berry, D., M.D. Olson, and K. Lartz, *Perceived Stability, Function, and Satisfaction Among Transfemoral Amputees Using Microprocessor and Nonmicroprocessor Controlled Prosthetic Knees: A Multicenter Survey*. American Academy of Orthotists and Prosthetists, 2009. **21**(1): p. 32-42.

- [34] Taylor, M.B., et al., *A comparison of energy expenditure by a high level trans-femoral amputee using the Intelligent Prosthesis and conventionally damped prosthetic limbs*. Prosthetics and Orthotics International, 1996. **20**: p. 116-21.
- [35] Berry, D., *Microprocessor Prosthetic Knees*. Phys Med Rehabil Clin N Am, 2006. **17**: p. 91-113.
- [36] Hafner, B.J., et al., *Evaluation of Function, Performance, and Preference as Transfemoral Amputees Transition From Mechanical to Microprocessor Control of the Prosthetic Knee*. Arch Phys Med Rehabil, 2007. **88**: p. 207-17.
- [37] Kahle, J.T., M.J. Highsmith, and S.L. Hubbard, *Comparison of nonmicroprocessor knee mechanism versus C-Leg on Prosthesis Evaluation Questionnaire, stumbles, falls, walking tests, star descent, and knee performance*. Journal of Rehabilitation Research & Development, 2008. **45**(1): p. 1-14.
- [38] Bellmann, M., et al., *Comparative biomechanical analysis of current microprocessor-controlled prosthetic knee joints*. Arch Phys Med Rehabil, 2010. **91**: p. 644-52.
- [39] Segal, A.D., et al., *Kinematic and kinetic comparisons of transfemoral amputee gait using C-Leg and Mauch SNS prosthetic knees*. Journal of Rehabilitation Research & Development, 2006. **43**(7): p. 857-70.
- [40] Kaufman, K.R., et al., *Gait and balance of transfemoral amputees using passive mechanical and microprocessor-controlled prosthetic knees*. Gait & Posture, 2007. **26**: p. 489-93.
- [41] Kaufman, K.R., S. Frittoli, and C.A. Frigo, *Gait asymmetry of transfemoral amputees using mechanical and microprocessor-controlled prosthetic knees*. Clinical Biomechanics, 2012. **27**: p. 460-65.
- [42] Gailey, R.S., et al., *The Amputee Mobility Predictor: An Instrument to Assess Determinants of the Lower-Limb Amputee's Ability to Ambulate*. Arch Phys Med Rehabil, 2002. **83**: p. 613-27.
- [43] Stepien, J.M., et al., *Activity levels among lower-limb amputees: Self-reported versus step activity monitor*. Arch Phys Med Rehabil, 2007. **88**: p. 896-900.
- [44] Coleman, K.L., et al., *Step activity monitor: Long-term, continuous recording of ambulatory function*. Journal of Rehabilitation Research and Development, 1999. **36**: p. 8-18.
- [45] Jaegers, S.M.H.J., J.H. Arendzen, and H.J. de Jongh, *Prosthetic Gait of Unilateral Transfemoral Amputees: A Kinematic Study*. Arch Phys Med Rehabil, 1995. **76**: p. 736-43.

- [46] Czerniecki, J.M., *Rehabilitation in Limb Deficiency. I. Gait and Motion Analysis*. Arch Phys Med Rehabil, 1996. **77**: p. S – 3-8.
- [47] Racic, V., A. Pavic, and J.M.W. Brownjohn, *Experimental identification and analytical modeling of human walking forces: literature review*. Journal of Sound and Vibration, 2009. **326**: p. 1-49.
- [48] Hollman, J.H., E.M. McDade, and R.C. Peterson, *Normative spatiotemporal gait parameters in older adults*. Gait & Posture, 2011. **34**: p. 111-18.
- [49] James, U., and K. Oberg, *Prosthetic gait pattern in unilateral above-knee amputees*. Scand J Rehab Med, 1975. **5**: p. 35-50.
- [50] Zachazewski, J.E., P.O. Riley, and D.E. Krebs, *Biomechanical analysis of body mass transfer during stair ascent and descent of healthy subjects*. J Rehabilitation Research and Development, 1993. **30**(4): p. 412-22.
- [51] Protopapadaki, A., et al., *Hip, knee, ankle kinematics and kinetics during stair ascent and descent in healthy young individuals*. Clinical Biomechanics, 2007. **22**: p. 203-10.
- [52] Muhaidat, J., et al., *Measuring foot placement and clearance during stair descent*. Gait & Posture, 2011. **33**: p. 504-506.
- [53] Hamel, K.A., et al., *Foot clearance during stair descent: effects of age and illumination*. Gait & Posture, 2005. **21**: p. 135-40.
- [54] Mian, O.S., et al., *Kinematics of stair descent in young and older adults and the impact of exercise training*. Gait & Posture, 2007. **25**: p. 9-17.
- [55] Hobara, H., et al., *Lower extremity joint kinematics of stair ascent in transfemoral amputees*. Prosthetics and Orthotics International, 2011. **35**(4): p. 467-72.
- [56] Hobara, H., et al., *Factors affecting stair-ascent patterns in unilateral transfemoral amputees*. Prosthetics and Orthotics International, 2012. **0**(0): p. 1-5.
- [57] Pavol, M.J., et al., *Mechanisms leading to a fall from an induced trip in healthy older adults*. Journal of Gerontology, 2001. **56A**(7): p. M428-37.
- [58] van den Bogert, A.J., M.J. Pavol, and M.D. Grabiner, *Response time is more important than walking speed for the ability of older adults to avoid a fall after a trip*. J. Biomechanics, 2002. **35**: p. 199-205.
- [59] Grabiner, M.D., et al., *Trunk kinematics and fall risk of older adults: Translating biomechanical results to the clinic*. Journal of Electromyography and Kinesiology, 2008. **18**(2): p. 197-204.

- [60] Vrieling, A.H., et al., *Obstacle crossing in lower limb amputees*. Gait & Posture, 2007. **26**: p. 587-94.
- [61] Crenshaw, J.R., K.R. Kaufman, and M.D. Grabiner, *Failed trip recoveries of above-knee amputees suggest possible fall-prevention interventions*, presented at the American Society of Biomechanics (ASB), Providence, RI, 2010.
- [62] Kaufman, K., et al., *Mechanisms of stumble recovery: non-microprocessor controlled compared to microprocessor-controlled prosthetic knees*. American Academy of Orthotists & Prosthetists: Journal of Proceedings, **38**, 2008.
- [63] Zatsiorsky, V., and V. Seluyanov, *The mass and inertia characteristics of the main segments of the human body*. Biomechanics VIII-B, 1983. **56**(2): p. 1152-59.
- [64] de Leva, P., *Adjustments to Zatsiorsky-Seluyanov's segment inertia parameters*. J. Biomechanics, 1996. **29**(9): p. 1223-30.
- [65] Dempster, W.T., and G.R. Gaughran, *Properties of body segments based on size and weight*. American Journal of Anatomy, 2005. **120**(1): p. 33-54.
- [66] Yeadon, M.R., *The simulation of aerial movement – II. A mathematical inertia model of the human body*. J. Biomechanics, 1990. **23**: p. 67-74.
- [67] Kingma, I., et al., *Segment inertial parameter evaluation in two anthropometric models by application of a dynamic linked segment model*. J. Biomechanics, 1996. **29**(5): p. 693-704.
- [68] Lulić, T.J., O. Muftić, and A. Sušić, *Design of the 3D model of human body oriented to biomechanical applications*. International Design Conference, Dubrovnik, 2004.
- [69] Miller, L.A., and D.S. Childress, *Problems associated with the use of inverse dynamics in prosthetic applications: An example using a polycentric prosthetic knee*. Robotica, 2005. **23**: p. 329-35.
- [70] Gitter, A., J. Czerniecki, and M. Meinders, *Effect of prosthetic mass on swing phase work during above-knee amputee ambulation*. American Journal of Physical Medicine & Rehabilitation, 1997. **76**(2): p. 114-21.
- [71] Fowler, E.G., et al., *Contrasts in gait mechanics of individuals with proximal femoral focal deficiency: Syme amputation versus Van Nes rotational osteotomy*. J. of Pediatric Orthopaedics, 1999. **19**(6): p. 720.
- [72] van der Linden, M.L., et al., *A methodology for studying the effects of various types of prosthetic feet on the biomechanics of trans-femoral amputee gait*. J. Biomechanics, 1999. **32**: p. 877-89.

- [73] Mattes, S.J., P.E. Martin, and T.D. Royer, *Walking symmetry and energy cost in persons with unilateral transtibial amputations: matching prosthetic and intact limb inertial properties*. Arch Phys Med Rehabil, 2000. **81**: p. 561-68.
- [74] Selles, R.W., et al., *Lower-leg inertial properties in transtibial amputees and control subjects and their influence on the swing phase during gait*. Arch Phys Med Rehabil, 2003. **84**: p. 569-77.
- [75] Goldberg, E.J., P.S. Requejo, and E.G. Fowler, *The effect of direct measurement versus cadaver estimates of anthropometry in the calculation of joint moments during above-knee prosthetic gait in pediatrics*. J. Biomechanics, 2008. **41**: p. 695-700.
- [76] Dempster, W.T., W.C. Gabel, and W.J. Felts, *The anthropometry of the manual work space for the seated subject*. American Journal of Physical Anthropology, 1959. **17**(4): p. 289-317.
- [77] Winter, D.A. *Biomechanics of human movement*. 2nd ed. New York: John Wiley & Sons, 1990.
- [78] Drillis, R., and R. Contini, *Body segment parameters*. Technical Report No. 1166.03. School of Engineering and Science, New York University, 1966.
- [79] McConville, J.T., et al., *Anthropometric relationships of body and body segment moments of inertia*. AFAMRL Technical Report 80-119. Wright-Patterson Air Force Base, Ohio, 1980.
- [80] Cham, R., and M.S. Redfern, *Changes in gait when anticipating slippery floors*. Gait & Posture, 2002. **15**: p.159-71.
- [81] Moyer, B.E., M.S. Redfern, and R. Cham, *Biomechanics of trailing leg response to slipping – evidence of interlimb and intralimb coordination*. Gait & Posture, 2009. **29**: p. 565-70.
- [82] Coley, B., and R. Cham, *Proactive postural adjustments during multiple exposures to trips*, presented at the American Society of Biomechanics (ASB), Providence, RI, 2010.
- [83] Stevens, W., B. Coley, and R. Cham, *Postural adaptations to repeated trips*, presented at the Biomedical Engineering Society (BMES), Pittsburgh, PA, 2009.
- [84] Legro, M.W., et al., *Prosthesis evaluation questionnaire for persons with lower limb amputations: assessing prosthesis-related quality of life*. Arch Phys Med Rehabil, 1998. **79**: p. 931-38.
- [85] Studenski, S., et al., *Predicting falls: the role of mobility and non-physical factors*. Journal of the American Geriatrics Society, 1994. **42**: p. 297-302.

- [86] Thies, S.B., et al., *Effects of ramp negotiation, paving type and shoe sole geometry on toe clearance in young adults*. J. Biomechanics, 2011. **44**: p. 2679-84.
- [87] United States Access Board, *Americans with Disabilities Act and Architectural Barriers Act accessibility guidelines*. July 23, 2004, p. 142-43, 164-67, 190.
- [88] Vickers, D.R., et al., *Elderly unilateral transtibial amputee gait on an inclined walkway: A biomechanical analysis*. Gait & Posture, 2008. **27**: p. 518-29.
- [89] Vrieling, A.H., et al., *Uphill and downhill walking in unilateral lower limb amputees*. Gait & Posture, 2008. **28**: p. 235-42.
- [90] Redfern, M.S., and J. DiPasquale, *Biomechanics of descending ramps*. Gait & Posture, 1997. **6**: p. 119-25.
- [91] Thies, S.B., J.K. Richardson, and J.A. Ashton-Miller, *Effects of surface irregularity and lighting on step variability during gait: a study in healthy young and older women*. Gait & Posture, 2005. **22**: p. 26-31.
- [92] Richardson, J.K., et al., *Interventions improve gait regularity in patients with peripheral neuropathy while walking on an irregular surface under low light*. J Am Geriatr Soc, 2004. **52**: p. 510-15.
- [93] Pijnappels, M., M.F. Bobbert, and J.H. van Dieën, *Contribution of the support limb in control of angular momentum after tripping*. J. Biomechanics, 2004. **37**: p. 1811-18.
- [94] Powell, L.E., and A.M. Myers, *The activities-specific balance confidence (ABC) scale*. Journals of Gerontology, 1995. **50A**: p. M28-34.
- [95] Gerzeli, S., A. Torbica, and G. Fattore, *Cost utility analysis of knee prosthesis with complete microprocessor control (C-Leg) compared with mechanical technology in transfemoral amputees*. Eur J Health Econ, 2009. **10**: p. 47-55.
- [96] Rabin, R., and F. de Charro, *EQ-5D: a measure of health status from the EuroQol Group*. Ann Med, 2001. **33**: p. 337-43.
- [97] Viccaro, L.J., S. Perera, and S.A. Studenski, *Is timed up and go better than gait speed in predicting health, function, and falls in older adults?* J Am Geriatr Soc, 2011. **59**: p. 887-92.
- [98] The EuroQol-Group, *EuroQol – a new facility for the measurement of health related quality of life*. Health Policy, 1990. **16**: p. 199-208.
- [99] Gauthier-Gagnon, C., M. Grise, and Y. Lepage, *The locomotor capabilities index: content validity*. J Rehabil Outcomes Meas, 1998. **2**: p. 40-46.

- [100] Dite, W. H.J. Connor, and H.C. Curtis, *Clinical identification of multiple fall risk early after unilateral transtibial amputation*. Arch Phys Med Rehabil, 2007. **88**: p. 109-14.
- [101] Startzell, J.K., P.R. Cavanagh, *A three-dimensional approach to the calculation of foot clearance during locomotion*. Human Movement Science, 1999. **18**: p. 603-11.
- [102] Mickelborough, J., et al., *Validity and reliability of a kinematic protocol for determining foot contact events*. Gait & Posture, 2000. **11**: p. 32-37.
- [103] Roerdink, M., et al., *Gait coordination after stroke: benefits of acoustically paced treadmill walking*. Phys Ther, 2007. **87**: p. 1009-22.
- [104] Moosabhoy, M.A., and S.A. Gard, *Methodology for determining the sensitivity of swing leg toe clearance and leg length to swing leg joint angles during gait*. Gait & Posture, 2006. **24**: p. 493-501.
- [105] Perry, J., *Gait analysis: normal and pathological function*. Thorofare: Slack Inc., 1992.
- [106] Ramstrand, N., and K.-A. Nilsson, *A comparison of foot placement strategies of transtibial amputees and able-bodied subjects during stair ambulation*. Prosthetics and Orthotics International, 2009. **33**(4): p. 348-55.
- [107] Wang, T.-Y., et al., *Adaptive control reduces trip-induced forward gait instability among young adults*. J. Biomechanics, 2012. **45**: p. 1169-75.
- [108] van der Burg, J.C.E., M. Pijnappels, and J.H. van Dieën, *The influence of artificially increased trunk stiffness on the balance recovery after a trip*. Gait & Posture, 2007. **26**: p. 272-78.
- [109] Carty, C.P., P. Mills, and R. Barrett, *Recovery from forward loss of balance in young and older adults using the stepping strategy*. Gait & Posture, 2011. **33**: p. 261-67.
- [110] Curtze, C., et al., *Balance recovery after an evoked forward fall in unilateral transtibial amputees*. Gait & Posture, 2010. **32**: p. 336-41.
- [111] Grabiner, M.D., J.W. Feuerbach, and D.W. Jahnigen, *Measures of paraspinal muscle performance do not predict initial trunk kinematics after tripping*. J. Biomechanics, 1996. **29**(6): p. 735-44.
- [112] Owings, T.M., M.J. Pavol, and M.D. Grabiner, *Mechanisms of failed recovery following postural perturbations on a motorized treadmill mimic those associated with an actual forward trip*. Clinical Biomechanics, 2001. **16**: p. 813-19.

- [113] Myers, J.A., *Handbook of equations for mass and area properties of various geometrical shapes*. Defense Technical Information Center. U.S. Naval Ordnance Test Station, California, 1962.
- [114] Chandler, R.F., et al., *Investigation of inertial properties of the human body*. Report No. AMRL-TR-74-137. Air Force Aerospace Medical Research Laboratory, Wright-Patterson Air Force Base, Ohio, 1975.
- [115] Moyer, B.E., et al., *Gait parameters as predictors of slip severity in younger and older adults*. *Ergonomics*, 2006. **49**(4): p. 329-43.
- [116] Patterson, K.K., et al., *Evaluation of gait symmetry after stroke: a comparison of current methods and recommendations for standardization*. *Gait & Posture*, 2010. **31**: p. 241-46.
- [117] Nagano, H., et al., *Ageing and limb dominance effects on foot-ground clearance during treadmill and overground walking*. *Clinical Biomechanics*, 2011. **26**: p. 962-68.